



NRL/FR/5317--12-10,210

Polarization Characteristics of Coherent Waves

IRWIN D. OLIN

Sotera Defense Solutions, Inc.
McLean, VA 22102-5011

Naval Research Laboratory Retiree

March 12, 2012

Approved for public release; distribution is unlimited.

| REPORT DOCUMENTATION PAGE | | | | Form Approved OMB No. 0704-0188 | |
|---|-----------------------------|---------------------------------|---------------------------------------|---|---|
| Public reporting burden for this collection of information is estimated to average 1 hour per response, including the time for reviewing instructions, searching existing data sources, gathering and maintaining the data needed, and completing and reviewing this collection of information. Send comments regarding this burden estimate or any other aspect of this collection of information, including suggestions for reducing this burden to Department of Defense, Washington Headquarters Services, Directorate for Information Operations and Reports (0704-0188), 1215 Jefferson Davis Highway, Suite 1204, Arlington, VA 22202-4302. Respondents should be aware that notwithstanding any other provision of law, no person shall be subject to any penalty for failing to comply with a collection of information if it does not display a currently valid OMB control number. PLEASE DO NOT RETURN YOUR FORM TO THE ABOVE ADDRESS. | | | | | |
| 1. REPORT DATE (DD-MM-YYYY) 12-03-2012 | | 2. REPORT TYPE Formal Report | | 3. DATES COVERED (From - To) 2000-2011 | |
| 4. TITLE AND SUBTITLE Polarization Characteristics of Coherent Waves | | | | 5a. CONTRACT NUMBER | |
| | | | | 5b. GRANT NUMBER | |
| | | | | 5c. PROGRAM ELEMENT NUMBER | |
| 6. AUTHOR(S) Irwin D. Olin* | | | | 5d. PROJECT NUMBER 53-9741-C-15 | |
| | | | | 5e. TASK NUMBER | |
| | | | | 5f. WORK UNIT NUMBER | |
| 7. PERFORMING ORGANIZATION NAME(S) AND ADDRESS(ES) Naval Research Laboratory 4555 Overlook Ave., SW Washington, DC 20375-5320 | | | | 8. PERFORMING ORGANIZATION REPORT NUMBER NRL/FR/5317--12--10,210 | |
| 9. SPONSORING / MONITORING AGENCY NAME(S) AND ADDRESS(ES) Office of Naval Research Code 31 1 Liberty Center 875 N. Randolph Street, Suite 1425 Arlington, VA 22203-1995 | | | | 10. SPONSOR / MONITOR'S ACRONYM(S) ONR | |
| | | | | 11. SPONSOR / MONITOR'S REPORT NUMBER(S) | |
| 12. DISTRIBUTION / AVAILABILITY STATEMENT Approved for public release; distribution is unlimited. | | | | | |
| 13. SUPPLEMENTARY NOTES * Sotera Defense Solutions, Inc., McLean, VA 22102-5011; Naval Research Laboratory retiree. | | | | | |
| 14. ABSTRACT Coherent polarized waves, propagating toward and receding from an observer, together with their representation in terms of orthogonal linearly and circularly polarized component pairs are described in some detail. Appropriate matrix formulation facilitates their bases interchange and enables a better understanding of their characteristics, especially in connection with radar or communications related subjects. Component parameters in terms of Poincaré Sphere locations are described and readily characterize measurable relationships among different polarizations. Polarization distortion effects using phased array apertures with dual polarized elements are emphasized and details concerning signal bit resolution and phase center coincidence effects are described and analyzed. An approach to polarization filtering is reviewed and the well known polarization related parameter characterizations, the Ludwig-3 cross-polarized component definition and the Huynen Fork representation of radar target parameters, are described and relevant analyses presented. An illustrative polarization related problem concerning ground-based systems and SATCOM interaction illustrates many of the parameter design considerations described within the report. Throughout the text, numerous derived parametric plots are illustrated which aid in an overall understanding of the major details of this important subject. | | | | | |
| 15. SUBJECT TERMS Linear and Circular Polarization, Cross-polarization, Poincaré Sphere, Scatter Matrix, Phased Arrays, Ludwig-3, Huynen Fork, Polarization Bandwidth, Bit Resolution, Geometric Effect, Satellite Communication | | | | | |
| 16. SECURITY CLASSIFICATION OF: | | | 17. LIMITATION OF ABSTRACT SAR | 18. NUMBER OF PAGES 75 | 19a. NAME OF RESPONSIBLE PERSON Dharmesh Patel |
| a. REPORT Unclassified | b. ABSTRACT Unclassified | c. THIS PAGE Unlimited | | | 19b. TELEPHONE NUMBER (include area code) (202) 767-3355 |

CONTENTS

| | |
|---|----|
| 1. VISUALIZATION AND REPRESENTATION..... | 1 |
| 2. GENERALIZED EW WAVE REPRESENTATION | 4 |
| 2.1 Basis, Real and Complex Polarization Vectors and Scalar Components..... | 5 |
| 2.2 Geometric Characteristics of Linearly Polarized Waves | 8 |
| 2.3 Elliptically Polarized Waves | 11 |
| 2.4 Circular Base Components..... | 14 |
| 3. POINCARÉ SPHERE REPRESENTATION | 15 |
| 3.1 Concept and Measures | 15 |
| 3.2 Relationship Between Differing Polarizations | 19 |
| 4. CO-AND CROSS-POLARIZATION; LUDWIG-3 REPRESENTATION | 20 |
| 5. PHASED ARRAYS | 23 |
| 5.1 Angle between E-fields: The Geometric Effect | 23 |
| 5.2 Combining Signals from Dual-Polarized Elements | 30 |
| 5.3 Cross-polarization and Parameter Precision | 33 |
| 5.4 Impact of Bit Resolution on Polarization Characteristics | 35 |
| 5.5 Combining Polarization Components | 37 |
| 6. PHASE CENTER COINCIDENCE..... | 41 |
| 7. POLARIZATION BANDWIDTH | 45 |
| 8. SCATTER MATRIX | 49 |
| 8.1 Other Scatter Matrix Forms | 50 |
| 8.2 Canonical Structures | 50 |
| 8.3 Co- and Cross-pol Nulls of Target Backscatter | 51 |
| 8.4 The Huynen Fork | 53 |
| 8.5 Scatter Matrix Decomposition | 53 |
| 8.6 Control of Polarization Axial Ratio and Ellipse Orientation | 55 |

| | |
|---|----|
| 9. POLARIZATION FILTER | 57 |
| ACKNOWLEDGMENTS..... | 59 |
| REFERENCES..... | 59 |
| APPENDIX A – Charts Depicting Polarization Loss | 61 |
| APPENDIX B – Satellite Communication..... | 65 |

POLARIZATION CHARACTERISTICS OF COHERENT WAVES

1. VISUALIZATION AND REPRESENTATION

Every polarized wave – linear, circular, or elliptical – can be visualized as combinations of two constant E-field amplitudes, one rotating clockwise, the other counter-clockwise. Each rotates at a constant angular velocity $\omega (=2\pi f)$ and propagates at the speed of light within its medium. If the amplitude of one is zero, then the “combined” polarization is defined by IEEE convention as right circular if it rotates clockwise wave when propagating away from an observer and left circular if propagating toward an observer. Combinations of unequal rotating pairs each with a constant phase difference δ or time difference $(=\delta/\omega)$ then defines all possible polarization states. In this context, circularly and linearly polarized waves are special cases of elliptically polarized waves that are defined by three independent, physically measurable parameters: *axial ratio*, *direction of rotation* and *major (or minor) axis orientation*. Implicit in this characterization is a reference coordinate system, typically Cartesian coordinates using a right-hand rectilinear system. Then the E-field vector for a vertically polarized wave can be in the X-O-Z plane as illustrated in Fig. 1(a), assuming OX is the vertical direction. Using the same coordinate system, the E-field vector of a right circularly polarized wave would appear as illustrated in Fig. 1(b).

Of course, combinations of pairs of circularly polarized components are not the only way a polarized wave can be represented or described. Advantageously the wave would be resolved into a pair of *orthogonal* components; right and left circular as described above. But the two amplitudes and the relative phase between them could also be a pair of vertical and horizontal polarized components, or any angularly rotated linear pair. One could envision a pair of orthogonal elliptically polarized components, or even a nonorthogonal pair. Control of their amplitudes and phases then defines the polarization state. But regardless of the pair used, they provide the *basis components* for wave description needed for further analyses, described by Rumsey, Deschamps, Kales, and Bonhert [1].

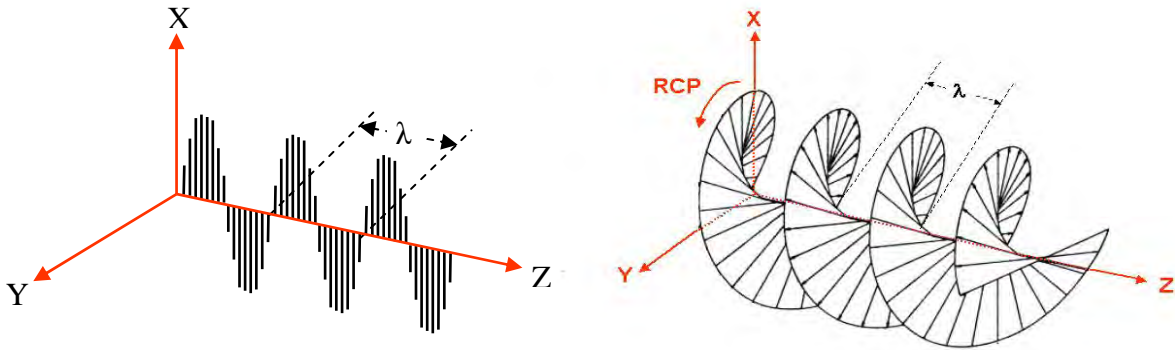


Fig. 1 – Rectangular coordinate linear (a) and circularly polarized (b) waves and their associated wavelength periodicity. λ is the wavelength in the propagating medium.

The relationship among observable parameters and the direction of propagation is further illustrated in Fig. 2.

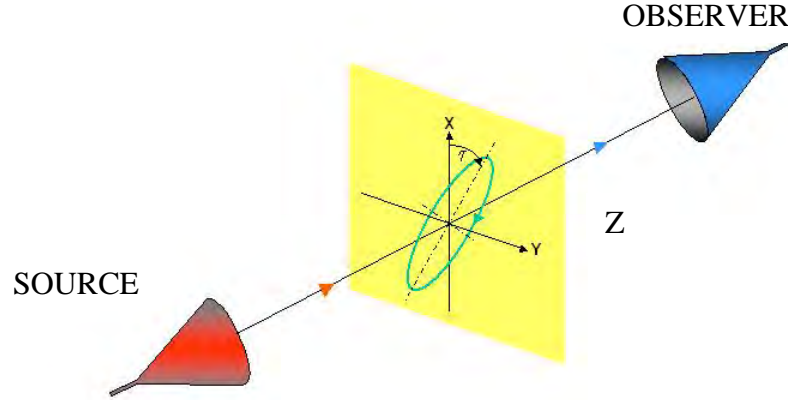


Fig. 2 – IEEE defines the rotational sense and the clockwise tilt angle from a reference direction, shown vertical, for a polarized wave looking in the propagating direction. The receiver (blue) observes a counter-clockwise tilt and an oppositely rotating wave.

For the circular basis representation, the E-field right and left circular components rotate oppositely at the same angular velocity of ω ($2\pi f$) radians per second, but with different amplitudes and a relative phase difference during the RF cycle. The waves spiral away along the “Z” axis, and for an observer *behind* the source, the right circular polarization (RCP) component rotates clockwise, and the left circular polarization (LCP) component rotates counterclockwise. But to an observer somewhere along the Z- axis and looking back toward the coordinate origin of the source, the rotation directions are reversed; RCP then rotates counterclockwise; LCP rotates clockwise.

Figures 3(a) and 3(b) represent two pairs of unequal amplitude, oppositely rotating circularly polarized waves viewed from behind the source. With equal phase between the waves initially aligned along the X-axis, the combination will always align along the X-axis. Assuming OX is a vertical axis, the polarization is purely vertical if $V_R = V_L$ and a vertically oriented elliptical polarization when they are unequal, as illustrated in Fig. 3(a). But if the waves are in-phase along the Y-axis, the combined polarizations will always be horizontally oriented, assuming OY corresponds to a horizontal axis, as in Fig. 3(b). Other alignments result when their phase difference is other than 0 or π , as illustrated in Fig. 4(a). But the locus of the total field vector by combining RCP and LCP fields with *equal* amplitudes will always be purely *linear* with an orientation represented by τ . With unequal amplitudes, the rotation rate of the combined field vector varies during a cycle, but is unidirectional. Within a plane, the locus of this vector is an ellipse with an axial ratio of E_{\max}/E_{\min} oriented about the maximum field during rotation, as illustrated in Fig. 4(b). The results of the analysis in Section 2.3 show that τ is just half of this difference. This representation is conceptually simple; the combined rotation (rotational sense) is the larger of the two components while the orientation of the major axis, whether representing linear or elliptical waves, is solely determined by their phase difference.

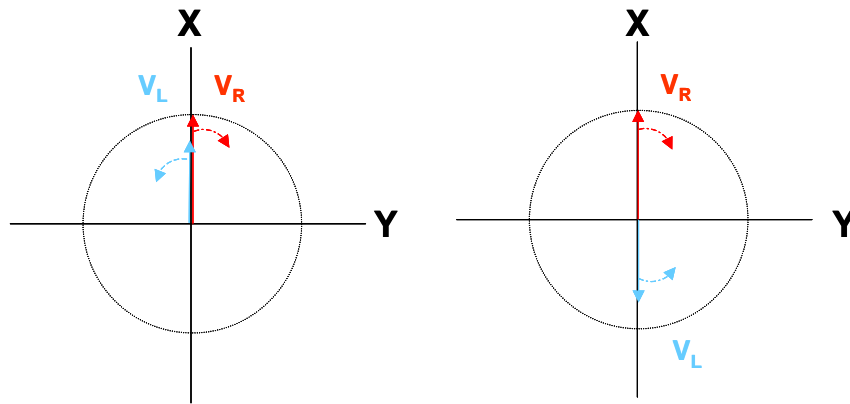


Fig. 3 – Rotating unequal components; vertically oriented elliptical polarization with 0° (a) and horizontal oriented elliptical with 180° phase difference (b) between the circular components. Axes origin corresponds to the OZ axis in Fig. 2.

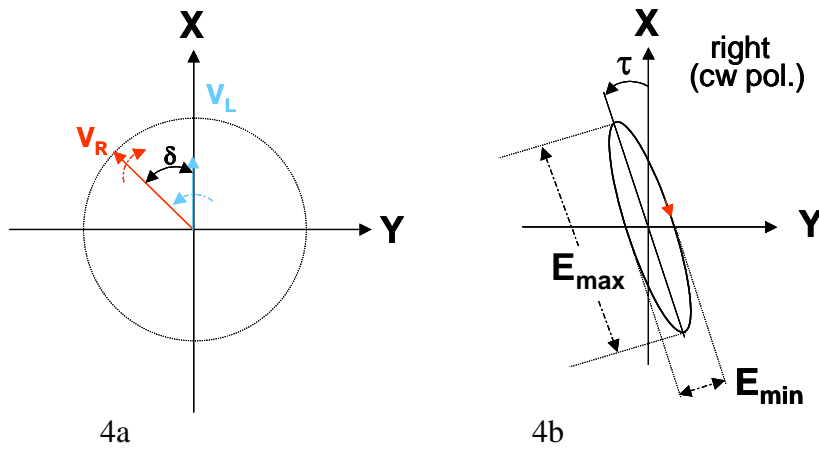


Fig. 4 – Phase difference δ between the two unequal circular components defines τ , the orientation of the major ellipse axis.

Accurate control of polarization is important in radar, electronic warfare, and communication. Efficient radar target detection is generally described in terms of matched transmit and received target polarization characteristics. Cross-polarization represents an unwanted loss and in tracking systems it can introduce errors. The effectiveness of electronic countermeasures (ECM) usually requires matching the attacker's characteristics. Maintaining a high axial ratio or the equivalent ratio of one sense with respect to the other is particularly important in SATCOM, where simultaneous use of RCP and LCP can enable two independent communication channels to occupy the same spectral space. In effect, sufficient separation between orthogonal components adds an independent polarization dimension to the available

spectral space. Often termed “frequency reuse,” its utility requires substantial isolation, sometimes as much as 40 dB to prevent cross-talk between the two circularly polarized channels.

Representing the amplitudes of the right and left circularly polarized E-field components by E_R and E_L , the maximum and minimum of their combined fields are $E_R + E_L$ and $E_R - E_L$. The ratio of these then defines the “ellipticity,” irrespective of its orientation:

$$\frac{E_{\max}}{E_{\min}} = \left| \frac{E_R + E_L}{E_R - E_L} \right|. \quad (1)$$

The ratio of the circular components, characterized as the *axial-ratio*, is then

$$\frac{E_R}{E_L} = \left| \frac{1 + E_{\max}/E_{\min}}{1 - E_{\max}/E_{\min}} \right|. \quad (2)$$

Figure 5 illustrates the decibel ratio of the circular components, $AR_{dB} = 20\log E_R/E_L$, in terms of the axial ratio, E_{\max}/E_{\min} , which is also expressed in decibels. The figure illustrates the nearly circular polarization that may be required. An axial ratio of 1 dB, defined by the relationship $AR_{dB} = 20\log(AR)$, appears nearly circular, but only represents a circular cross-polarization isolation of about 25 dB. Measures of cross-polarization depend on the polarization bases and therefore are not specific to pairs of circularly polarized waves. Frequently, the cross-polarization for the vertical and horizontal components may be used when the dominant system associated component is polarized along one of these directions. Circular polarization was chosen in connection with SATCOM because it is immune from Faraday magneto-optical field rotational effects; therefore, axial ratio is an appropriate measure of polarization purity.

2. GENERALIZED EW WAVE REPRESENTATION

Arbitrarily polarized waves are conveniently represented in terms of a pair of *basis* vectors. Although the X (vertical) and Y (horizontal) linear basis are most frequently used, the circular basis enables a comparatively easy understanding of the general characteristics of polarized waves. In this section, the analysis is extended using pairs of *orthonormal* vectors, i.e., the basis vectors are pair-wise orthogonal and each of unit length. To generalize this further, these unit vectors and the associated scalar parameters can also be complex.

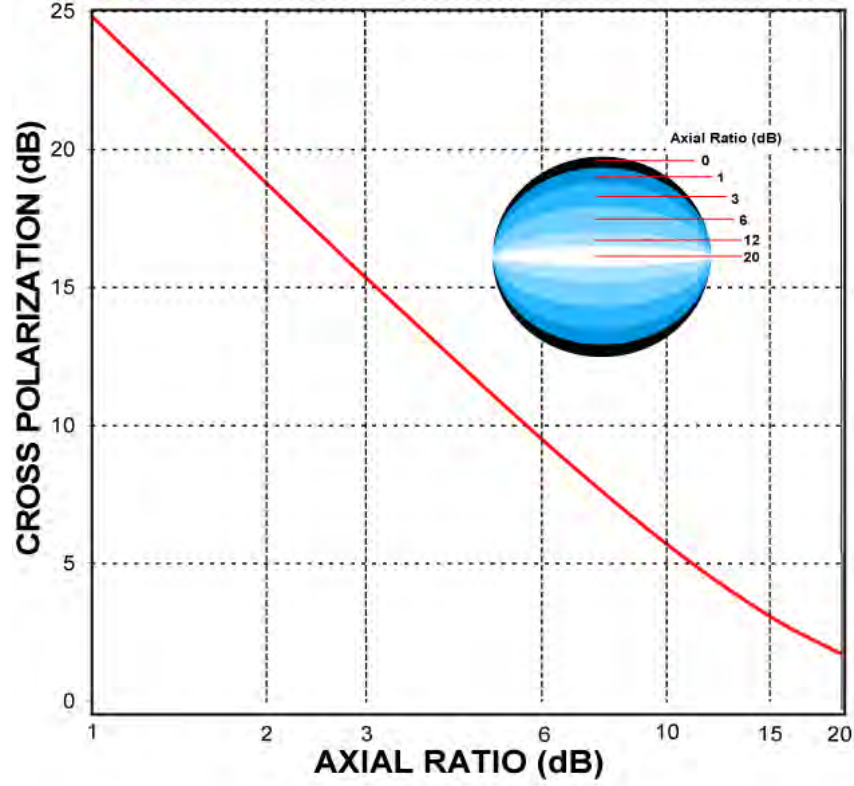


Fig. 5 – Circularity and representation of cross-polarization ratio and axial ratio

2.1 Basis, Real and Complex Polarization Vectors and Scalar Components

The E-field vector during an RF cycle is conveniently represented by the scalar parameters of an appropriate unit vector basis. Numerous differing vector bases, each spanning the polarization space, can and are used. Among many possibilities are the two linear bases: a vertical and horizontal pair, and a pair slanted 45° and 135° with respect to the vertical, and the clockwise and counterclockwise circular basis, illustrated in Section 1. But regardless of the basis used, the combined E-field vector (which defines polarization in electromagnetic problems, as contrasted with that used in optics) equivalence must connect the representation in different basis.

For a selected basis pair, polarization is defined in terms of projections, i.e., components, of the field along a pair of unit amplitude reference vectors \hat{e}_1 and \hat{e}_2 :

$$\vec{E} = (\vec{E} \cdot \hat{e}_1^*) \hat{e}_1 + (\vec{E} \cdot \hat{e}_2^*) \hat{e}_2 = E_1 \hat{e}_1 + E_2 \hat{e}_2. \quad (3)$$

The dot products $(\vec{E} \cdot \hat{e}_1^*)$ and $(\vec{E} \cdot \hat{e}_2^*)$ are the complex scalars that define the projection of the E-field vector onto the pair of complex base vector fields, \hat{e}_1 and \hat{e}_2 , simply the components of the vector in the unit vector directions. For orthonormal basis vectors, two conditions must be fulfilled:

$$(\hat{e}_1 \cdot \hat{e}_2^*) = (\hat{e}_1^* \cdot \hat{e}_2) = 0 \text{ and } (\hat{e}_1 \cdot \hat{e}_1^*) = 1, (\hat{e}_2 \cdot \hat{e}_2^*) = 1. \quad (4)$$

This expression defines the two unit length vectors, \hat{e}_1, \hat{e}_2 , which are also orthogonal.

In the familiar vertical and horizontal component pair, $(\hat{e}_x, \hat{e}_y) \equiv (\hat{e}_v, \hat{e}_h)$, illustrated in the right-hand coordinate system shown in Fig. 1, each is a real unit vector. Their components, each with some amplitude and phase, then form complex scalars. For example, the time-dependent complex scalar form of an arbitrarily polarized wave propagating in the +Z direction, i.e., away from an observer, can be represented in terms of these unit vectors:

$$\vec{E} = \hat{e}_x E_x \cos(\omega t - \beta z + \phi_x) + \hat{e}_y E_y \cos(\omega t - \beta z + \phi_y). \quad (5)$$

$\beta = 2\pi/\lambda$ and ϕ_x, ϕ_y characterize the phase relationships of the two components, where the equivalent polar form is

$$\vec{E} = \Re \left\{ \hat{e}_x E_x \epsilon^{j(\omega t - \beta z + \phi_x)} + \hat{e}_y E_y \epsilon^{j(\omega t - \beta z + \phi_y)} \right\}. \quad (6)$$

Since only the phase difference between these components is significant, using $\delta = \phi_x - \phi_y$ this can be written as

$$\vec{E} = \Re \left\{ \left[\hat{e}_x E_x + \hat{e}_y E_y \epsilon^{j\phi} \right] \cdot \epsilon^{j(\omega t - \beta z)} \right\}. \quad (7)$$

Of particular significance is the result with $E_x = E_y = 1$ and $\phi = \pm\pi/2$:

$$\vec{E} = \hat{e}_x \cos(\omega t - \beta z) \mp \hat{e}_y \sin(\omega t - \beta z). \quad (8)$$

Within any plane Z, the temporal characteristics are those of a unit length vector rotating clockwise if $\phi = +\pi/2$ and counterclockwise if $\phi = -\pi/2$. Furthermore, in this representation, the polarized wave is traveling in the +Z direction and away from an observer in the right-hand coordinate system illustrated in Fig. 1. Following IEEE convention, the rotational sense of a clockwise rotating wave, in the propagating direction, i.e., away from an observer, is right circular, and left circular with counterclockwise rotation, as illustrated in Fig. 2. In terms of the function $\exp(j\omega t - j\beta z)$ from Eq. (7), unit vectors and their associated scalar components define the circular-to-linear basis equivalence. Right and left circular polarized unit vectors are therefore

$$\hat{e}_R^+ = \frac{1}{\sqrt{2}} (\hat{e}_x - j\hat{e}_y) \quad (9a)$$

and

$$\hat{e}_L^+ = \frac{1}{\sqrt{2}} (\hat{e}_x + j\hat{e}_y). \quad (9b)$$

In these equations, the “+” exponent denotes propagation away from an observer, and the $1/\sqrt{2}$ factor accounts for the difference between the magnitude of the time-dependent rotating vector and its averaged value during one rotational period.¹

For an arbitrary polarized wave, the RCP and LCP equivalent components are

$$E_R = \vec{E} \cdot \hat{e}_R^* = \vec{E} \cdot \frac{1}{\sqrt{2}}(\hat{e}_x + j\hat{e}_y) \quad (10a)$$

and

$$E_L = \vec{E} \cdot \hat{e}_L^* = \vec{E} \cdot \frac{1}{\sqrt{2}}(\hat{e}_x - j\hat{e}_y) \quad (10b)$$

The matrix form describing the relationships of the scalar components is then

$$\begin{bmatrix} E_R^+ \\ E_L^+ \end{bmatrix} = \frac{1}{\sqrt{2}} \begin{bmatrix} 1 & j \\ 1 & -j \end{bmatrix} \cdot \begin{bmatrix} E_x^+ \\ E_y^+ \end{bmatrix} \quad (11)$$

For example, the linearly polarized components of a purely vertically polarized wave of unit amplitude is expressed $\{E_x^+, E_y^+\} = \{1, 0\}$. Then, the circularly polarized components $\{E_R^+, E_L^+\} = 1/\sqrt{2} \{(1, 1)\}$, also with a unity combined amplitude. For a horizontally polarized wave of unit amplitude, $\{E_x^+, E_y^+\} = \{0, 1\}$, or $\{E_R^+, E_L^+\} = 1/\sqrt{2} \{(j, -j)\}$, again with unit amplitude, but with a 180° phase difference between the circular components. The inverse relationship describing the linearly polarized components from their circular component equivalents then simply involves a matrix inversion. Since the inverse of a complex matrix $[T]$ is $[\tilde{T}]^*$, the X,Y components in terms of the circularly polarized components are

$$\begin{bmatrix} E_x^+ \\ E_y^+ \end{bmatrix} = \frac{1}{\sqrt{2}} \begin{bmatrix} 1 & 1 \\ -j & j \end{bmatrix} \cdot \begin{bmatrix} E_R^+ \\ E_L^+ \end{bmatrix} \quad (12)$$

For wave components traveling toward an observer, also using the right-hand coordinates of Fig. 1, a reversal in one of the coordinate frames is required for their combination. For the pair of vertical and horizontal components (E_x, E_y) , a simple sign reversal of the horizontal component is required.

In terms of the scalar components matrix, this is accomplished by a conjugate operation. The total set of operations among these scalar components is then

$$\{E_R^+, E_L^+\} = [T] \cdot \{E_x^+, E_y^+\}, \quad (13)$$

¹ The $1/\sqrt{2}$ factor actually takes into account the difference between the magnitude of the time-dependent rotating vector and its averaged (rms) value during one rotational cycle (NRL Memo Report M1474, Oct. 1963).

$$\{E_X^+, E_Y^+\} = [T^{-1}] \cdot \{E_R^+, E_L^+\}, \quad (14)$$

$$\{E_R^-, E_L^-\} = [T^*] \cdot \{E_X^-, E_Y^-\}, \quad (15)$$

$$\{E_X^-, E_Y^-\} = [\tilde{T}] \cdot \{E_R^-, E_L^-\}, \quad (16)$$

where

$$[T] = \frac{1}{\sqrt{2}} \begin{bmatrix} 1 & j \\ 1 & -j \end{bmatrix}. \quad (17)$$

Each of these equations describes the relationship between the complex scalars in the linear and circular basis. In this context, the linear temporal form, $E \cos(\omega t + \phi)$, would be written as previously described.

Regardless of the changes in coordinate basis or propagating directions, the mathematical transform from one basis to another must leave the field vector unchanged. The matrix form of this transformation facilitates this conversion using a simple matrix transform that conserves the equivalent fields:

$$[E_{1,2}] = [M] \cdot [E_{3,4}].$$

$[M]$ is a unitary matrix, so that,

$$[M] \cdot [M]^{-1} = [M] \cdot [\tilde{M}]^* = [I],$$

where $[I]$ is the identity matrix (ones in the principal diagonal). For example:

$$\frac{1}{\sqrt{2}} \begin{bmatrix} 1 & 1 \\ -j & j \end{bmatrix} \cdot \frac{1}{\sqrt{2}} \begin{bmatrix} 1 & j \\ 1 & -j \end{bmatrix} \equiv \begin{bmatrix} 1 & 0 \\ 0 & 1 \end{bmatrix} = I. \quad (18)$$

2.2 Geometric Characteristics of Linearly Polarized Waves

Linear and circular polarized waves are characterized as special cases of general elliptically polarized waves, the parameters of which are important in polarization metrics. The polarization of signals radiated or received by an antenna is defined by the polarization of the antenna in the direction of interest. Although this may appear somewhat trivial, all antennas, whether simple horns, illuminated parabolas or phased arrays, exhibit polarization *angular* dependence, further motivating a better understanding within any system design.

Some early measurements of a simple X-band rod antenna excited to radiate circular polarization in the axial direction are illustrated in Fig. 6 and show substantial variation in the measured off-axis polarization characteristics. Linearly polarized horns exhibit similar characteristics. The central axis beam may be linearly polarized, but away from its axis the single polarization radiator “acquires” a cross-polarized component. For many applications this characteristic presents little difficulty, since only the main beam direction is important. But the directionality of phased arrays is the result of element signal weighting of the fixed constituent elements, *each* with wide angular coverage. Therefore, array element

off-axis polarization characteristics are relevant to overall antenna performance. Problems and solution approaches specific to phased arrays are described later in Section 5.

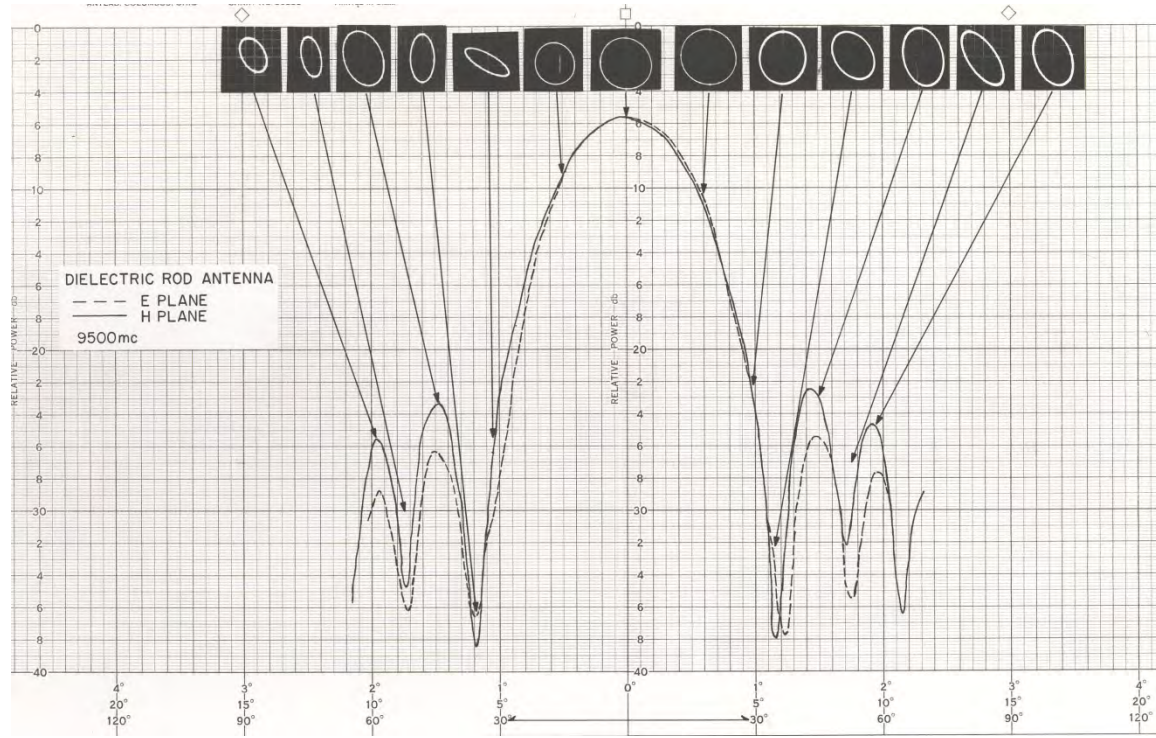


Fig. 6 – Rod-antenna-polarization characteristics. The axial pure circularity is severely degraded near the first null.

The parameters of any elliptically polarized wave can be described in terms of the locus of the sinusoidal field vector components in directions defined by the orthonormal vectors, \hat{e}_x and \hat{e}_y as a function of time for the wave traveling in the +Z direction. Within any X,Y plane, illustrated in Fig. 7, these are assumed:

$$x = E_x \cos(\omega t + \phi_x) \quad (19)$$

$$y = E_y \cos(\omega t + \phi_y) \quad (20)$$

The total field, $\vec{E} = \hat{e}_x E_x \cos(\omega t + \phi_x) + \hat{e}_y E_y \cos(\omega t + \phi_y)$, is then readily visualized by the rotating vector Fig. 7. Polarization sense, i.e. right or left, is determined by the direction of the temporal variation of ξ , shown here as the angle of the combined field vector relative to the X-Y axes, where $r = E_x/E_y$:

$$\xi = \tan^{-1} r \frac{\cos(\omega t + \phi_x)}{\cos(\omega t + \phi_y)} \quad (21)$$

The rate of change of this angle is:

$$\frac{d\xi}{dt} = \frac{r\omega}{r^2 \cos^2(\omega t + \phi_X) + \cos^2(\omega t + \phi_Y)} \cdot \sin(\phi_Y - \phi_X). \quad (22)$$

As a result, along the +Z direction, $d\xi/dt$ is negative when $\phi_Y > \phi_X$, therefore clockwise rotation; right elliptical (or circular) polarization. Left elliptical (or circular) polarization results when $\phi_Y < \phi_X$, and thus counter-clockwise rotation.

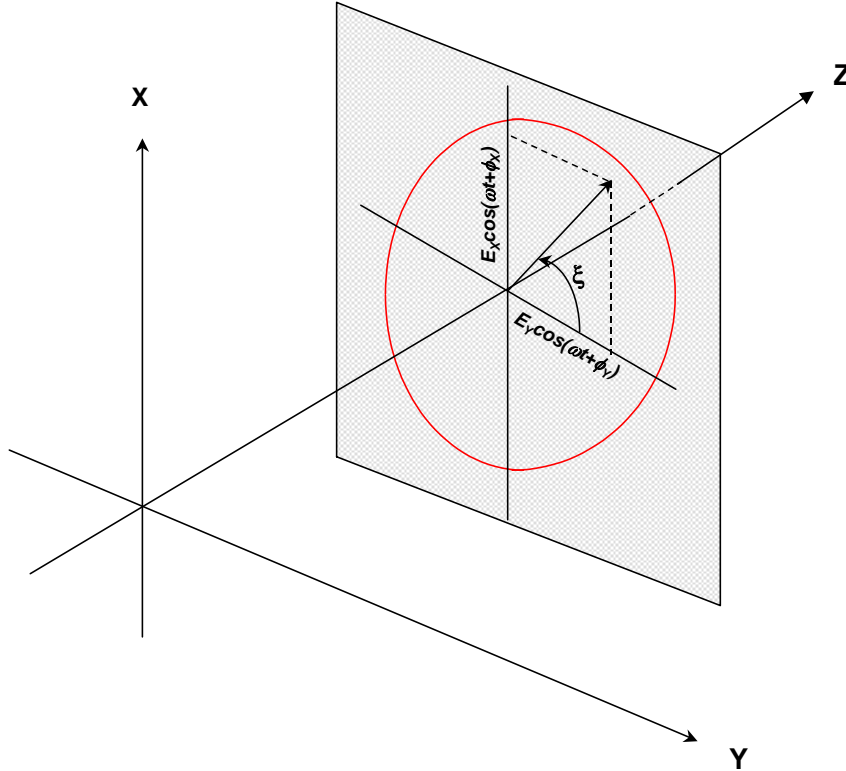


Fig. 7 – Rotating E-field within one X-Y plane along the Z – axis

The clear distinction between circularly polarized and elliptically polarized waves of different axial ratios is illustrated by the change in rotation rates of the E-field vector from Eq. (22) and plotted in Fig. 8 for various axial ratios. (These also correspond to the ratios of the orthogonal linearly polarized components, each with a 90° phase shift.) A constant rotation rate would correspond to a purely circularly polarized wave, while a nearly linearly polarized wave would show high, nearly discontinuous rotation rates during the RF cycle. As shown, the peak value of the -20 dB ratio scales beyond the ordinate scale to a value of 500 deg/s, within a short period, closer to that of a purely linearly polarized wave. For purely linearly polarized waves the field vector instantaneously changes so the ellipse is narrowed to a line, its polarization angle can be vertical, horizontal or any other depending on the component amplitudes, E_x and E_y . Circular and linear polarizations are then visualized as special cases of the general elliptically polarized wave. But in terms of the duality between linear and circularly polarized waves, the *linear* basis axial ratio of a wave polarized either mostly vertical or mostly horizontal will approach zero or infinity, but its circularly polarized equivalents, measured in a *circular* basis will be near unity.

Except for purely circularly polarized waves, the angular velocity of the E-field varies during one period. But as is the case for circularly polarized waves, for a wave traveling away from an observer, the right elliptical polarization (REP) and left elliptical polarization (LEP) are respectively defined by

$$(\phi_X - \phi_Y) > 0 \text{ or } (\phi_X - \phi_Y) < 0. \quad (23)$$

It is just the phase lead or lag of one of components of the rotating vector with respect to the other as depicted in Fig. 7, which defines the rotational direction, therefore the characterized sense.

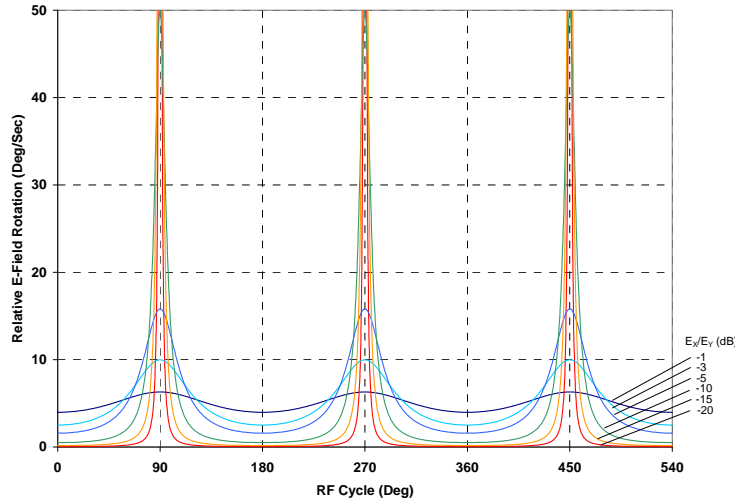


Fig. 8 – Effect of linearly polarized components amplitude ratio on field rotation rate

2.3 Elliptically Polarized Waves

The pictorial character of polarized waves is best visualized in terms of the geometric trace of the rotating vector shown in Fig. 7. In general terms, this is an ellipse defined by axial ratio, major axis inclination and rotational sense. The parameters of this ellipse are defined by the combined components and can be readily determined by a parametric solution in ωt of the “x” and “y” components of Eqs. (19) and (20). Equivalently, these are:

$$x = a \cos \omega t - b \sin \omega t \quad (24a)$$

and

$$y = c \cos \omega t - d \sin \omega t, \quad (24b)$$

where $a = E_X \cos \phi_X$, $b = E_X \sin \phi_X$, $c = E_Y \cos \phi_Y$, $d = E_Y \sin \phi_Y$. (24c)

Equations (24a, 24b) can then be combined for the parametric solution in ωt :

$$\tan \omega t = \frac{cx - ay}{dx - by}. \quad (25)$$

Substituting the corresponding sine and cosine values into Eqs. (24a, 24b), combining terms in the variables, x and y , and representing the phase difference by $(\phi_x - \phi_y) = \delta$, the result is the familiar equation for an ellipse:

$$Ax^2 + Bxy + Cy^2 = 1, \quad (26a)$$

with
$$A = \frac{1}{(E_x \sin \delta)^2}, \quad B = \frac{-2 \cos \delta}{E_x E_y \sin^2 \delta}, \quad C = \frac{1}{(E_y \sin \delta)^2}. \quad (26b)$$

If the coefficient $B \neq 0$, the major and minor axes of the ellipse are aligned with an orthogonal pair of axes $X'-Y'$, at an angle τ , from $X-Y$ as illustrated in Fig. 9, since the components E_x , E_y were defined with respect to the $X-Y$ axes. Their intercepts on these axes then define the axial ratio. If $B=0$, then $\tau=0$ and the axial ratio is defined with respect to the $X-Y$ axes. From the figure, the relationship between two pairs of components, $X'-Y'$ and $X-Y$ is

$$\begin{pmatrix} x' \\ y' \end{pmatrix} = \begin{pmatrix} \cos \tau & \sin \tau \\ -\sin \tau & \cos \tau \end{pmatrix} \cdot \begin{pmatrix} x \\ y \end{pmatrix}, \quad (27a)$$

and the corresponding inverse relationship:

$$\begin{pmatrix} x \\ y \end{pmatrix} = \begin{pmatrix} \cos \tau & -\sin \tau \\ \sin \tau & \cos \tau \end{pmatrix} \cdot \begin{pmatrix} x' \\ y' \end{pmatrix}. \quad (27b)$$

For both of these equations, τ is the inclination angle of the ellipse and can be derived from the temporal characteristics depicted in Fig. 9:

$$\tau = \tan^{-1} \left(\frac{E_x \cos(\omega \hat{t} + \phi_x)}{E_y \cos(\omega \hat{t} + \phi_y)} \right). \quad (28)$$

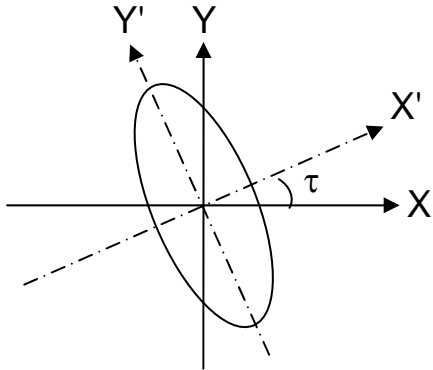


Fig. 9 – General form of the ellipse defined by Eqs. (26a) and (26b)

The orientation of the ellipse about the rotated X' , Y' axes, found by substituting the values from Eq. (27b) into Eq. (26a) is then

$$A'X'^2 + C'Y'^2 = 1, \quad (29)$$

in which

$$A' = \frac{1}{2}[(A + C) + (A - C)\cos 2\tau - B\sin 2\tau], \quad (30)$$

$$C' = \frac{1}{2}[(A + C) - (A - C)\cos 2\tau + B\sin 2\tau], \quad (31)$$

with

$$\tan 2\tau = \frac{B}{C - A}. \quad (32)$$

In terms of the components, E_x , E_y and δ ,

$$\tan 2\tau = \frac{2r}{r^2 - 1} \cos \delta, \quad (32a)$$

where $r = E_x/E_y$. The ratio of the components along X' and Y' defines the axial ratio or ellipticity of the component wave:

$$\left(\frac{x'}{y'}\right) = \sqrt{\frac{(A + C) + (A - C)\cos 2\tau - B\sin 2\tau}{(A + C) - (A - C)\cos 2\tau + B\sin 2\tau}}. \quad (33)$$

Substituting the “A, B, C” values from Eq. (26b), the axial ratio² is:

$$AR = \frac{x'}{y'} = \sqrt{\frac{\left(\frac{r^2 + 1}{r^2 - 1}\right)\cos 2\tau + 1}{\left(\frac{r^2 + 1}{r^2 - 1}\right)\cos 2\tau - 1}}. \quad (34)$$

The fact that the major and minor axes of the ellipse correspond to the time \hat{t} (or phase, $\omega\hat{t}$) when the total field vector is a maximum or a minimum, may also be used to define the relevant parameters, i.e., axial ratio, orientation and rotational sense. This interpretation further reinforces the concept that polarized waves, irrespective of their specific parameters, are characterized within a plane as a rotating vector. For a square of the field amplitude, V^2 , this is found by equating the derivative to zero:

$$\frac{dV^2}{dt} = \frac{d[E_x^2 \cos^2(\omega t + \phi_x) + E_y^2 \cos(\omega t + \phi_y)]}{dt} = 0. \quad (35)$$

The orientation angle of the ellipse, which corresponds to that in Fig. 9 is

² Axial ratio is generally defined when $x'/y' \geq 1$, while ellipticity is often defined by the inverse.

$$\tau = \tan^{-1} \left(\frac{E_X \cos(\omega \hat{t} + \phi_X)}{E_Y \cos(\omega \hat{t} + \phi_Y)} \right). \quad (36)$$

One cautionary note is that the transform depicted in Fig. 9 using Eqs. (27a, 27b) does not define an angle specific to the major or minor axes of the ellipse. Additionally, while the association between the propagating direction and the ellipse parameters can be deduced from Eqs. (8) and (26a, 26b), the parameters are only two-dimensional. Therefore, directionality will need to be considered when the radar response to target backscatter, a jamming signal, or even different radar needs to be accounted for.

2.4 Circular Base Components

In this basis, combining two differing but constant amplitude circularly polarized waves results in a rotating field vector, the terminus of which traces an ellipse as illustrated in Figs. 4(a) and 4(b). Axial ratio and orientation are functions of the amplitudes and phases of the circular waves, the angular velocity of the combined field vector varies during an RF cycle as indicated in Eq. (22). Its amplitude and velocity are constant only if a single component, V_R or V_L , is present.

With two equal amplitude circularly polarized components, which results in a linearly polarized wave, the amplitude of the combined vector varies sinusoidally over an RF cycle but its alignment appears stationary and in a direction that is half the difference in phase between the circular component waves (θ_L and θ_R).

The utility of circular base components is generally favored in subsequent field analyses. The rotational directions (or sense) are determined directly, i.e., the larger of the two components, while the angle of the major axis of the ellipse, τ , irrespective of the axial ratio, is just half the phase angle difference between the two circular components. The axial ratio is expressed in a simple form, as shown in Eq. (38). Assuming a wave traveling away from an observer, the circular base field components are given by:

$$\vec{E} = \vec{u}_R E_R \mathcal{E}^{j(\omega t - \beta z + \theta_R)} + \vec{u}_L E_L \mathcal{E}^{-j(\omega t - \beta z + \theta_L)}. \quad (37)$$

The magnitude of this rotating field vector in terms of the difference in circular components amplitude and phase is $|E|^2 = E_R^2 + E_L^2 + E_R E_L \cos(2\omega t - 2\beta z + \theta_R - \theta_L)$, with maximum and minima occurring when $\arg(\cos) = 0, \pi/2$, respectively. The axial ratio is then defined, as cited in Section 1 as

$$AR = \left| \frac{E_R + E_L}{E_R - E_L} \right|, \quad (38)$$

and the rotational sense is just the larger of either E_R or E_L . The elliptical characteristic of this field can be observed in any plane along the Z-axis as a function of time, as illustrated in Fig. 7. But the angular orientation of the ellipse considered here is measured from the x-axis. Therefore, to determine this angle, a transform to the X-Y- linear basis is required.

For the general pair of circular components, written as: $\{E_R \mathcal{E}^{j\theta_R}, E_L \mathcal{E}^{j\theta_L}\}$ and assuming propagation away from an observer, the equivalent linear base components from Eq. (12) are

$$\begin{bmatrix} E_X \\ E_Y \end{bmatrix} = \frac{1}{\sqrt{2}} \begin{bmatrix} 1 & 1 \\ -j & j \end{bmatrix} \cdot \begin{bmatrix} E_R \mathcal{E}^{j\theta_R} \\ E_L \mathcal{E}^{j\theta_L} \end{bmatrix} = \frac{1}{\sqrt{2}} \begin{bmatrix} (E_R \cos \theta_R + E_L \cos \theta_L) + j(E_R \sin \theta_R + E_L \sin \theta_L) \\ (E_R \sin \theta_R - E_L \sin \theta_L) + j(E_L \cos \theta_L - E_R \cos \theta_R) \end{bmatrix}. \quad (39)$$

Expanding these and substituting the linear components into Eq. (27a), the result for the tilt angle τ is simply

$$\tau = \frac{\theta_R - \theta_L}{2}. \quad (40)$$

Note that this result, independent of the axial ratio when expressed in circular base coordinates, is consistent with the specialized vertically and horizontally polarized cases described in connection with Fig. 2. The circular basis wave description, therefore, provides a direct and simple way to completely describe the three basic parameters (axial ratio, tilt, and rotation sense) of a polarized wave and, by extension those of antennas, radar targets, and jammers.

3. POINCARÉ SPHERE REPRESENTATION

3.1 Concept and Measures

The multiple dimensionality of a polarized wave makes it difficult to assess, much less analyze, the relationship between differently polarized waves. These can be the radar transmitted and target reflected waves, the uplink and downlink of a SATCOM system or the interception and jamming of an EW signal. In a three-page paper in 1892, Poincaré (p. 275-277, H. Poincaré, “Theorie Mathematique de la Luminiere II,” Gauthier-Villars, Paris, 1892) described a very useful representational and analytical tool to simplify the relationships among different polarizations.

The radius of the Poincaré Sphere corresponds to the normalized power of the represented polarizations. Its surface, illustrated in Fig. 10 maps a one-to-one correspondence with all possible polarizations. Points located in a specific hemisphere and along the same latitude represent the same axial ratio. Points along the same longitude represent polarizations with the same orientation but varying degrees of axial ratio or ellipticity. Points along an equatorial circle represent purely linear polarization states. All points in the upper hemisphere represent left elliptical states while points in the lower hemisphere represent right elliptical states.

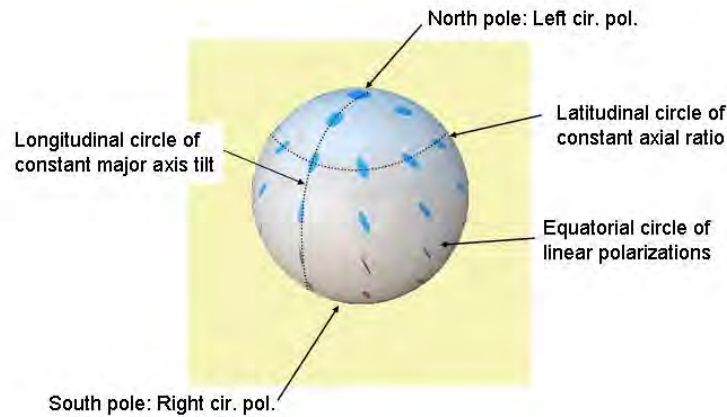


Fig. 10 – Representation of polarization states on the Poincaré Sphere

The four pairs of polarization states illustrated in Fig. 11 represented by diametrically opposed points *anywhere* on the sphere are orthogonal. For example, the two linearly polarized pairs, “V” and “H,” and another at inclined angles, the “RCP” and “LCP” pair or the “REP” and “LEP,” are each orthogonal. So if one represents the polarization of a wave traveling toward a receiver and the other that of the receiver, the 180° arc between them represents an infinite signal loss. The measure of the arc length, ℓ , between any two of these points is then a measure of their similarity or difference. In terms of decibel (dB) loss a simple expression for this relationship is

$$L_{dB} = 20 \log \left(\cos \frac{\ell}{2} \right). \quad (41)$$

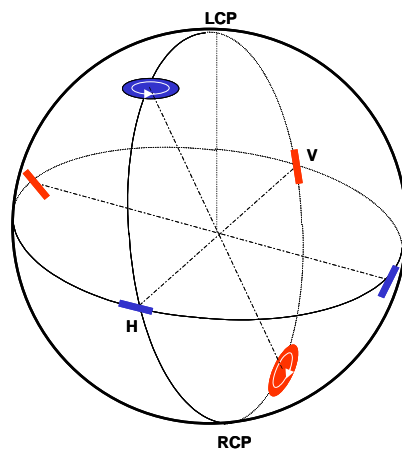


Fig. 11 – Orthogonal polarizations on the Poincaré Sphere. Polarizations represented by any two diametrically opposite points are orthogonal.

This result, plotted in Fig. 12, is independent of the disposition of one point about the other and shows a small polarization loss or difference even with modest arc lengths. However, it should be noted that in comparing transmitted and received waves on a single sphere, account must be taken of the differences in the rotation and major axis tilt.

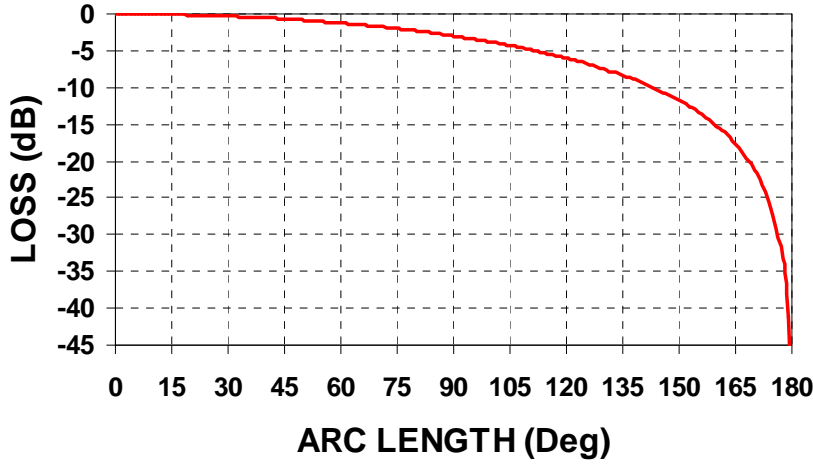


Fig. 12 – Polarization loss between any pair of points on the Poincaré Sphere separated by an arc length ℓ

Recall that the major axis tilt and field vector rotation direction of a wave viewed in opposite directions, i.e., toward or away from an observer, is reversed. Therefore, one can represent the polarization of an incident wave by the point that corresponds to the antenna that best receives it. This is a useful representation, for example, when estimating the polarization difference between an incident wave and a jamming signal that accounts for both the correct sense of the incident wave and that of the jamming signal.

Figure 13 illustrates one quadrant of the upper Poincaré hemisphere. A point “P” is sufficiently described by a complex scalar in the appropriate basis. For linear X-Y basis this is simply:

$$r\mathcal{E}^{j\delta} = \frac{E_X}{E_Y} \mathcal{E}^{j(\phi_X - \phi_Y)}, \quad (42)$$

and Eq. (42) can then be used in defining the sides and angles of the associated right spherical triangle outlined in the figure.

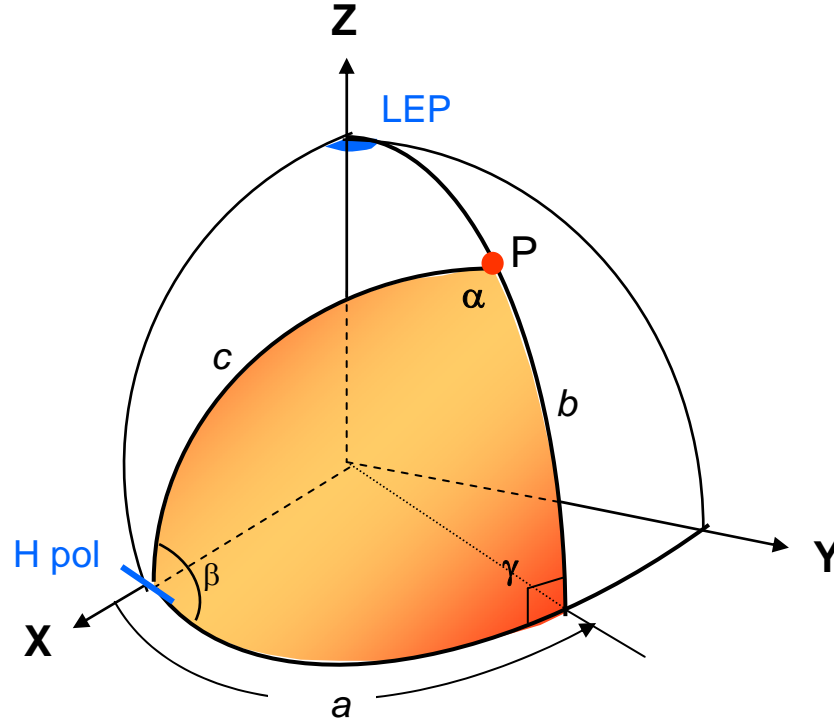


Fig. 13 – Upper hemisphere Poincaré Sphere quadrant. Angles and sides of a right spherical triangle define the location of a single polarized wave at “P.”

The latitudinal angle, side “b,” is related to the axial ratio AR. Since axial ratios of linearly and circularly polarized waves are “ ∞ ” and “1,” respectively, while b is “0°” and “90°,” respectively, the axial ratio is represented by an angular arc of $2 \tan^{-1} 1/AR$. Using Eqs. (32a) and (34) and appropriate trigonometric equivalents:

$$b = 2 \tan^{-1} \frac{1}{AR} = \sin^{-1} \left(\frac{2r}{r^2 + 1} \sin \delta \right). \quad (43)$$

Longitudinal angles, for example side “a,” are a measure of polarization angular tilt. Like the Earth’s Greenwich location, horizontal polarization universally serves as the reference longitudinal direction. Orthogonal polarizations along the equatorial plane and planes parallel to the equatorial plane are 180° apart, so polarization angular tilt, τ , is represented by an angular arc “a” of 2τ , as defined in Eq. (32a):

$$a = 2\tau = \tan^{-1} \left(\frac{2r}{r^2 - 1} \cos \delta \right). \quad (44)$$

Using the right spherical triangle relationship, $\sin a = \tan b \cot \beta$, then angle β is simply represented by

$$\beta = \delta. \quad (45)$$

Side “c” can be determined from the right spherical triangle trigonometric identity as $\cos c = \cos a \cos b$, then

$$\tan c/2 = 1/r. \quad (46)$$

Finally, using the identities $\cot \alpha \cot \beta = \cos a \cos b$, the remaining angle, α , in terms of “r” is

$$\tan \alpha = \frac{r^2 + 1}{r^2 - 1} \cot \delta. \quad (47)$$

3.2 Relationship Between Differing Polarizations

Systems analyses or designs invariably involve the association of one polarization with another. Basically the question that must be answered is: “How close is one polarization to another?” For example, target detection may involve the relationship between the polarization of the transmitter and that of the target or clutter. Electronic Warfare (EW) applications can involve the relationship between the polarization of a radar and that of a jammer. In a SATCOM application, the effectiveness of frequency reuse depends on maintaining the orthogonality between polarization channel pairs for effectiveness. The differences mean propagation direction as well as the usual parametric measures. The approach taken in analyzing such problems can be in terms of polarization sphere metrics or classic complex waves analyses. Both are therefore briefly outlined.

On the polarization sphere, two different polarizations can be represented by their locations that can be referenced to any pair of base polarizations. Figure 14 illustrates polarizations located by points P_1 and P_2 referenced to horizontal polarization at the point $(x, y, z) = (1, 0, 0)$. The arc length ℓ and the associated decibel (dB) difference illustrated in Fig. 12 then define the difference in their polarizations. Generally, the *proximity* rather than the *disposition* of these points is important, so a variety of parameter changes can be applied assuming the goal is to match or reject one or the other.

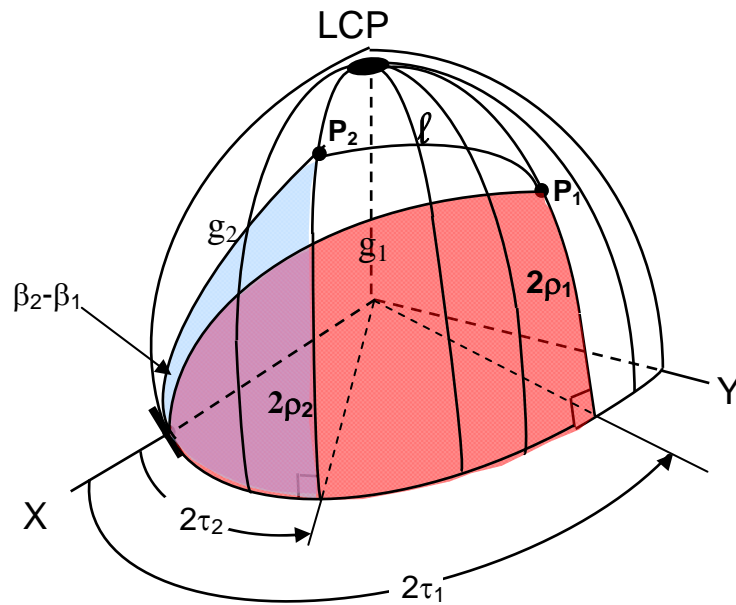


Fig. 14 – Polarizations represented by points P_1 and P_2 and the reference horizontal polarization define an oblique spherical triangle, enabling calculation of the arc ℓ .

The arc length ℓ can be defined in terms of the polarizations defined by their component field ratios r and the phase difference δ , or by the axial ratios and tilt angles. The sides, g_1 and g_2 , of the two right spherical triangles in terms of the axial ratio and tilt angles are determined using the relationship:

$$\cos g_n = \cos 2\tau_n \cos 2\rho_n, \quad n=1,2. \quad (48)$$

Angles β_1, β_2 in terms of these parameters are defined by

$$\tan \beta = \frac{\tan 2\rho}{\sin 2\tau}. \quad (49)$$

The sides, g_1, g_2 , the angular difference $\beta_1-\beta_2$, and the arc $\overline{P_1P_2}$ ($=\ell$) define an oblique spherical triangle. In terms of the two sides, ρ_1, ρ_2 , and the included angle $(\tau_1 - \tau_2)$, which are defined in terms of the axial ratio and tilt of the component polarizations $\cos \ell$ is then:

$$\cos \ell = \cos 2\rho_1 \cos 2\rho_2 \cos 2(\tau_1 - \tau_2) + \sin 2\rho_1 \sin 2\rho_2. \quad (50)$$

The formalism using complex field components yields the same results. Coupling or isolation between two different fields can be expressed in terms of the projection of one field component on the other. Assume the components a receiver and transmitter expressed in a linear X-Y basis are:

$$\vec{E}_{Rec} = E_1 \hat{e}_X + E_2 \hat{e}_Y \quad \text{and} \quad \vec{E}_{Trans} = E_3 \hat{e}_X + E_4 \hat{e}_Y, \quad (51)$$

in which E_1, E_2, E_3 and E_4 are complex scalars. Assume the scalar components are

$$E_1 = E_{X1} \mathcal{E}^{j\phi_{X1}}, E_2 = E_{Y2} \mathcal{E}^{j\phi_{Y2}}, E_3 = E_{X3} \mathcal{E}^{j\phi_{X3}}, E_4 = E_{Y4} \mathcal{E}^{j\phi_{Y4}}. \quad (52)$$

Then, normalize the power represented by each scalar so that

$$|E_1|^2 + |E_2|^2 = |E_3|^2 + |E_4|^2 = 1. \quad (53)$$

The coupling or isolation is then determined by the projection of one component on the other, represented by the dot product:

$$E = \vec{E}_{Rec} \cdot \vec{E}_{Trans}^*. \quad (54)$$

4. CO-AND CROSS-POLARIZATION; LUDWIG-3 REPRESENTATION

There is a recognized and explicable ambiguity in the IEEE definition of co-polarization and cross-polarization field components when describing the characteristics of an antenna. A simple unambiguous definition defines the co-polarization as one the antenna is intended to radiate, while the cross-polarization is that which is orthogonal. These can be defined in terms of any basis pair, but regardless of the basis used, a “*reference direction*” cited by the IEEE definition is needed. There is no ambiguity concerning the co-polarization of the E-field from a single short dipole along the OY axis as illustrated in

Fig. 15. The reference direction is the OY axis. In any plane containing the dipole the co-pol field varies as the cosine of the angle from its axis, while it is invariant in any orthogonal plane. The characteristics are the same for a small dipole aligned with the OX axis. Then the reference direction would be OX. With both dipoles the co-polarized field may be represented by one dipole along the reference direction, and the cross-polarized field by the other dipole. This definition implies orthogonality between their fields, but as described in connection with Section 5.1, these fields are only geometrically orthogonal in a single direction: azimuth = elevation = 0° , as shown in Fig. 19.

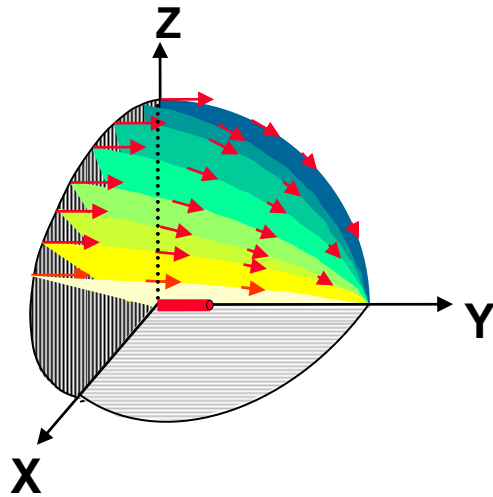


Fig. 15 – Representation of the E-fields around a small dipole, illustrating a cosine axial variation, none in the transverse direction.

Complete antenna patterns need to deal with both the problems of depicting a spherical projection of the pattern on a flat surface as well as a meaningful polarization representation. The former problem is a familiar one in cartography while the latter must deal with the ambiguity inherent in the IEEE characterization of co-pol and cross-pol components. Various mapping transforms, the most popular being the Mercator projection, adequately represent most area features defined by unit vectors $(\hat{r}, \hat{e}_\theta, \hat{e}_\phi)$, but within up to elevation (latitudinal) angles of about 60° . Area distortion at higher angles is familiar to everyone. But antenna patterns usually require accurate amplitude *and* angular definition over wider angles, so the manner in which these are made involves practical matters concerning antenna rotation about two orthogonal axes. Concerning far-field patterns, practicality usually favors elevation-over-azimuth rotation. Azimuth “cuts” for each value of fixed elevation angle are recorded often using a single linearly polarized transmit signal, defined along unit directions \hat{e}_x, \hat{e}_y and receiving the signals from the pair of orthogonal antenna ports representing the E_θ, E_ϕ components along unit directions $\hat{e}_\theta, \hat{e}_\phi$. As long as the angles are properly recorded, complete spherical coverage can be realized. At any angular point within the coverage, the components of both pairs are defined orthogonal, but like the curvature of longitudinal spherical lines viewing a global sphere, or their projection on a plane surface, there is an

increasing rotation of one pair with respect to the other with increasing (or decreasing) latitude as the longitude is changed. The affect and the transform that accounts for this rotation and distortion is then equivalent to the polarization representation proposed by the third of Ludwig's alternative representations.

Ludwig [2] in a classic paper of only four pages in a transactions communication note more than 30 years ago, Roy and Shafai [3], and Knittel [4] have defined co-polarized and cross-polarized components in a manner that better resolves the ambiguity in the IEEE definition. Among many possibilities, Ludwig's third variant that defines the components in a manner equivalent to those measured on an antenna pattern range using an elevation over azimuth mount, is widely accepted, provided a single linearly polarized illuminator is first aligned with the antenna under test at azimuth = elevation = 0° . This assures that *in this direction* the fields from a dual orthogonal-port antenna are properly defined co-pol and cross-pol. Then, with successive azimuth ϕ angle cuts, each at a different fixed elevation angle θ , the fields are measured along the \hat{e}_θ and \hat{e}_ϕ directions.

Figure 16(a) illustrates two dipoles, the longer of which, along the OY axis, represents a co-polarized component, and the smaller, along the OX axis represents the cross-polarized component.

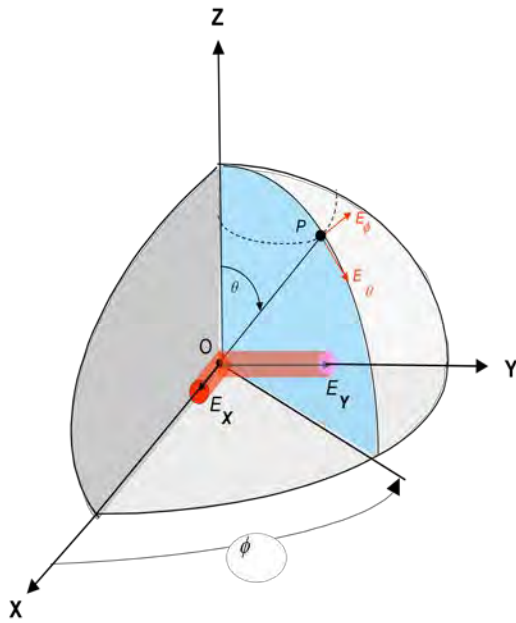


Fig. 16(a) – Dipole fields E_x , E_y and their equivalent polar components E_θ , E_ϕ .

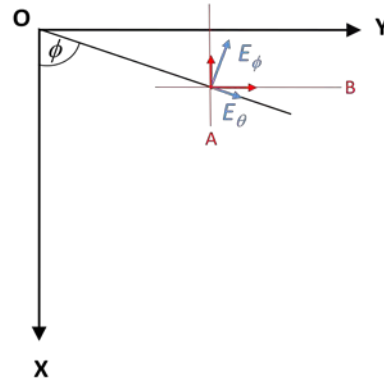


Fig. 16(b) – Rotation of the component fields, E_θ , E_ϕ , relative to the azimuth angle, ϕ .

Along a line-of-sight direction, OP, their spherical basis fields, (E_θ, E_ϕ) would be measured. These same fields are shown in Fig. 16(b) with an added rectilinear coordinate pair A and B. The components along these coordinates is a function of angle ϕ :

$$\begin{bmatrix} E_B \\ E_A \end{bmatrix} = \begin{bmatrix} \sin \phi & \cos \phi \\ \cos \phi & -\sin \phi \end{bmatrix} \cdot \begin{bmatrix} E_\theta \\ E_\phi \end{bmatrix} \quad (55)$$

Then, since the co-polar and cross-polarized components were defined along the OY and OX axes, their equivalence and thereby the Ludwig-3 components are then:

$$\begin{bmatrix} E_{co-pol} \\ E_{cross-pol} \end{bmatrix} = \begin{bmatrix} \sin \phi & \cos \phi \\ \cos \phi & -\sin \phi \end{bmatrix} \cdot \begin{bmatrix} E_\theta \\ E_\phi \end{bmatrix}. \quad (56)$$

This result is followed by the rotational transform of the measured components along the unit vector directions $\hat{e}_\theta, \hat{e}_\phi$. Of course, the same result can be realized by an equivalent rotation of the measurement probe polarization during pattern measurements, as suggested by Maters and Gregson [5]. A similar measurement rotation approach was also described by Roy and Shafai [4].

5. PHASED ARRAYS

Phased arrays consist of numerous elemental radiators in a pattern matrix on a surface that is usually planar, but can be occasionally cylindrical. Control of their amplitude and phase excitations then enable beam formation and direction within a large azimuth elevation region using a physically immovable structure. Versatility and responsiveness are its main advantages, but complexity and matrix structure are its main disadvantages. Elements can consist of single or multiple polarized dipoles, slots or waveguides and individually connected to signal sources or receivers, or by interconnection through multiple sub-apertures. The wide angular coverage of each radiator or subaperture provides the signal coverage that is generally complex weighted to provide the required pattern control. In terms of polarization performance, array design always encounters the distortion shown in Fig. 6, since beam formation must involve these off-axis characteristics of its constituent elements.

5.1 Angle between E-fields: The Geometric Effect

When the antenna array plane is fixed, but its collimated beam is directed over a wide coverage volume, polarization control requires appropriate weighting of the element pairs. Usually these are vertically and horizontally polarized and accurately orthogonal aligned, one with the other. Two factors need to be considered, the elements cross-polarization characteristics and the spatial angular relationship between their radiated (or received) fields in the beam direction. Consider the cross-pol level of a single dual linearly polarized element within a matched array or array port. Examine the far field in a direction normal to the array. For vertical excitation, the ratio of measured horizontal to vertical polarization then represents the cross-polarization characteristics of that element. On reception, the signal from a vertically polarized source also results in a small horizontally polarized signal. Like the rod antenna in Fig. 6, the E-field polarization from the (only) port of the rod antenna deteriorated at angles outside the rod's axis. For a phased array, this is likened to a distortion in the matrix structure.

A simple illustration of a representative array rectangular matrix grid shows this distortion and is readily interpreted as an angular change between the fields of its linear "elements." Shown from the same distance, the square grid in the left photo in Fig. 17 is distorted and their angular orientations changed as shown in the illustration at the right of the same grid portrayed at 45° azimuth and 30° elevation. Of course, photos, while serving to illustrate the effect described, are also subject to some degree of approximation that may concern the purists among us. In an exact case, i.e., without the camera view, the polarization target plane is normal to this LOS and the angle between orthogonally polarized "elements" can be readily calculated. But a photo, taken from any finite distance shows a range-dependent distortion; parallel lines do not appear exactly parallel. (Recall the "vanishing point" used in artistic renditions.) The

variability of this effect can be shown analytically by replacing the camera “lens” with a pinhole in an opaque plane through which all rays from an element points must pass. Their intersection with another distant parallel plane then provides the element “image” at that distance that also enables a simple calculation of the angles between lines. Of course these “images” on that plane are inverted, but has no effect on the results, which disclose that only image portions at the center are undistorted. Other parts show a range dependent distortion. For the elevation of 30° and an azimuth of 45° and distance used in this figure, a correct result should have been 63.43° , but actual measured angles of the photo print varied within 63° to 70° .

Problematic of phased arrays, element phasing can optimize beam gain in a given direction, albeit lessened by the reduced projected aperture area. But full accounting of the beams polarized components directions must also account for this geometric distortion. This effect is commonly experienced and not very different than looking at a room ceiling corner from various angles. Its correction is especially important in the control of the polarization characteristics of phased arrays because, as noted earlier, their beams are not confined to their plane normal. The solution involves the *availability and control of two signal ports*. Typically, although not essential, these may be aligned with the X-Y axes as shown by the dipole elements in Fig. 18.

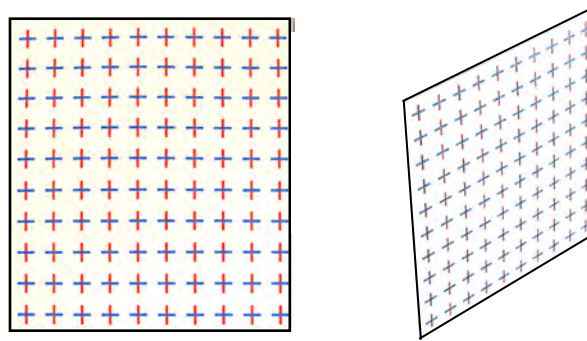


Fig. 17 –Two illustrations of a representative phased array grid of vertical and horizontal polarized elements viewed in a direction orthogonal to the aperture plane (left) and at 45° azimuth, 30° elevation (right).

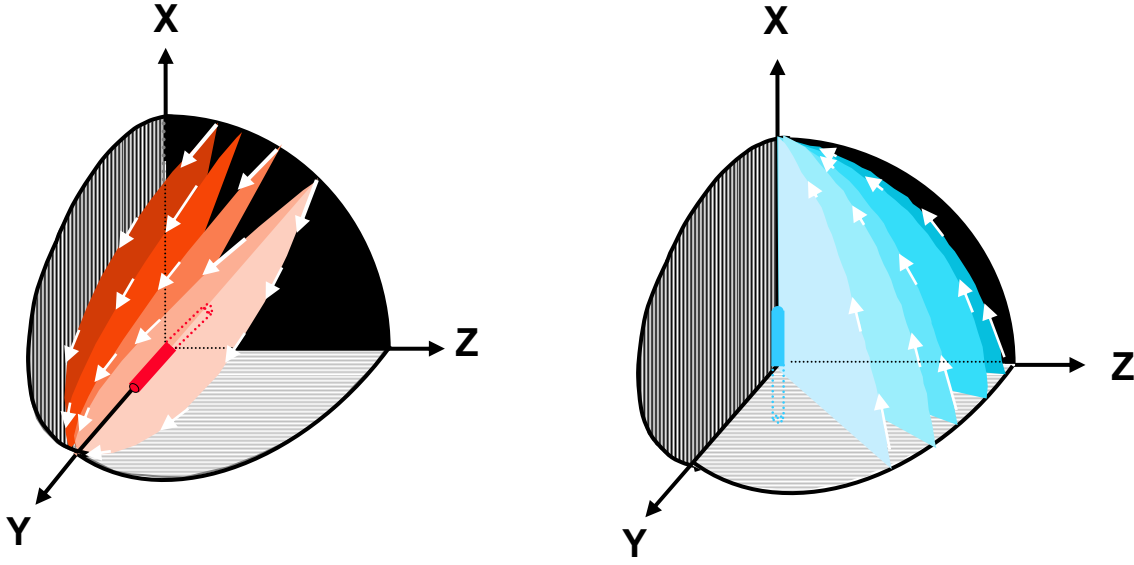


Fig. 18 – Fields from horizontal and vertical dipole elements are within planes parallel to the element axes.

Along a line-of-sight defined by a specific azimuth and elevation angle, the planes of an element fields intersect at an angle, ξ , as shown in Fig. 19. If the line-of-sight is normal to the AOB plane, then the planes of these fields intersect at 90° . For a circularly polarized performance benchmark, equal amplitude excitation with a 90° phase difference provides purely circular polarization along the OZ direction. At other angles, the circularity rapidly deteriorates. Their polarization planes, AOP and BOP, intersect at a point “P” along the line-of-sight direction. The angle ξ represents the angle between the two field vectors in a plane normal to the line-of-sight or, equivalently the angle between the two polarization planes. Then, assuming the fields around their respective axes are sufficiently omnidirectional, their magnitudes and phases can be observed over wide angular elevation and azimuth angles. (Although only a dipole pair is illustrated, in terms of polarization analyses this dipole pair can also represent the orthogonal ports of an entire phased array.)

Angle ξ is also the same as the angle between the normals of their polarization planes, so that the required field angle can be determined by calculating the angle between these plane normals. Assuming a unit radius sphere, the Cartesian coordinates of points defining these planes are:

$$P(x, y, z) = (\cos E \sin A, \sin E, \cos E \cos A), \quad (57a)$$

$$A(x, y, z) = (1, 0, 0), \quad (57b)$$

$$B(x, y, z) = (0, 1, 0), \quad (57c)$$

and

$$O(x, y, z) = (0, 0, 0). \quad (57d)$$

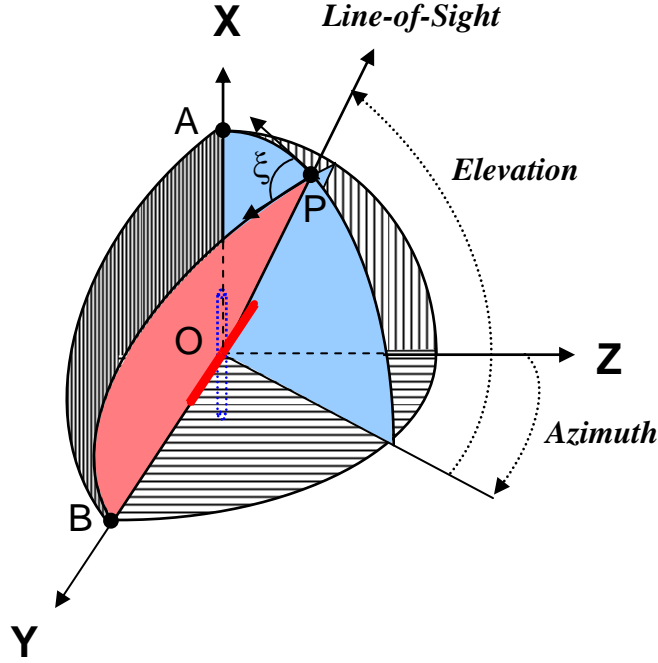


Fig. 19 –Line-of-sight azimuth and elevation angles from a dipole pair aligned with the X – Y axes.

Defining unit vectors along the X, Y, and Z axes by $\hat{e}_x, \hat{e}_y, \hat{e}_z$, the determinant form of the vector equations defining planes AOP and BOP are then

$$AOP: \begin{vmatrix} \hat{e}_x & \hat{e}_y & \hat{e}_z & 1 \\ 1 & 0 & 0 & 1 \\ 0 & 0 & 0 & 1 \\ \cos E \sin A & \sin E & \cos E \cos A & 1 \end{vmatrix} = 0 \quad (58)$$

and

$$BOP: \begin{vmatrix} \hat{e}_x & \hat{e}_y & \hat{e}_z & 1 \\ 0 & 1 & 0 & 1 \\ 0 & 0 & 0 & 1 \\ \cos E \sin A & \sin E & \cos E \cos A & 1 \end{vmatrix} = 0. \quad (59)$$

The angle ξ between the normals to these planes is given by:

$$\cos \xi = \frac{\vec{F} \cdot \vec{Q}}{\|\vec{F}\| \cdot \|\vec{Q}\|}, \quad (60)$$

in which \vec{F} and \vec{Q} are the vectors defining planes AOP and BOP , respectively. Completing the solutions to Eqs. (57, 58, 59, 60), the angle between the two planes is given simply by:

$$\cot \xi = \tan A \sin E. \quad (61)$$

This equation is plotted in Fig. 20 for several constant field angle values. It illustrates, for example, that for an array beam steered angle of 45° azimuth and 15° elevation, the angle between the field components, due to geometry alone, is nearly 15° less than the 90° at broadside. Near a typical phased array scan limit of 60° azimuth, 60° elevation, the angle between the E-fields of the orthogonal elements, or equivalent array ports, is less than 40° . This doesn't preclude radiating a purely circular polarization by properly phasing the elements, but the penalty is the reduction in power.

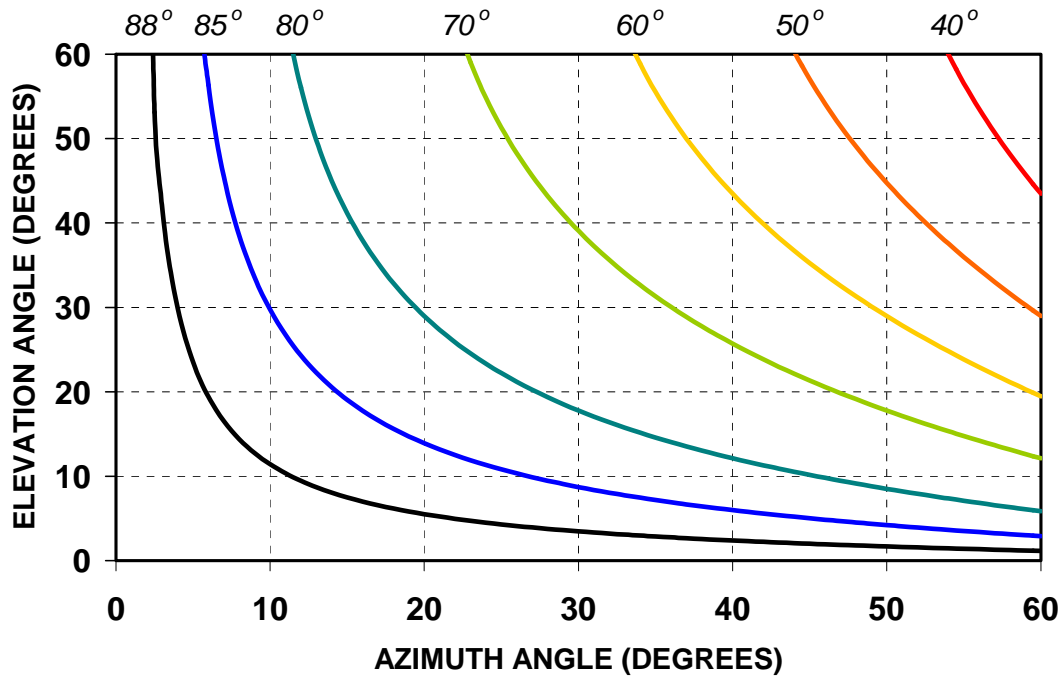


Fig. 20 – Angle (ξ) between vertical and horizontal field components as a function of azimuth and elevation relative to the plane of the elements.

Equation (61) described the angle between the E_x and E_y field vectors in the LOS plane in terms of spherical coordinate angles ($\theta = A_z$) and ($\phi = E_L$). However, an equivalently alternative representation in terms of angles α, γ is illustrated in Fig. 21. It describes the fields along the slant plane shown in the

figure. These planes also correspond to the IEEE definition (#2.193) of intercardinal planes, although the single one at $\gamma = 45^\circ$ is the one most referred. Their relationship at any point $P(x, y, z)$, is readily shown.

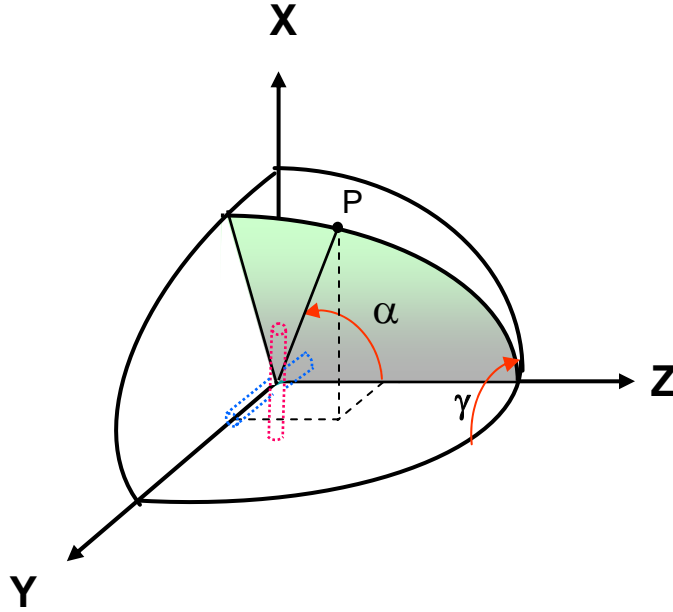


Fig. 21 – Components of a vector \overrightarrow{OP} defined by angles α, γ

The components of the vector \overrightarrow{OP} in terms of each of the two reference angles are in spherical coordinates:

$$x = \sin \phi \quad (62a)$$

$$y = \cos \phi \sin \theta \quad (62b)$$

$$z = \cos \phi \cos \theta \quad (62c)$$

In slant plane coordinates:

$$x = \sin \alpha \sin \gamma \quad (63a)$$

$$y = \sin \alpha \cos \gamma \quad (63b)$$

$$z = \cos \alpha \quad (63c)$$

Since these represent the same components of the vector, Eq. (61) can be defined:

$$\cot \xi = \frac{\sin^2 \alpha \sin 2\gamma}{2 \cos \alpha} \quad (64)$$

Figure 22 illustrates the substantial change in this spatial angle within the intercardinal plane.

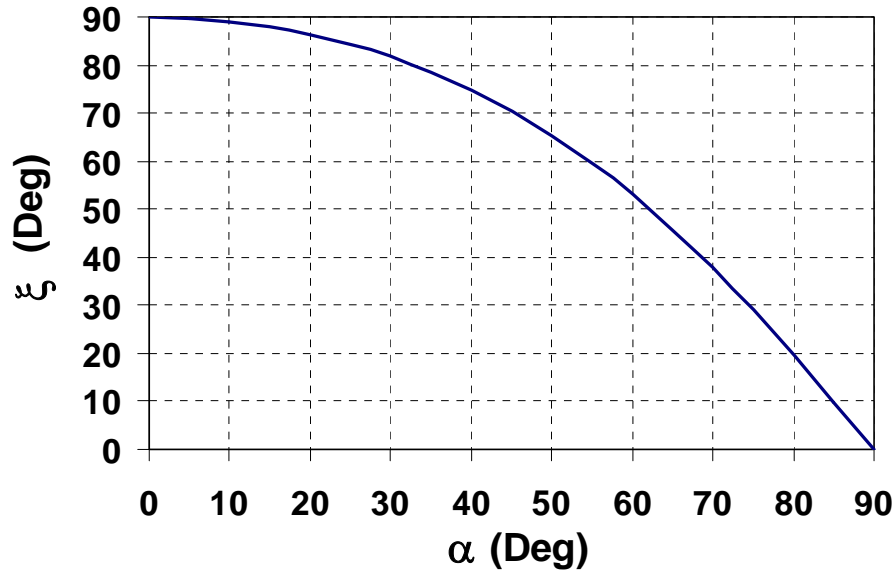


Fig. 22 – Geometric effect; the variation of the spatial angle ξ between fields in the LOS plane defined by a scan angle α for an intercardinal angle, $\gamma = 45^\circ$.

The spatial field angular relationship is a matter of geometric projection of the component fields. Excite both V- and H- ports and measure the spatial angle between the radiated fields as a function of observation angle. When the direction is normal to the array plane, the spatial angle between the two fields is 90° . However, as the direction of observation is changed, the spatial angle between the two fields decreases.

When the observation angle is $60^\circ \times 60^\circ$ with respect to the array normal, the calculated spatial angle is only about (less than) 40° . A compensation for this angular change can be made when it is required that a specified polarization be radiated in this direction. For example, if purely right or purely left circular polarization is required, the two ports would need to be driven by equal amplitude signals that differed in phase by $180^\circ \pm 40^\circ$. (Normal to the array, when the spatial angle between two exciting fields is 90° , the circular polarization requirement is met with the familiar phase shift values of $\pm 90^\circ$.) In a similar manner, the compensation for generating a specifically oriented linear polarization in a specified direction can be determined in terms of an excitation ratio of two equal-phased signals.

Figure 5 illustrated the relationship between axial ratio and the cross-polarization of a wave expressed in terms of equivalent circularly polarized components. Eq. (61) defined an effective geometric angle ξ in terms of a line-of-sight defined by azimuth and elevation angles. Except for quadrature phased equal amplitude components when $A_z = 0^\circ$, the result for an inter-cardinal scan effectively define elliptically polarized waves with varying axial ratios. Figure 23 illustrates the distinct differences in the axial ratio due to the angular change, ξ . The larger the axial ratio, the more elliptical the polarization is. The effect not unlike the changes shown in Fig. 6, clearly show the importance of compensation at the element or sub-array level, if consistent polarized performance is to be maintained.

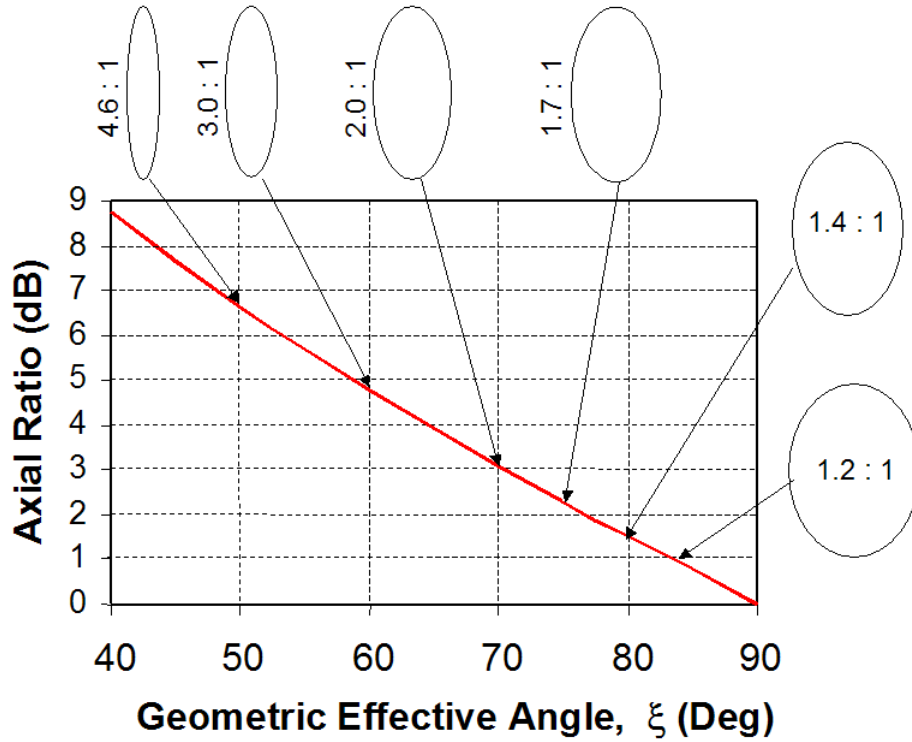


Fig. 23 –Axial ratio and circularity as a function of ξ

5.2 Combining Signals from Dual-Polarized Elements

In this analysis, no restriction is placed on their relative values, so it applies equally to a single element pair or the dual ports of combined elements of an array or subarray. Although appropriate phase and amplitude weighting is required, neither axes orthogonality nor in the case of many types of phased array elements, is phase center coincidence conditional. The phase centers need not be actually coincident, but these as well as axes orthogonality will impact the “*polarization bandwidth*.” This is defined in Section 7 as the signal bandwidth within which a prescribed level of cross-polarization is maintained or exceeded for a fixed set of amplitude and phase weights. By example, the goal here is circularly polarized purity, but any other requirement can be similarly met. Generally some form of phase compensation will be required and it is important to keep in mind that phase realized components or a computer algorithm is distinct from a phase factor ($\beta d = 2\pi/\lambda \cdot d$) due to a physical length “ d .” The conditional wavelength dependent equivalence represents a paradox that can lead to errors. Assuming equal amplitude components, their phase relationship *must* differ by 90° . For widest bandwidth this means a wavelength independent 90° . A line length d is unacceptable, as may be an algorithm such as CORDIC.

Figure 24 illustrates two complex scalar fields, $E_1 e^{j\phi_1}$ and $E_2 e^{j\phi_2}$, components of two linear orthogonal reference vectors (\hat{e}_x, \hat{e}_y). In order to include the geometric effect described previously, assume that their physical angular orientation with respect to the Y-axis is ξ_1 and ξ_2 . As a result, neither

spatial nor signal orthogonality is assumed. An appropriate performance measure is the cross-polarization of a circularly polarized wave and this parameter is used here and elsewhere in the analyses.

The respective scalar field components to be combined are

$$E_X = (E_1 \cos \xi_1 \cos \phi_1 + E_2 \sin \xi_2 \cos \phi_2) + j(E_1 \sin \xi_1 \sin \phi_1 + E_2 \sin \xi_2 \sin \phi_2), \quad (65)$$

$$E_Y = (E_1 \sin \xi_1 \cos \phi_1 + E_2 \cos \xi_2 \cos \phi_2) + j(E_1 \cos \xi_1 \sin \phi_1 + E_2 \cos \xi_2 \sin \phi_2). \quad (66)$$

The relationship between the scalar components and the equivalent circularly polarized components in terms of the unit vectors (\hat{e}_R, \hat{e}_L) , assuming the case for transmission, is, from Eq. (11):

$$\begin{bmatrix} E_R \\ E_L \end{bmatrix} = \frac{1}{\sqrt{2}} \begin{bmatrix} 1 & j \\ 1 & -j \end{bmatrix} \bullet \begin{bmatrix} E_X \\ E_Y \end{bmatrix}. \quad (11)$$

Substituting Eqs. (65) and (66) into Eq. (11), the equivalent circularly polarized components are

$$|E_R| = \sqrt{\frac{E_1^2 + E_2^2 + 2E_1E_2 \cos[(\xi_1 - \xi_2) - (\phi_1 - \phi_2)]}{2}}, \quad (67)$$

$$|E_L| = \sqrt{\frac{E_1^2 + E_2^2 + 2E_1E_2 \cos[(\xi_1 - \xi_2) + (\phi_1 - \phi_2)]}{2}}. \quad (68)$$

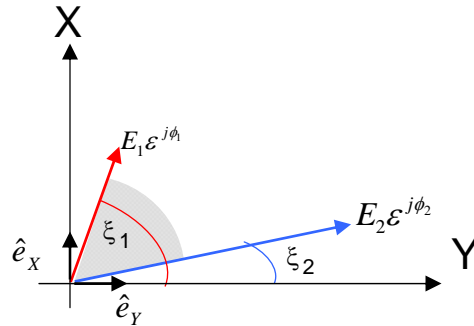


Fig. 24 – Location of two complex E-field components relative to orthogonal X – Y axes.

An appropriate measure of the circularity of the field derived by combining two linearly polarized waves is simply the ratio of its equivalent circularly polarized components, as expressed in Eqs. (67) and (68). It conveniently describes its circularity, and the decibel value also measures its conformity with SATCOM “dual-use” requirements, typically –25 dB to –30 dB. Expressing the ratio of the two component amplitudes by $r = E_1/E_2$ and the physical angle and phase difference respectively by ξ and δ :

$$\left| \frac{E_R}{E_L} \right| = \sqrt{\frac{r^2 + 2r \cos(\xi - \delta) + 1}{r^2 + 2r \cos(\xi + \delta) + 1}}. \quad (69)$$

This form agrees with the general notion that a purely circularly polarized wave results by combining two equal spatially orthogonal linearly polarized components that differ in phase by 90° . The cosine argument of these expressions also indicates that the physical angle between the two linearly polarized components is combined with the phase difference between these components. Therefore *spatial non-orthogonality due to the geometric effect*, i.e., $\xi \neq 90^\circ$, can be offset by adjusting the component phases. This fact is important and provides the means by which a dual-polarized phased array can maintain good circularity throughout its scan volume. But the price to be paid is the gain loss associated with the rebalancing of the component amplitudes that accompanies this compensation.

The results using Eq. (69), plotted over a narrow range of phase and amplitude ratio values, assuming $\xi = 90^\circ$, are shown in Fig. 25.

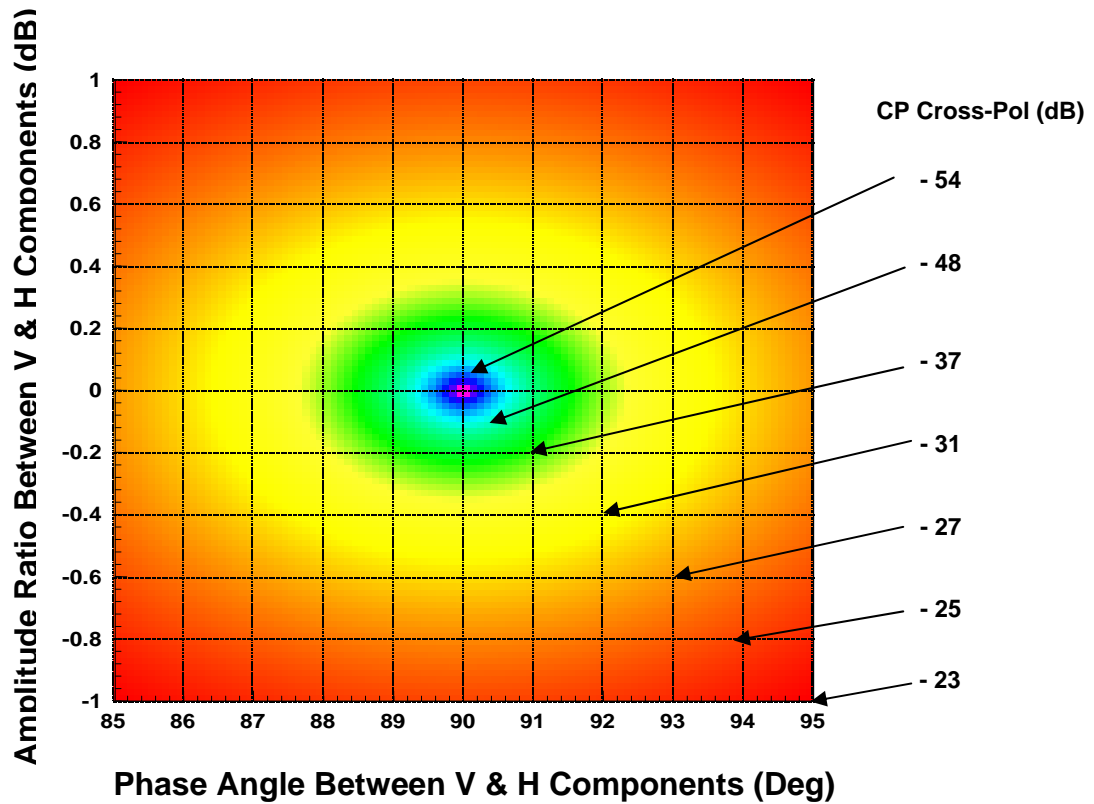


Fig. 25 – Circular cross-pol, by combining linear polarization components

For other angles, the results can be closely represented by linear translations to a point about the changed null point in the figure center. Good cross-polarization performance for a benchmark *circular polarization* or to meet any other specification requires tight control of the basis components amplitudes and phases that are combined. This is readily accomplished by controlling the combined amplitude and

phase of a dual-pol element or array antenna ports. The combination of coherent signals from *both* of the element terminals or the combined array ports is then required to maintain one field with low cross-polarization. Of course, when signals are received and the components noise figures set to satisfactory levels, the same signals can be combined in multiple ways to meet multifunction operation requirements. These may include any or all of the required surveillance, tracking, ID, and EW functions.

5.3 Cross-polarization and Parameter Precision

Within the combining networks, precision in both amplitude and phase are important, but each impacts the cross-polarization differently. Figure 26 shows axial ratio between the right and left circularly polarized components as a function of the two linearly polarized fields that are combined with the phase required to maximize this ratio. The two curves, for geometric effect angles $\xi = 35^\circ$ and $\xi = 90^\circ$, are the typical limits within the scan volume of a phased array, defined by Eq. (61) for $A_Z = E_L = 60^\circ$, or 0° . Assuming good circularity is required, the performance deteriorates with just a little amplitude imbalance, so careful control will generally be required. For a representative dual-use circular cross-pol goal of -25 dB, linear components must be balanced to about $\frac{3}{4}$ dB.

In Fig. 27, the same ordinate and abscissa plot the result of phase error; each of the plots represents an error of just one degree in phase from the optimum value given by $\delta = (180^\circ - \xi)$. Comparing these two results, amplitude errors affect the cross-polarization to a greater degree than phase errors. This can impact any tradeoff between numbers of bits in amplitude and phase precision necessary to maintain or exceed a specific cross-polarization level.

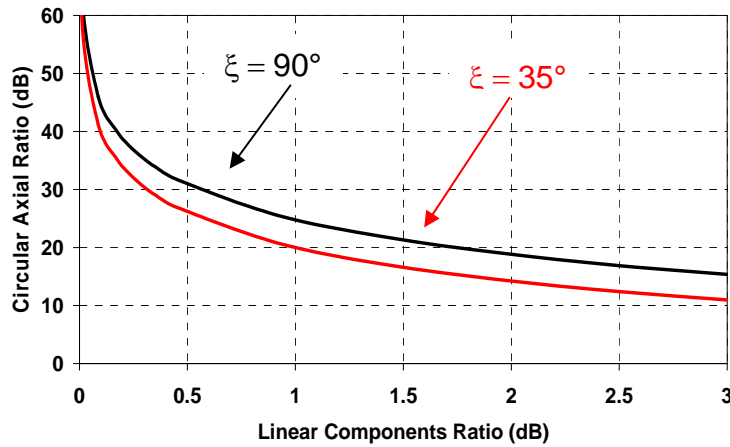


Fig. 26 – Maximum ratio of circularly polarized components by combining linearly polarized components within the scan volume of a typical phased array.

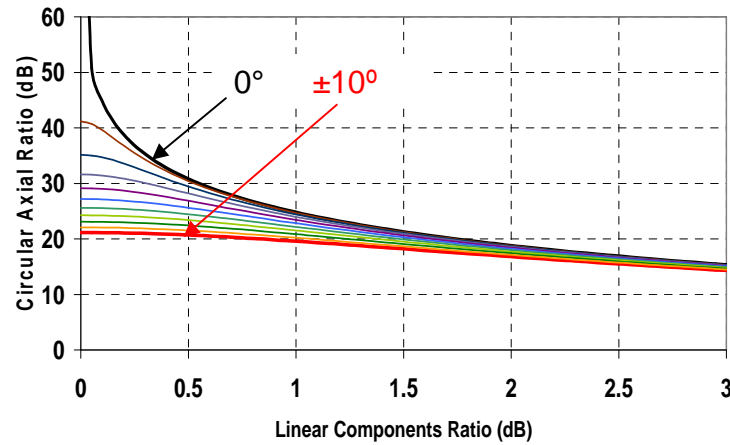


Fig. 27 – Circular components ratio combining linear components with various phase errors. Phase errors shown in 1° increments.

From Fig. 27, it is observed that when the two combining amplitudes are equal, i.e., their linear components ratio equals 0 dB, the circularly polarized axial ratio is very large, but with one linear component reduced to half the other, the circular components axial ratio is reduced to 10 to 15 dB. From Fig. 28 a similar reduction occurs, but is less sensitive to phase errors.

The loss of the *purely* circular polarized field when the two equal linearly polarized field components are optimally combined is illustrated in Fig. 28. Using Eq. (68) with $r = 1$, changing δ results in this optimization within the limits of ξ shown. Although the cross-pol level is zero, the optimization results in significant co-pol loss. Effectively, this loss is due to the geometric effect alone. Regardless of the geometric effect angle, assuming $r = 1$, a compensating phase, δ , will result in a purely circularly polarized wave. But the penalty is a loss in this wave. Of course, for an array, this loss is in addition to the scan loss due to the effective aperture loss with scan.

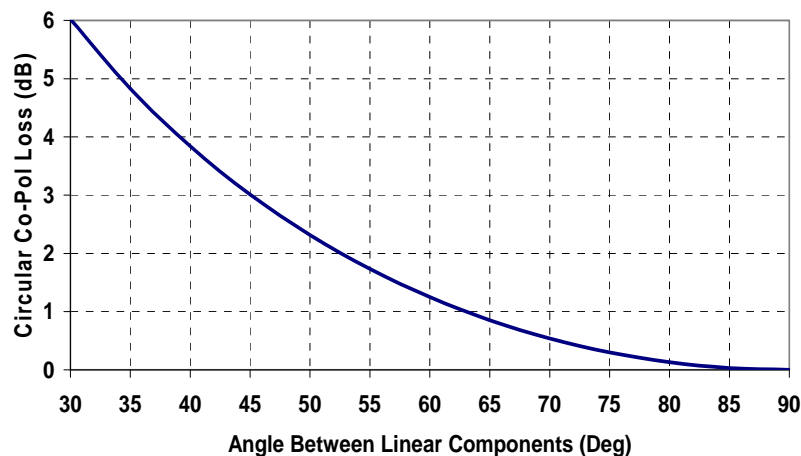


Fig. 28 – Circular polarization loss, with two equal amplitude vertical and horizontal polarized components combined, as a function of the geometric effect angle, ξ .

A representative problem involves determining the parameters and losses associated with phase compensation of imperfect vertical and horizontal polarized elements to generate (or receive) circular polarization. Performance quality is a function of two factors, the cross-polarization of the elements and the signal power division or other amplitude difference between the element polarizations. Establishing and maintaining pure circular polarization (RCP or LCP) requires balancing both amplitudes and phases of the element radiating (or receiving) signals throughout the angular lines-of-sight of interest. Using a combination of vertical and horizontal polarized elements, Eq. (69) conveyed the requirements in which ξ is the physical angle between E_V and E_H when projected on a plane orthogonal to the line-of-sight and the applied phase, δ = phase between E_V and E_H , with a specific amplitude ratio, r . Irrespective of that ratio, the phase shift that compensates the geometric effect represented by ξ , as shown in Fig. 19, can be expressed in terms of an optimization problem for the ratio $|E_R/E_L|$. Figure 29 shows some results of that optimization in terms of that ratio. These curves bound most lines-of-sight of interest and illustrate that a proper combination of angles ξ and δ enables compensation of the “geometric effect” using phase shift alone. Regardless of “ r ,” optimum circularity (lowest cross-pol) results when $(\xi + \delta) \approx 180^\circ$. But the *best* circularity also requires good amplitude balance, for which phase is ineffective. A further accounting must also include the cross-polarization levels of the elements. Signal input to the vertical port of a dual-polarized element results in a small horizontally polarized component.

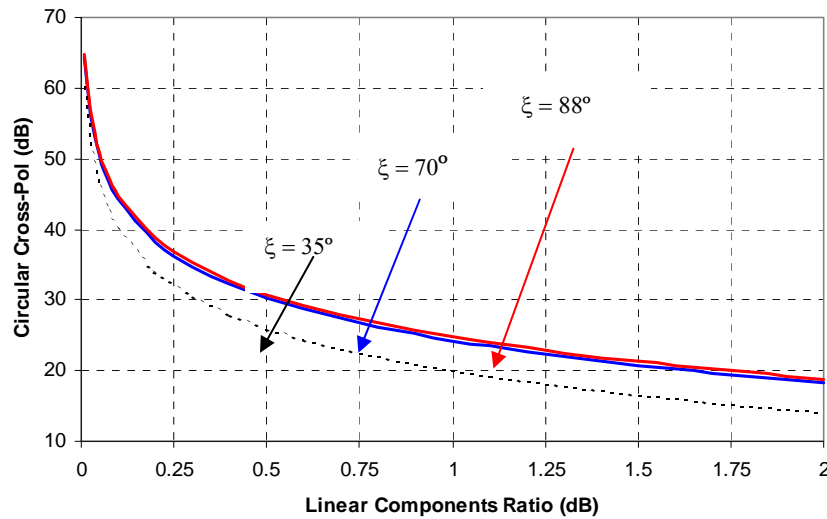


Fig. 29 – Optimized circular cross-pol level as a function of linear component ratio for geometric effect angles between 35° and 88° .

5.4 Impact of Bit Resolution on Polarization Characteristics

The parameters required to achieve and maintain a specific polarization with acceptable cross-polarization values over a wide field of view, are readily calculated. Assuming these are all implemented digitally, the actual performance will be a function of the bit accuracy of the constituent parameters, whether amplitude or phase is required. Figure 20 illustrated the substantial change in the geometric field

angle between a pair of vertical and horizontal polarized elements as a function of viewing angle requiring compensation. For circular polarization, Eq. (69) described the ratio of the circularly polarized components in terms of their linear amplitudes and phases. Assuming equal amplitudes, this ratio is

$$\frac{E_R}{E_L} = \sqrt{\frac{1 + \cos(\xi - \delta)}{1 + \cos(\xi + \delta)}}, \quad (70)$$

in which ξ and δ represent the geometric angular and component signal phase differences. Then, for purely right circular polarization, $\delta = \pi - \xi$. Clearly errors in setting δ , due to bit quantization results a finite E_L component, therefore less than infinite circular cross-polarization ratio.

In general, a number X within an interval of values $0 \leq X \leq X_{\max}$ can be divided into N binary bits, with the least significant bit (LSB) defined by

$$LSB = \frac{X_{\max}}{2^N}. \quad (71)$$

Assuming five-bits will represent the phase within a 180° phase interval, the LSB is 5.625° and the possible binary values range from $[00000] = 0^\circ$ to $[11111] = 174.375^\circ$. The required phase shift δ could be approximated by the nearest N -bit value within the interval. This too involves an approximation, the simplest of which is using either the rounded or truncated values. For example, the closest five-bit binary value for a required phase of 121.877° with $X_{\max} = 180$ is $[10101] = 118.125^\circ$. Within element spatial angles, illustrated in Fig. 20, rounding the required phase to one digit, then using this value results in a slightly better result than truncating to two digits. Using Eq. (70), Fig. 30 illustrates the cross-polarization performance with the phase quantized to four, five, six and seven bits. Five or six-bits provide good performance, however the combination of bit accuracy of both angle and amplitude need to be considered.

Numbers of bits are critical costs factors in designing antenna systems, especially in large phased array systems with large numbers of elements. For the circular polarization benchmark, Fig. 31 illustrates the poorest (highest dB level) circular cross-polarization achievable for various bit levels.

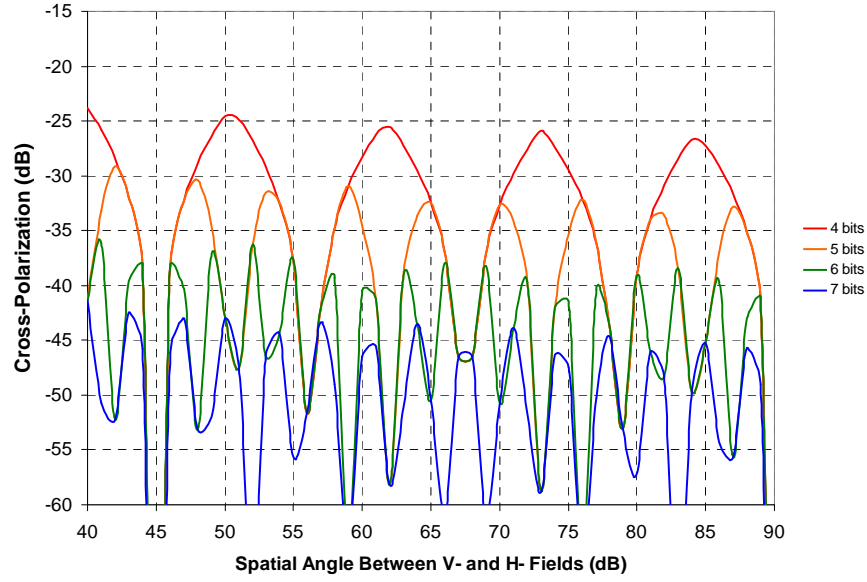


Fig. 30 – Effect of bit approximation of phase compensation angles on circular cross-polarization ratio for equal amplitude components.

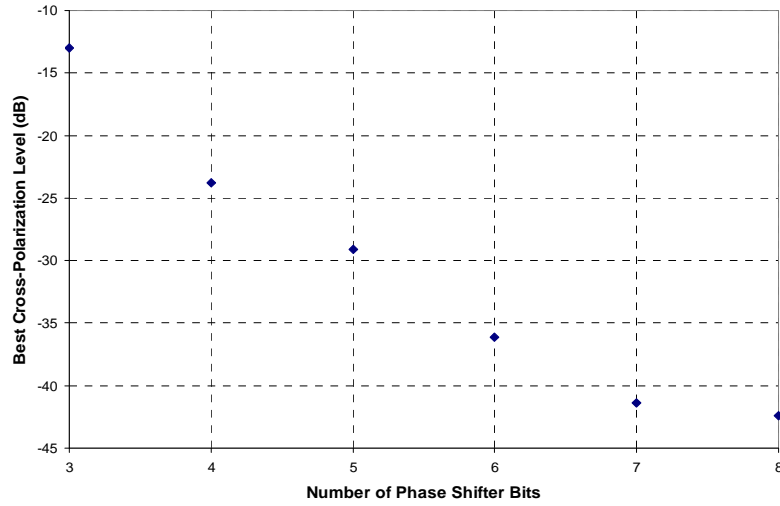


Fig. 31 – Required phase shifter bits for different ratios of circular cross-polarization.

5.5 Combining Polarization Components

The general case where the fields from both vertical and horizontal ports each have cross-polarized components associated with them is illustrated in Fig. 32. These four field components then combine and their resultant is examined in the line-of-sight plane defined by the azimuth and elevation angles shown. As before, the directions along which the fields are combined define geometric effect angle ξ . These can then be resolved in terms of their circularly polarized equivalents using Eq. (11). The components shown in the figure, correspond to the following parallel (\parallel) and cross- (\perp) polarized components: $E_{V1} = E_{\parallel}$,

$E_{H1} = E_{1\perp}$, $E_{H2} = E_{2\parallel}$, $E_{V2} = E_{2\perp}$. Assuming lossless elements, $E_{1\parallel}^2 + E_{1\perp}^2 = 1$ and $E_{2\parallel}^2 + E_{2\perp}^2 = 1$. Then, expressing the dB ratios of the co- and cross-polarized components by $\eta = 20 \log E_{\perp}/E_{\parallel}$, the four radiating components are

$$\begin{aligned} a = E_{1\parallel} &= \frac{1}{\sqrt{1 + 10^{\eta_1/10}}} & b = E_{2\perp} &= \frac{10^{\eta_2/20}}{\sqrt{1 + 10^{\eta_2/10}}} \\ c = E_{2\parallel} &= \frac{1}{\sqrt{1 + 10^{\eta_2/10}}} & d = E_{1\perp} &= \frac{10^{\eta_1/20}}{\sqrt{1 + 10^{\eta_1/10}}} \end{aligned} \quad (72)$$

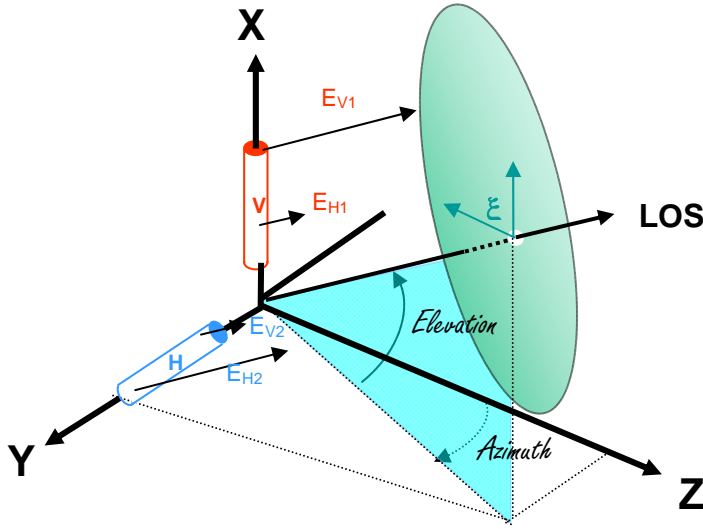


Fig. 32 – Representation of the fields from a linear dual-polarized element in a line-of-sight plane

A further factor concerns the ratio of the element drive signals. To some extent these drive signals could also account for any other amplitude imbalance between the element ports. Figure 33 accounts for this by just using a relative amplitude “k” and also adding the phase control “δ.”

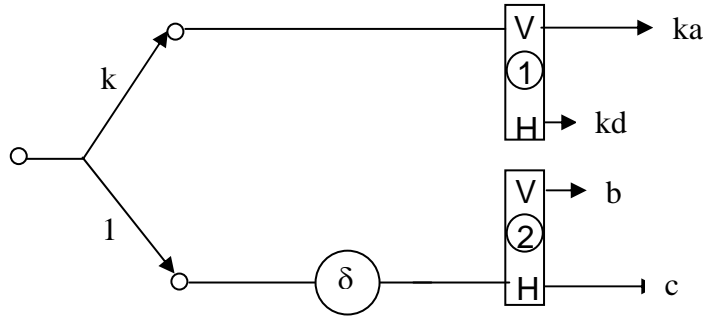


Fig. 33 – Signal excitation of a dual linearly polarized element

The resulting linearly polarized components are then

$$\begin{aligned}
 ka = E_{1\parallel} &= k \frac{1}{\sqrt{1+10^{\eta_1/10}}} & kd = E_{1\perp} &= k \frac{10^{\eta_1/20}}{\sqrt{1+10^{\eta_1/10}}} \\
 c = E_{2\parallel} &= \frac{1}{\sqrt{1+10^{\eta_2/10}}} & b = E_{2\perp} &= \frac{10^{\eta_2/20}}{\sqrt{1+10^{\eta_2/10}}}
 \end{aligned} \tag{73}$$

In terms of combining orthogonal pairs, it is seen that the polarization *direction* represented by $E_{1\perp}$ is the same as that of $E_{2\parallel}$ and that of $E_{2\perp}$ is the same as that of $E_{1\parallel}$ so their respective pairs can be combined, as long as their phase weightings and differences, either laterally or normal to their surface plane are also included. A representation of the combined fields, including these phase weightings used to control the equivalent circular polarization components is then shown in Fig. 34. The X-Y- axes are an orthogonal pair in the LOS plane illustrated in Fig. 33. The total vertical (or horizontal) component is the phase adjusted sum of the co-polarized component from element “1” (or “2”) and the cross-polarized component from element “2” (or “1”). Combining all of the component scalars, the components are:

$$E_X = (ka\varepsilon^{j\delta_1} + b\varepsilon^{j\delta_2})\sin \xi_1 + (c\varepsilon^{j\delta_2} + kd)\sin \xi_2 \tag{74}$$

$$E_Y = (ka\varepsilon^{j\delta_1} + b\varepsilon^{j\delta_2})\cos \xi_1 + (c\varepsilon^{j\delta_2} + kd)\cos \xi_2 \tag{75}$$

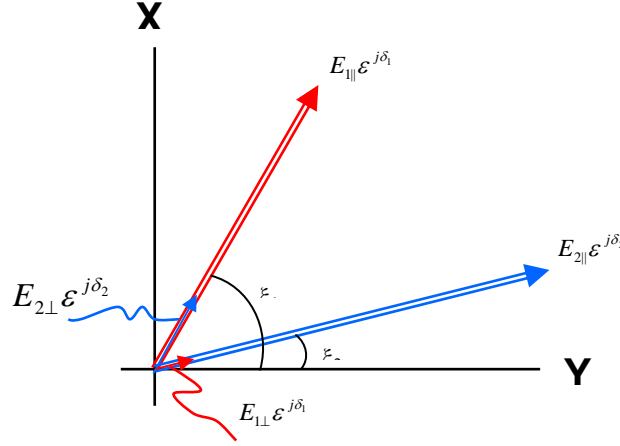


Fig. 34 – Parallel and orthogonal fields in the line-of-sight plane

Then the equivalent circular basis (transmission) components from Eq. (11) are

$$\begin{bmatrix} E_R^+ \\ E_L^+ \end{bmatrix} = \frac{1}{\sqrt{2}} \begin{bmatrix} 1 & j \\ 1 & -j \end{bmatrix} \begin{bmatrix} E_X^+ \\ E_Y^+ \end{bmatrix}. \quad (11)$$

Substituting the linear components defined by Eqs. (73, 74, 75) into this equation, the circularly polarized quality, i.e., the combinations with the least cross-polarization can be determined. Assuming specific signal divisions, k , solution for the best phase $(\delta_2 - \delta_1)$, for various geometric angles, $(\xi_2 - \xi_1)$ can be found which minimizes one of the two circularly polarized components. Clearly the various possible combinations are endless. Three groups were chosen. These use values for “ k ” of 0, -0.5, and -1 dB. Within these groups, the phase settings δ , which minimize the combined right circularly polarized component, were determined using the gradient search technique available in Excel© for 12 combinations of linearly polarized elements with prescribed cross-pol characteristics defined by η_1 and η_2 . The tabulated results are the requisite phase settings, the cross-pol ratio expressed as $|E_R/E_L|_{dB}$ and the loss in the co-pol components, E_L . The results are tabulated and printed in Appendix A. Although these results were independently calculated, all of the phase settings for the same elements defined by η_1 and η_2 are essentially identical. While the results are not shown for $\xi = 90^\circ, \delta = 90^\circ$; as expected, setting $\eta = -100$ dB essentially removed any cross-pol contributions from the elements. But cross-pol values are best (smallest value of E_R) when $k = 0$ dB, since the amplitudes of the combined components can be identical. Although the sources of the somewhat random values for $|E_R/E_L|$ are not immediately obvious, the phase contributions of element “2” polarization impact the combination component scalars in different ways. Unsurprisingly, the overall results verify the importance of elements cross-polarization characteristics and amplitude balance. With poor elements accurate phase trimming may help, but ultimately detailed parameters need to be measured and both amplitude and phase compensation included.

6. PHASE CENTER COINCIDENCE

The phase center of an orthogonal element pair consists of two distinct parts, one due to their common physical intersection and another resulting from their field excitation (or reception) points. As a result ascribing the term “coincident phase center” can be interpreted as either of the two effects or their combination.

The effective radiating center for a single notch type or Vivaldi radiator varies along the throat as a function of frequency. An orthogonal intersecting pair that is aligned at their base therefore has *identical* radiating centers at the same frequencies, so the term “common radiating center” is appropriate. Their fields viewed along angles away from their common axis also issue from a common point. Of course if the polarized elements are physically separated, their radiating centers differ, resulting in a line-of-sight angular dependent path difference. Field excitation combines the propagation time within the element and that of the circuitry to the excitation ports. Differences then introduce frequency dependence between combined ports, which ultimately constrains polarization bandwidth. A compensating line should be effective, although differences in media propagation times will impact the result.

Within the grid of array elements mechanical and electronic interconnections provide dual linearly polarized ports, which can then be combined to maintain a prescribed polarization characteristic throughout the antenna scan coverage. Line interconnections also need to account for differences in media propagation times.

Assuming the elements are physically oriented orthogonal to each other, their excitation center's can be displaced normal to the array plane, as illustrated in Fig. 35. The LOS is defined by angle α within the array plane oriented at angle γ . Except for issues concerning their individual cross-polarization characteristics, described in Section 4, any required polarization in any line-of-sight direction normal to the array plane is achievable, but *only* at a single frequency. This is due to the equivalence between a phase displacement, $\Delta\phi$, and that from a physical line length, $\Delta\phi = \beta d = (2\pi/\lambda)d$. As a result, differences in their physical phase centers constrain the bandwidth within a specified nominal value. Assuming the phase center displacement is along the OZ axis as illustrated in Fig. 35, the unequal distance, d , can be *approximately* offset by an equivalent line interconnection, assuming equivalence in propagating velocity is maintained. (Theoretically, a small uncorrectable difference between the field vectors in a plane orthogonal to the line-of-sight remains.)

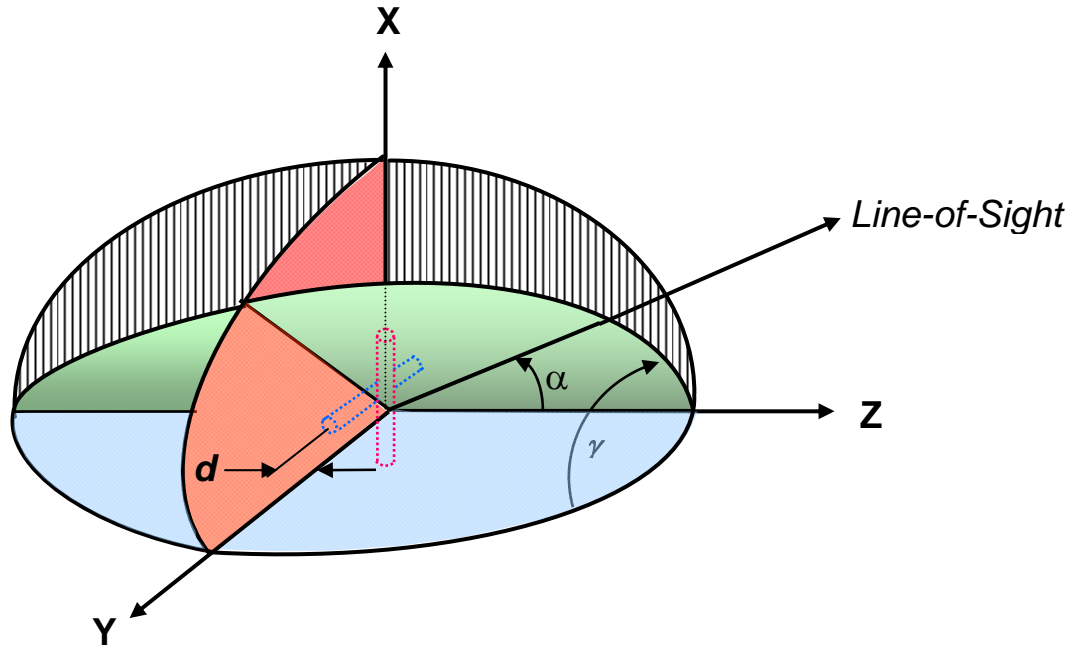


Fig. 35 – As in Fig. 21, with element phase centers displaced normal to the array plane, XOY.

In this report, polarization characteristics are described in terms of representative ideal dipole elements. These are readily visualized and served in characterizing the basic polarization characteristics of phased array elements and their combination. They are geometrically orthogonal with a common terminal drive or reception phase center point at the coordinate's origin. Among current multiple array arrays elements, the flared notch (Vivaldi) radiator is foremost. The effective radiating center of the Vivaldi element varies along its throat as a function of frequency, enabling the element alone to have wideband performance. But in combination with orthogonal Vivaldi elements, lateral displacement of their phase centers, as suggested in Fig. 36, constrains bandwidths, since any displacement results in wavelength-dependent phase differences in their combination.

This is illustrated in the array rendition in the detail representation on the right. It can be shown that the angle ξ between the two linearly polarized fields is independent of the displacement in the phase centers. Therefore, defined by the geometric effect described in Section 5.1, the angle ξ between their fields remains as given by Eq. (61) is $\cot \xi = \tan A \sin E$. The same accommodation in the element signals combination enables maintaining specific polarization parameters throughout the angular coverage of the array. However, the substantive range difference to the line-of-sight plane due to the lateral elements displacement can greatly impact the polarization bandwidth. This can be shown using the illustration in Fig. 37.

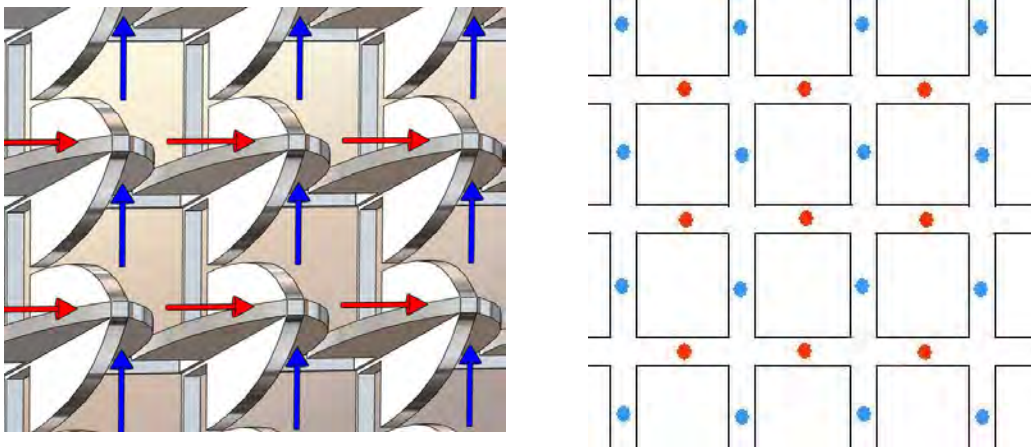


Fig. 36 – Representation of Vivaldi-type element radiators with laterally displaced phase centers. These introduce unequal phase delays in the LOS direction during scan.

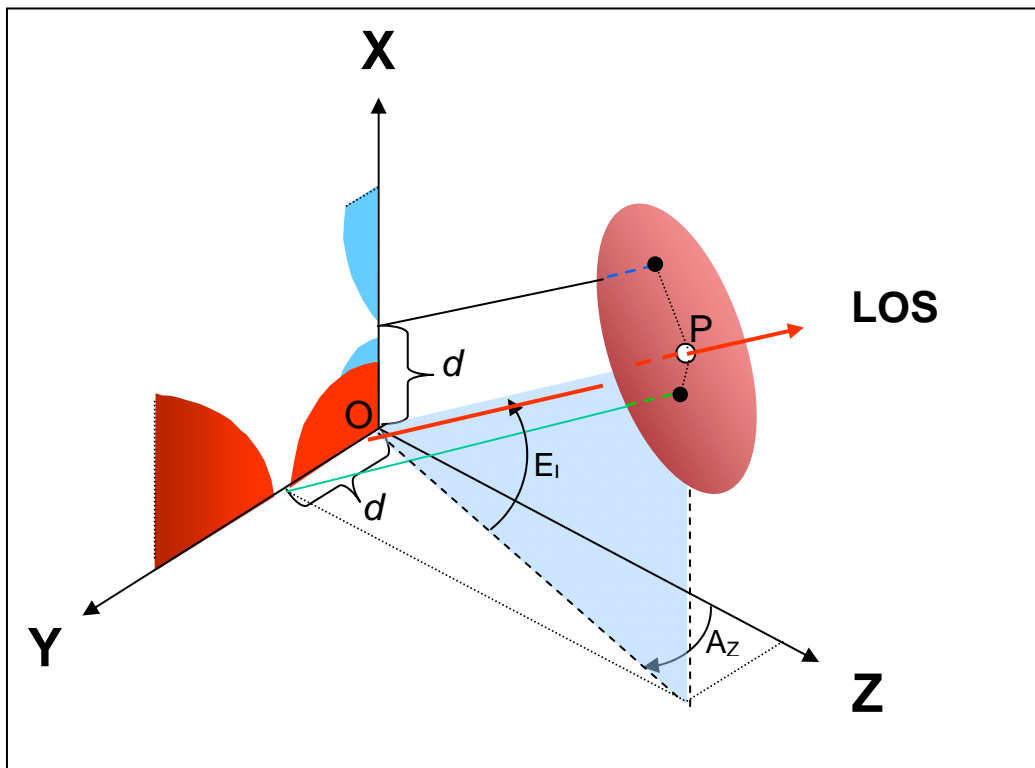


Fig. 37 – Representation of Vivaldi-type element radiators with non-coherent phase centers. Distances to a plane orthogonal to the LOS are unequal functions of azimuth and elevation.

The general equation for a plane at distance D from the origin of the X-Y-Z coordinates is $Ax + By + Cz + D = 0$. For a length $OP = 1$, point “P” is defined in terms of the azimuth and elevation angles by $P(x, y, z) = \sin E_L, \cos E_L \sin A_Z, \cos E_L \cos A_Z$. The constants A, B, C, D of the line-of-sight plane orthogonal to OP are then: $A = \sin E_L, B = \cos E_L \sin A_Z, C = \cos E_L \cos A_Z, D = -1$. The shortest distance from a point defined by coordinates (a', b', c') to the LOS plane is given by the well-known equation:

$$S = \left| \frac{a'A + b'B + c'C + D}{\sqrt{A^2 + B^2 + C^2}} \right|. \quad (76)$$

Referring to Fig. 37, the difference in lengths between the lines containing the points $(d, 0, 0)$ and $(0, d, 0)$ is then

$$\Delta S = d |\cos E_L \sin A_Z - \sin E_L|. \quad (77)$$

For a wavelength normalized separation, ΔS_λ , this is equivalent to $2\pi\Delta S_\lambda$ radians and can greatly impact both phase compensation and polarization bandwidth. Without sacrificing polarization bandwidth, the sole alternative is the design of element pairs with coincident phase centers. One more recent design, due to Pickels, Rao, Patel, and Mital [6] at NRL is conceptually illustrated in Fig. 38. In this design, improved symmetry in the two radiators and associated baluns structural layout results in no lateral or radial (axial) differences of the phase centers, thereby enabling the widest range of polarization characteristics with the widest polarization bandwidth.

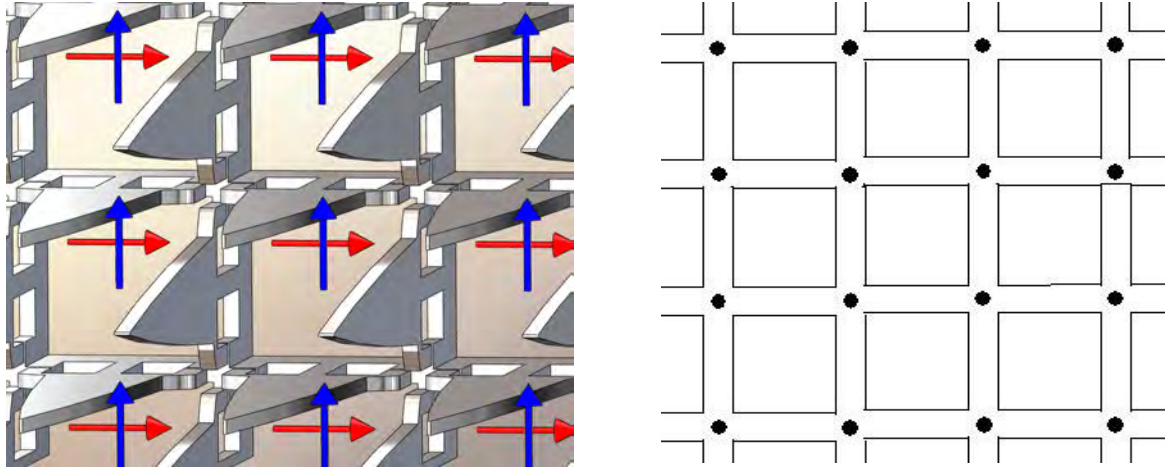


Fig. 38 – Intersecting Vivaldi linearly polarized elements designed at NRL with coincident phase centers, illustrated in the drawing at right.

7. POLARIZATION BANDWIDTH

This is defined as the maximum bandwidth within which the cross-polarized component is equal or less than a specified value. Beam steering and polarization control of a physically fixed phased array both require phase weighting of the elements. But the control processes are somewhat different. Beam steering results from appropriate element signal delays or line lengths. The familiar expression for the phase from a line length is $\ell : \theta = \beta \ell$, where $\beta = 2\pi/\lambda$, expresses the equivalence between the phase and line length, but *only* at a single wavelength. Maintaining circular polarization, for example, requires a phase difference of $\pi/4$ radians between orthogonal equal amplitude linear polarized components, regardless of the wavelength. However, unwanted wavelength dependence occurs using an equivalent line length. Wideband array steering control can benefit using coincident phase center elements together with true time delay steering, but this does not necessarily negate phase control of polarization and potential bandwidth constraints.

The phase difference for a differential length ΔS for two frequencies, f_o and f_1 is

$$(\beta_1 - \beta_o)\Delta S_o = \frac{2\pi}{c}(f_1 - f_o)\Delta S \text{ (radians),} \quad (78)$$

where “c” is the speed of light in the propagating medium. The geometric effect also impacts the combined fields radiated (or received) by the element pair. Assume that a compensating phase, δ , offsets the effects of signal path differences and noncoincident phase centers, as shown in Fig. 39.

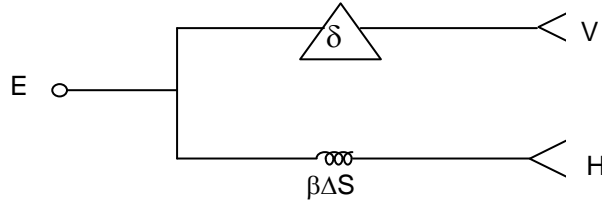


Fig. 39 – Element signal paths combining the effects of signal path differences and noncoincident phase centers $\beta\Delta S$ and the compensating phase δ .

The equivalent components along a pair of X – Y axes resulting from the combined effects of these factors and the geometric effect angle ξ are

$$E_x = \frac{E}{\sqrt{2}} \epsilon^{j\delta} + \frac{E}{\sqrt{2}} \epsilon^{j\beta\Delta S} \cos \xi, \quad (79a)$$

$$E_y = \frac{E}{\sqrt{2}} \epsilon^{j\beta\Delta S} \sin \xi. \quad (79b)$$

The equivalent right and left circularly polarized components for waves traveling away from an observer from Eq. (11) are

$$\begin{bmatrix} E_R \\ E_L \end{bmatrix} = \frac{1}{\sqrt{2}} \begin{bmatrix} 1 & j \\ 1 & -j \end{bmatrix} \cdot \begin{bmatrix} E_X \\ E_Y \end{bmatrix}. \quad (11)$$

Substituting the relevant terms, the ratio of right to left circularly polarized components is

$$\left| \frac{E_R}{E_L} \right| = \sqrt{\frac{1 + \cos(\xi + \beta\Delta S - \delta)}{1 + \cos(\xi - \beta\Delta S + \delta)}}. \quad (80)$$

A purely right circularly polarized wave at a *single frequency*, f_o , results if the left circularly polarized component is zero, which requires the compensating phase

$$\delta_o = \pi + \beta_o \Delta S - \xi. \quad (81)$$

This compensation, for any specific ξ , is exactly correct at a single frequency. The polarization of finite spectral content signals is then degraded, i.e. operating bandwidth within a prescribed cross-pol level is restricted. Defining the bandwidth in terms of frequencies normalized to a band center, f_o , the bandwidth is closely defined by:

$$\Delta B = 2 \left(\frac{f}{f_o} - 1 \right). \quad (82)$$

Applying the compensation expressed by Eq. (81) to the circular components ratio expressed by Eq. (80), the result in terms of wavelength normalized separation, ΔS_λ , is

$$\left| \frac{E_R}{E_L} \right| = \sqrt{\frac{1 - \cos(\pi \Delta B \Delta S_\lambda)}{1 - \cos(\pi \Delta B \Delta S_\lambda - 2\xi)}}. \quad (83)$$

Regardless of the source of the difference, ΔS , bandwidth defined within specific polarization parameters is a significant array design issue. The impact of path length differences, ΔS_λ in constraining polarization bandwidth is illustrated in Figs. 40 and 41 within an intercardinal scan. (The relationship between the azimuth and elevation angles and an intercardinal angle, α , in a plane defined by $\gamma = \pi/4$, as shown in Fig. 22, facilitates an understanding defining the geometric effect angle ξ , in which $\cos \xi = 2 \cos \alpha / \sin^2 \alpha$.) Dual use typically requires circular cross-pol levels of -25 dB or better within the signal spectral space, so the available bandwidth for elements spaced $\lambda/2$ apart, for example is very restrictive. Figures 42 and 43 depict the same conditions as those for Figs. 40 and 41 except the ordinates are expressed as axial ratios of the polarization ellipses.

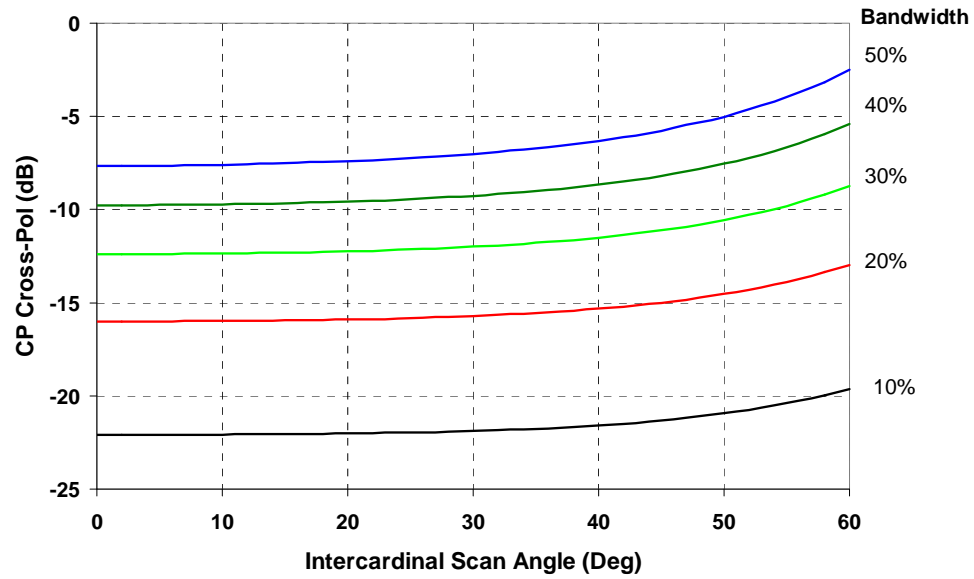


Fig. 40 – Circular cross-pol bandwidth characteristics for element centers spaced $\lambda/2$ apart.

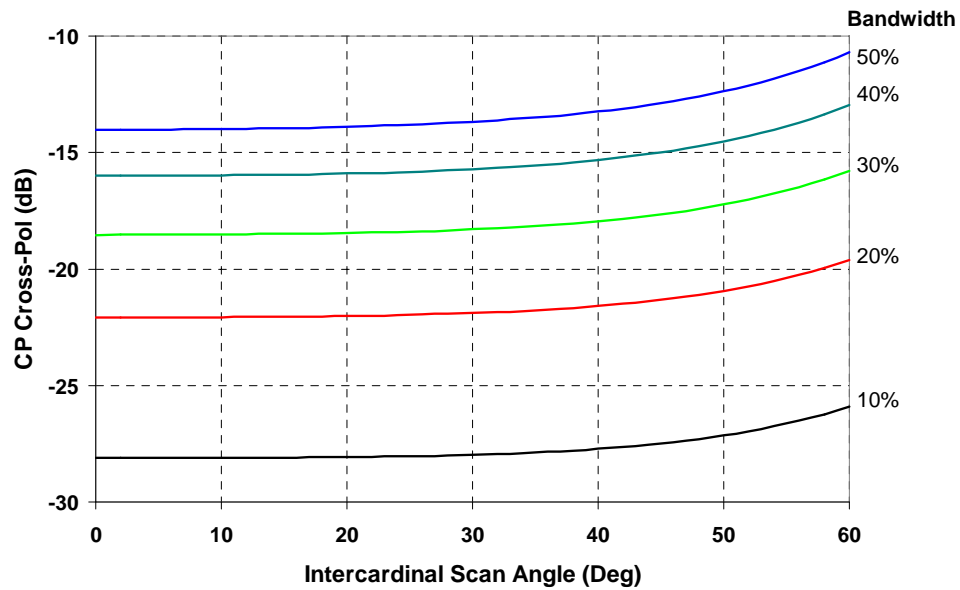


Fig. 41 – Circular cross-pol bandwidth characteristics for element centers spaced $\lambda/4$ apart.

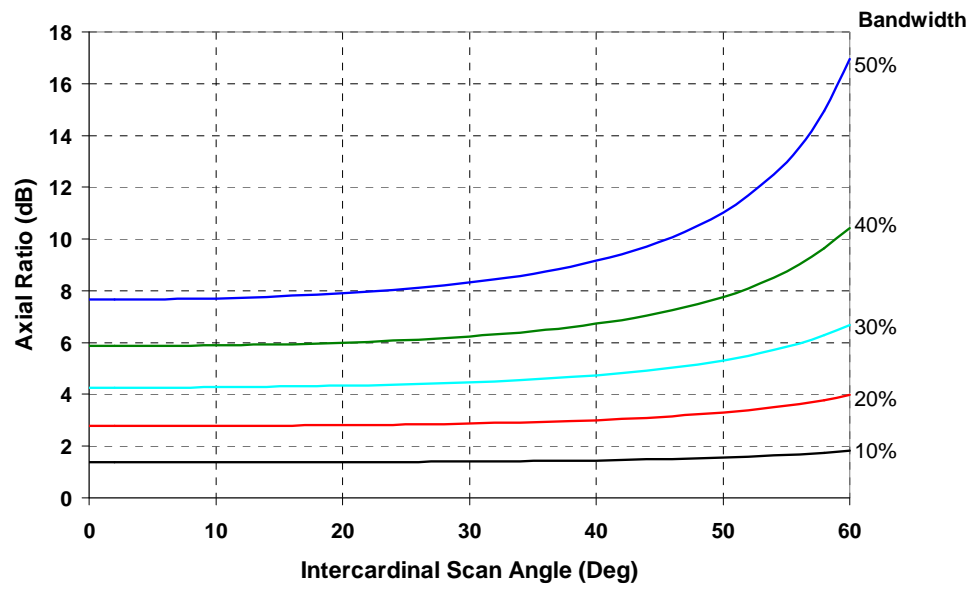


Fig. 42 – Equivalent circular cross-pol bandwidth characteristics for element centers spaced $\lambda/2$ apart.

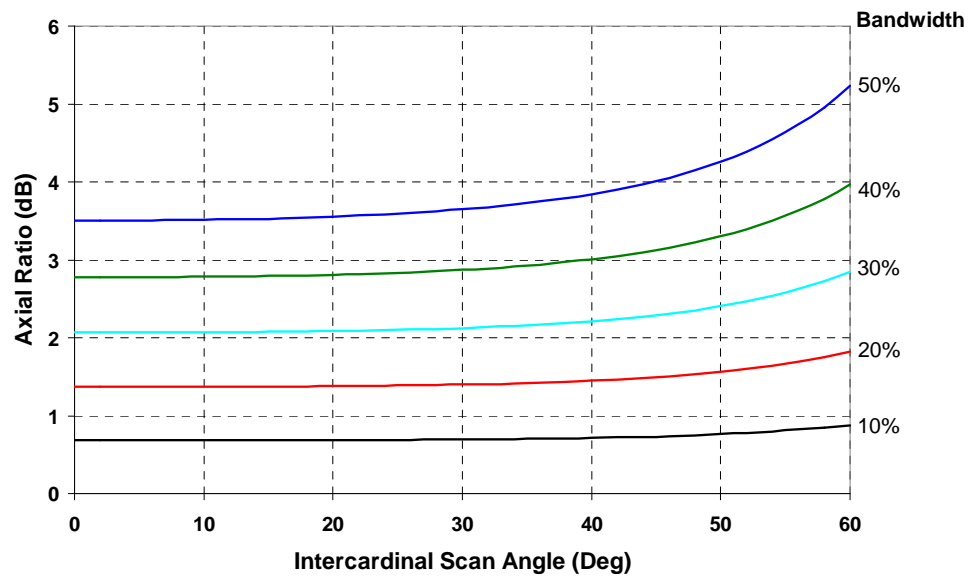


Fig. 43 – Equivalent circular cross-pol axial ratio bandwidth characteristics for element centers spaced $\lambda/2$ apart.

8. SCATTER MATRIX

The network formalism that relates network output versus network input carries over to the relationship between radar target polarization illumination and the target polarization backscatter in the form of the scatter matrix. In this case the target functions as a transformer of a polarized transmitted incident wave to a reflecting polarized wave impinging on the receiving antenna. The utility of the scatter matrix for use in matching, rejecting or identifying a target requires that its characteristics be described in terms of known basis coordinates. This doesn't mean that the basis is unique, nor does it mean that any identifiable target characteristics require a specific basis. Uniqueness is a characteristic of the target not the descriptive basis.

A fully polarametric radar, as described by Huynen [7], will measure all parallel and orthogonal basis components as well as the phase between them. For duplexed radar, one with common transmit and receive antennas, the collective result at one frequency within the radar time-volume cell is a description of the scatter matrix. Typically, for a known incident polarization, the backscattered polarization would be measured. Assuming vertical and horizontal polarization is used, the scatter matrix, in which "xx" means vertical transmission and reception, "xy" vertical transmission, but horizontal reception and "yy" means horizontal transmission and reception is defined by

$$[S] = \begin{bmatrix} s_{11} & s_{12} \\ s_{12} & s_{22} \end{bmatrix} = \begin{bmatrix} xx & xy \\ xy & yy \end{bmatrix}. \quad (84)$$

Each component term is generally complex so ignoring a common range dependent phase, there are a maximum of five independent parameters. These five, together with X-Y basis polarizations are all that is known about the target within a specific time-volume cell. But while the matrix is polarization basis specific, knowing that basis enables determining an exactly equivalent form in any other basis. So even though the two scatter matrices may appear completely different, they will equally describe the same target within the same time-volume cell. If the column vector represents the incident polarized wave $\begin{Bmatrix} E_1^i & E_2^i \end{Bmatrix}$, then the backscattered field at the antenna in the same polarization basis is:

$$\begin{bmatrix} E_1^s \\ E_2^s \end{bmatrix} = \begin{bmatrix} s_{11} & s_{12} \\ s_{12} & s_{22} \end{bmatrix} \cdot \begin{bmatrix} E_1^i \\ E_2^i \end{bmatrix} = \begin{bmatrix} s_{11}E_1^i + s_{12}E_2^i \\ s_{12}E_1^i + s_{22}E_2^i \end{bmatrix}. \quad (85)$$

It should be recognized that as two-dimensional components, E_1^s, E_2^s only describes a polarization ellipse in terms of the components basis. It conceals anything concerning the operating process. Also, a third dimension, the "handedness" of the equivalent rotating field vector must also be accounted for to properly characterize the received voltage at the terminals of a radar antenna. Although seemingly trivial it is understood that within a specific time-volume cell of the target and at one operating frequency, measurement of the scatter matrix completely describes everything that can be learned about the target. The scatter matrix can also be measured at any one basis, and a corresponding matrix readily written for any other. Most commonly, the matrix of the same target may be written in a linear X-Y basis or a circular, R-L basis. Each exhibit target characteristics in a different, sometimes more feature recognizable manner. Since targets move and cells change it doesn't appear to be very much. But the matrix basis is of lesser importance than invariant characteristics of the target, essentially what Huynen [7] termed the "phenomenology" of the target.

8.1 Other Scatter Matrix Forms

Conceptually, the polarization characteristics of a radar target are simple and were so defined in matrix form in a widely referenced M.Sc. thesis by E.M. Kennaugh written in 1952 [8]! Subsequently, his matrix form burgeoned. This matrix is sometimes termed a Sinclair matrix, a Mueller matrix, occasionally a Kronecker matrix, and at times as a Jones matrix. (Technically, differences between these matrices concern component coherency; subjectively, they concern scientific field, i.e., electromagnetic vs optics: F.T. Ulaby and C. Elachi [9] and Mott [10]. The 2×2 scatter matrix form is elemental insofar as coherent components polarization description is concerned. In its basic form it simply relates the coherent field backscattered from a target as a result of a particular coherent incident field. It differs little from the basic relationship for a microwave network that is so well expressed in the MIT Radiation Lab book, following World War II: $[B] = [S] \cdot [A]$; output $[B]$ from a network described by a matrix $[S]$, for a specific input $[A]$.

However, other derived or more readily measured forms appear in the literature. Foremost among these is the power scatter matrix, first proposed by C.D. Graves [11]. This form is based on the total power incident and back scattered from a target. It conveniently describes the backscattered power for any polarized illuminating power, but omits the phase reference necessary for the complete matrix description. In terms of the Poincaré Sphere, the wave polarization power could be located at any point along any great circle, an infinite number of possibilities! Another form, necessary for the description of collectively time varying (within the radar time-volume cell) scatterers, is its representation as the Mueller matrix with the wave characteristics represented by Stokes parameters, which accommodate partially coherent waves in terms of time averaged power components. Still other forms include covariance and coherency matrices.

Much of the early experimental work was also limited by the inability to conveniently vary the polarization coordinates of the transmitter and receiver. The use of vertical and horizontal components dominated the work. Then phase measurements were not always convenient, adding further to the difficulty in accurately describing the complete target scattering matrix, even for one angle aspect or range segment. But phase can be determined by adding an additional pair of linearly polarized measurements, e.g., slant right 45° and slant left 45° . For a static target and measurement, this can lead to a proper scatter matrix for one measurement basis, i.e., vertical and horizontal, but targets can exhibit characteristics such that a linear basis measurement yields inaccurate scatter matrix. For example, a simple flat plate may be better characterized by measurements using a circular basis, since the rotational sense of the wave from a plate is better observed. Nonetheless a single scatter matrix, regardless of its accuracy and derivation will only provide a characteristics snapshot and alone will not enable target classification. Even so, the characteristics of even a single matrix have been and are of interest. The scatter matrix is essentially independent of the basis used for its measurement. But if accurate it readily discloses polarizations that would result in a maximum signal, the co-polarized characteristic, as well as the polarization that would result in zero, i.e., a null polarization.

8.2 Canonical Structures

In theory, any target could be reduced analytically to an assembly of small points, a bit larger, then spheres or plates, but there are some basic structures with readily visualized polarization characteristics that taken together, i.e., within a single radar time-volume resolution cell, comprise the collective radar target. While not canonical in the purest sense, the four matrixes in the Table, expressed in a linear V-H basis and in terms of a rotational angle θ , are most often described.

Alone none of these matrices can completely describe the scatter matrix of most targets; their visualization as part the complete target is palliative in its interpretation. The sphere or flat plate could also include a trihedral corner, but in the linear basis the transmitted and received components are identical. The dipole orientation defines its transmitted and received components orientation. The dihedral essentially combines two plates but is nonetheless a basic structure because it includes an important and well-known effect.

Table 1 – Canonical Radar Targets in a Linear V-H

| Structure | Rotation angle | [S] |
|----------------------|----------------|--|
| Sphere or Flat Plate | Any | $\begin{bmatrix} 1 & 0 \\ 0 & 1 \end{bmatrix}$ |
| Dipole at θ | 2θ | $\begin{bmatrix} 1 + \cos 2\theta & \sin 2\theta \\ \sin 2\theta & 1 - \cos 2\theta \end{bmatrix}$ |
| Dihedral at θ | 2θ | $\begin{bmatrix} \cos 2\theta & \sin 2\theta \\ \sin 2\theta & -\cos 2\theta \end{bmatrix}$ |
| Helix | Any | $\begin{bmatrix} 1 & \pm j \\ \pm j & -1 \end{bmatrix}$ |

In terms of the radar environment, each reflection results in an inversion of the rotational direction of a circularly polarized transmitted component. This effect can be exploited in radar target detection. The reversal in polarization sense of rain, considered single bounce contrasted with targets that include other multiple bounce effects could be separated with radar using a circular polarization.

8.3 Co- and Cross-pol Nulls of Target Backscatter

Target backscatter usually includes components both parallel and orthogonal to the illumination. However, in the case of four target illumination polarizations this doesn't occur. These are of particular interest since they offer some target categorization uniqueness. Two polarizations describe target backscatter polarizations that are exactly orthogonal to the illumination polarization and while the remaining two polarizations are for the backscatter without any cross-polarized component. The first pair has been described as "Co-polarization nulls" since all of the illumination that is backscattered is orthogonal to that of the incident polarization, i.e., exactly mismatched. (Not good for radar attempting target detection!) The second pair, described as "Cross-polarization nulls" represents a match between illuminating and backscatter polarizations, since no backscattered component is orthogonal to the polarization incident on the target. The significance of these polarizations is a representation of the inherent target properties, as contrasted to the scatter matrix that only represents these properties in one of any number of possible bases. Assuming the scatter matrix and basis is completely described, both co- and cross-pol nulls can be determined. Nonetheless, any measurement or appropriate null representations all describe ellipses. These, in turn are characterized by the ellipse geometry: axial ratio, angular orientation and the rotational sense of the generating rotating field. The latitudinal and longitudinal coordinates of the Poincaré Sphere then provides a convenient mapping to further visualize all of the targets characteristics.

Among the numerous papers and publications dealing with the derivation of null characteristics from a specific scatter matrix, those by Huynen [15], Boerner, El-Arni, Chan, Saatchi, Ip, Mastoris, Foo, and He [12] and Cloude [13] are foremost, although earlier Kennaugh described the problem in his M.Sc. thesis. It is recognized that although the mathematics appear similar to a conventional eigenvalue/eigenvector problem, propagating directional differences (illumination vs backscatter) make the solution much more difficult and all have avoided this “pseudo-eigenvalue” problem. But the goals are the same; unitary transforms are sought that will either diagonalize the scatter matrix, thereby describing the cross-polarization nulls, or result in a matrix with zero main diagonal terms, thereby describing the co-polarization nulls.

The basic work assumes a transform of the scatter matrix using a general unitary transform matrix, $[T]$, with complex scalar coefficients in the same scatter matrix basis, to a new matrix in a new basis with either diagonal or off-diagonal zeros. The general form of the transform matrix is:

$$[T] = \frac{1}{\sqrt{1 + \rho\rho^*}} \begin{bmatrix} 1 & -\rho^* \\ \rho & 1 \end{bmatrix}. \quad (86)$$

The corresponding scatter matrix terms, from the transform $S' = TST^{-1}$, represented with primed superscripts, are then:

$$s'_{11} = (1 + \rho\rho^*)^{-1} [s_{11} + \rho^2 s_{22} + \rho(s_{12} + s_{21})] \quad (87a)$$

$$s'_{12} = (1 + \rho\rho^*)^{-1} [-\rho^* s_{11} + \rho s_{22} + s_{12} - \rho\rho^* s_{21}] \quad (87b)$$

$$s'_{21} = (1 + \rho\rho^*)^{-1} [-\rho^* s_{11} + \rho s_{22} + s_{21} - \rho\rho^* s_{12}] \quad (87c)$$

$$s'_{22} = (1 + \rho\rho^*)^{-1} [\rho^{*2} s_{11} + s_{22} - \rho^*(s_{12} + s_{21})] \quad (87d)$$

Then by setting $s'_{11} = 0$ and $s'_{22} = 0$, the transformed matrix defines the co-polarization nulls, in which $s_{12} = s_{21}$, to represent a duplexed, monostatic transmitter/receiver:

$$\rho^{co-pol} = \frac{-s_{12} \pm \sqrt{s_{12}^2 - s_{11}s_{22}}}{s_{22}}. \quad (88)$$

Setting s'_{12} and $s'_{21} = 0$, then the transformed scatter matrix, as shown by Boerner et al. [12], results in the corresponding scalar (defining the cross-polarization nulls) :

$$\rho^{cross-pol} = \frac{-b \pm \sqrt{b^2 - 4ac}}{2a}, \quad (89)$$

where the quadratic coefficients are

$$a = s_{22}s_{21}^* + s_{11}^*s_{21}, \quad (90a)$$

$$b = -[|s_{22}|^2 - |s_{11}|^2], \quad (90b)$$

and

$$c = -a^* \quad (90c)$$

8.4 The Huynen Fork

An inferential “so-what” implied by detailed calculations or measurements was recognized by Huynen and depicted on the Poincaré Sphere. Although just four complex null parameters can hardly be expected to sufficiently classify a target, they do serve to depict the target in a manner that is independent of the scatter matrix and therefore more closely aligned with a radar target from a conceptual sense.

Unsurprisingly, the quadratics in Eqs. (88) and (89) provide the four polarizations unique to the scatter matrix defined in Eq. (85). Huynen, Boerner and others have shown that these are displaced within a single plane, as illustrated in Fig. 44. Moreover, while the plane is diametrical, it may be inclined at any angle. An examination of the disposition of the “fork tines” reveals that all four polarizations need not be shown, only two are necessary. The co-polarization nulls are always 180° apart and while the locations of the two cross-polarization nulls always bisect the line of the co-polarization nulls, a target specific solution with the two cross-polarization nulls coalesce are also possible. Therefore knowledge of a few points can enable a calculation of the complete scatter matrix. In a sense the Huynen Fork fulfills the objective for a phenomenological description of a radar target. Its independent basis requires only a few parameters and is readily visualized. But there are infinite numbers of targets and many likely duplications or finely separated “forks” possible and the description doesn’t say anything directly about the target itself.

8.5 Scatter Matrix Decomposition

There is a certain familiarity concerning anticipated backscattered polarizations following illumination of simple targets with specific polarizations. The backscatter from an inclined wire or the edge of a sheet will be linear and at the same angle as the wire or sheet. The backscatter from a sphere or to some degree a rain drop will return with a circular polarization of an opposite sense. If a flat sheet is illuminated with one sense of circular polarization, the backscatter will be circularly orthogonal. Reflections from flat plates and corners are very different.

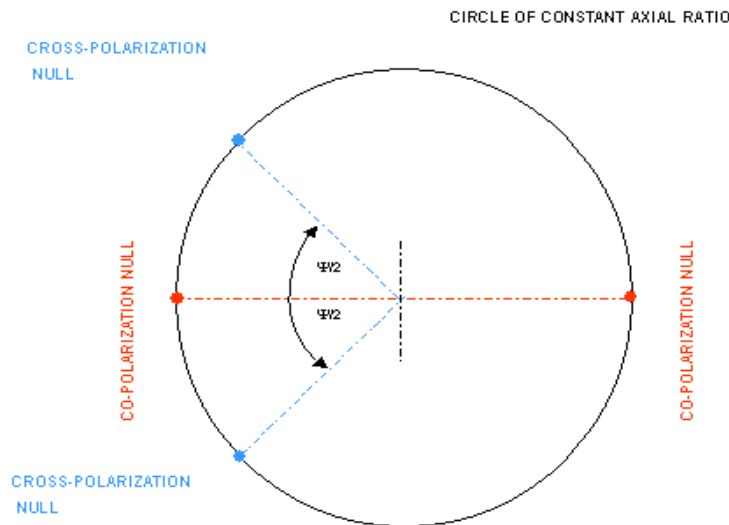


Fig. 44 – A principal plane of the Poincaré Sphere containing the target co-polarization and cross-polarization nulls.

Figure 45 shows a simple navigation buoy illuminated with circular polarization. As a radar reflector for use in navigation, it is mostly an assembly of corner reflectors. For the representative measurements, the buoy was tethered and it rotated during measurements. The polarization changes and even the pattern widths, based on physical dimensions, have the unmistakable character of a rotating corner. Sometimes the backscatter appears as a broad double-bounce effect, resulting in same-sense circular backscatter within the corner view, then followed by brief, narrow, opposite-sense polarizations, essentially as a flash from a single side, which is plainly visible in the plot.

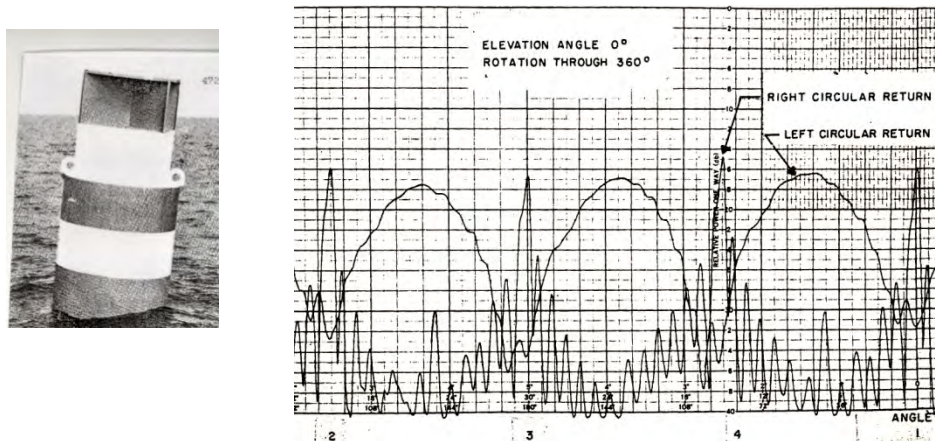


Fig. 45 – Left and right circularly polarized returns from a buoy, similar to the photo with angular rotation.

Other structures will show different identifiable characteristics, each with known parametric matrixes and all combined within a single scatter matrix range-angle-time cell. If their numbers are not too small, the scatter matrix as a sum of these basic, canonical matrix forms can be written so that each matrix coefficient defines the magnitude of the associated reflectors. This then bears a closer association to the “phenomenology” goal first proposed by Huynen, which only identifies the collective co-pol and cross-pol components of the scatter matrix. Of course, each is a complete analytic representation of the scatter matrix, so it can be interchangeably derived.

Rewriting matrixes as sums of simple elementary forms is well known in the quantum mechanics community as a means to separately identify specific characteristics. The Pauli Spin matrixes represented particle spins about each of the three axes, such that each rotation described a specific characterization. These results have been reported in the literature. But like the Huynen Fork, it is more an interpretation of the scatter matrix than identifying the detailed physical structure of a target. It may be useful, but much more is needed if that is among the goals of specific radars.

A mainstay of the radar remote sensing community is the synthetic aperture radar (SAR). It provides useful detail of large areas filled with collections of scatterers of interest. The familiar two-dimensional mappings with buildings, roads, rail lines, vehicles, trees, farm crops, etc., are distinguishable to most readers, but can be further enhanced by decomposing the scatter matrix into summed components of canonical scatterers. Each of these confers amplitudes of specific matrix components that are then distinguished using a false color representation. Numerous scatter sets have been suggested. Work in optics uses Pauli matrixes, but one that assumes decomposition into components of a sphere, a diplane at

a specified angle θ , and a helix, appears to have favored Krogager [14], but their equivalence using appropriate constants can be shown:

$$[S] \propto k_{sphere} \begin{bmatrix} 1 & 0 \\ 0 & 1 \end{bmatrix} + k_{diplane} \begin{bmatrix} \cos 2\theta & \sin 2\theta \\ \sin 2\theta & -\cos 2\theta \end{bmatrix} + k_{helix} \begin{bmatrix} 1 & \pm j \\ \pm j & -1 \end{bmatrix}. \quad (91)$$

An impressive number of papers have and continue to be written concerning “radar scatter matrix decomposition,” Internet search engines can fill report pages, for which the reader is recommended. Of course, all concern a static representation of the scatter matrix as the sum of known simple geometric targets in one form or another, i.e., some underlying assumptions are always made. The components used in any decomposition of the scatter matrix are all justified by assumptions concerning the physical properties of the target structure. Unsurprisingly these will be diverse and have been analyzed, demonstrated, and extensively reported in the literature. However, if the resolved time-volume cell is very small, i.e., it contains a single representative scatterer, then there would be no differences. But this is not the case. So, as a result, approaches to decomposition are sometimes argumentative. Some of the relevant background is described by Huynen [15]. But future work could well recount very early polarization work in which motion, e.g., the target or components movement or rotation, added a still further classification dimension. In early work associated with satellite orbiting, it was shown that satellite spin was readily measured using a polarization technique, as Fig. 46 suggests. Basically irrespective of any target composition, its rotation, or any of its components’ rotation, results in a measurable frequency translated backscattered component.

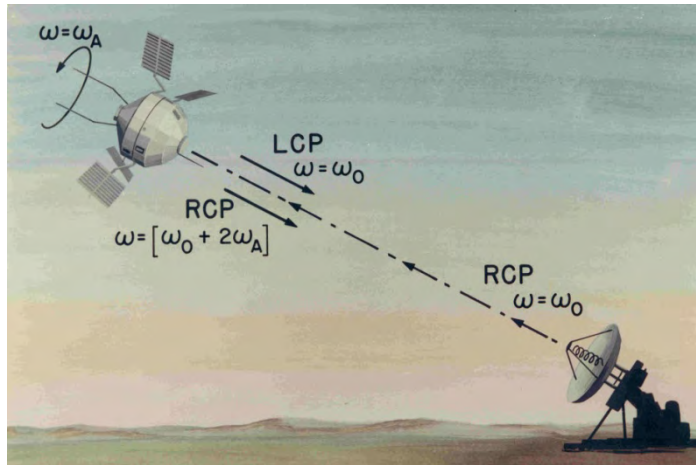


Fig. 46 – Circa 1950 representation of polarization frequency translation from a spinning satellite

8.6 Control of Polarization Axial Ratio and Ellipse Orientation

A coherently polarized wave has been characterized in terms of the axial ratio and angular orientation of the ellipse traced by a rotating field vector. Radar targets can be illuminated by specifically characterized polarized waves to achieve a specific objective, such as illuminating a rotating target to

facilitate identification, as in the case for Fig. 46. An electronic warfare application may require transmission of a polarized wave with a specific axial ratio and orientation. Such parameter specific polarizations can be simply developed by controlling transformations of just a few basic structures, as illustrated in Fig. 47.

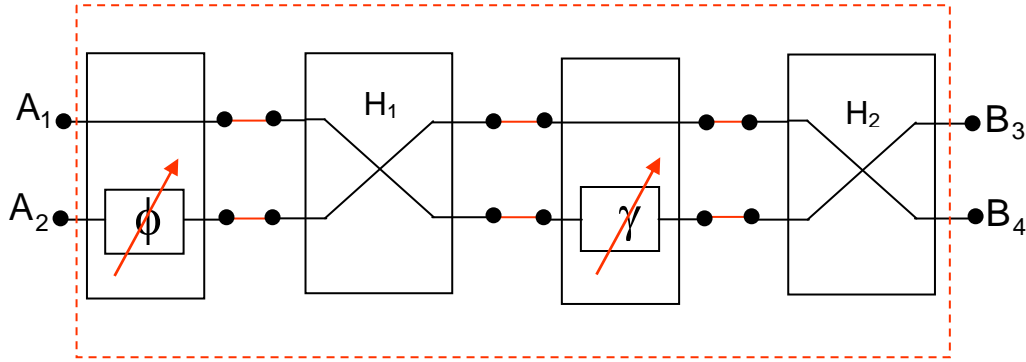


Fig. 47 – Cascade circuit enabling control of axial ratio and ellipse orientation.

In this particular example, unit vertical and horizontal polarized inputs applied to a circuitry cascade of adjustable phase shifters and waveguide quadrature hybrids enable *independent* control of the axial ratio and orientation of the output polarization. The axial ratio of the combined B_3/B_4 output components is a function of the phase shift ϕ , while the orientation of the ellipse is a function of the phase shift γ . The circuit essentially operates the same as a radar target, the polarization at the input is controlled and transformed to another at its output.

An analysis of this circuit is facilitated using the familiar combinations of network matrices. Using the generalized notation, noted in Section 8.1, $B = S \cdot A$, the 4-port scatter matrix of the first phase shifter is given by

$$S_{\phi} = \begin{bmatrix} 0 & 0 & 1 & 0 \\ 0 & 0 & 0 & \epsilon^{j\phi} \\ \hline 1 & 0 & 0 & 0 \\ 0 & \epsilon^{j\phi} & 0 & 0 \end{bmatrix}. \quad (92)$$

The equivalent form for the quadrature hybrid is given by

$$S_{Hy} = \begin{bmatrix} 0 & 0 & j & 1 \\ 0 & 0 & 1 & j \\ \hline j & 1 & 0 & 0 \\ 1 & j & 0 & 0 \end{bmatrix}. \quad (93)$$

Each is assumed lossless and fulfills the unitary condition $S \cdot S^* = I$. The parameters of the combined network can be found by assuming the output of one, B_3, B_4 , serves as the inputs, A_1, A_2 , for the one following. For the lossless elements, $B_1 = B_2 = 0$, and:

$$B_3 = \{(-1 + \cos \gamma)E_1 - [\sin \phi + \sin(\phi + \gamma)E_2]\} + j\{E_1 \sin \gamma + [\cos \phi + \cos(\phi + \gamma)E_2]\}, \quad (94)$$

$$B_4 = \{[\cos \phi - \cos(\phi + \gamma)]E_2 - E_1 \sin \gamma\} + j\{(1 + \cos \gamma)E_1 + [\sin \phi - \sin(\phi + \gamma)]E_2\}. \quad (95)$$

Since $|B_3/B_4| = r$, and $\arg(B_3 - B_4) = \delta$, Eqs. (32a) and (34), respectively, determine the ellipse orientation and axial ratio.

Other circuit combinations using waveguides or their printed circuit equivalents most certainly are possible, which can then be used to readily control the generation and reception of polarized waves.

9. POLARIZATION FILTER

In a general sense, the performance and characteristics of a filter are defined in terms of the preferential selectivity of one of its input characteristics over others. For a frequency filter, characteristics can be defined in terms of the gain or loss of one or a group of input components over others. Alternatively, the frequency selectivity, relative bandwidth or quality “Q” of a resonant circuit can be

defined in terms of its phase response near its maximum design frequency, ω_r : $Q = \frac{1}{2} \omega_r \cdot \left[\frac{\partial \theta}{\partial \omega} \right]_{\omega=\omega_r}$.

A polarization filter can also be designed to exhibit a preferred output for one or a group of similarly polarized input components using the polarization selectivity inherent in an array, waveguide or other RF circuit element. The selectivity is limited and based on the mode selectivity of the element. A vertical dipole or TE₁₀ waveguide ideally rejects horizontal polarization; a right circular spiral rejects left circular polarization. Plotted on a Poincaré Sphere, the rejection is defined by a 180° arc. The loss for other polarizations, defined by an arc are given by Eq. (41) and plotted in Fig. 12. The polarization difference or loss between two polarized signals is readily determined.

Figure 48 illustrates two points located on a sphere quadrant by the usual θ, ϕ coordinates. In the Poincaré Sphere notation, ϕ corresponds to twice the angle of the major ellipse axis and as a function of the axial ratio, $\theta = \pi/2 - 2 \tan^{-1}(1/\rho)$, where ρ represents the axial ratio, AR with respect to the reference horizontal polarization.

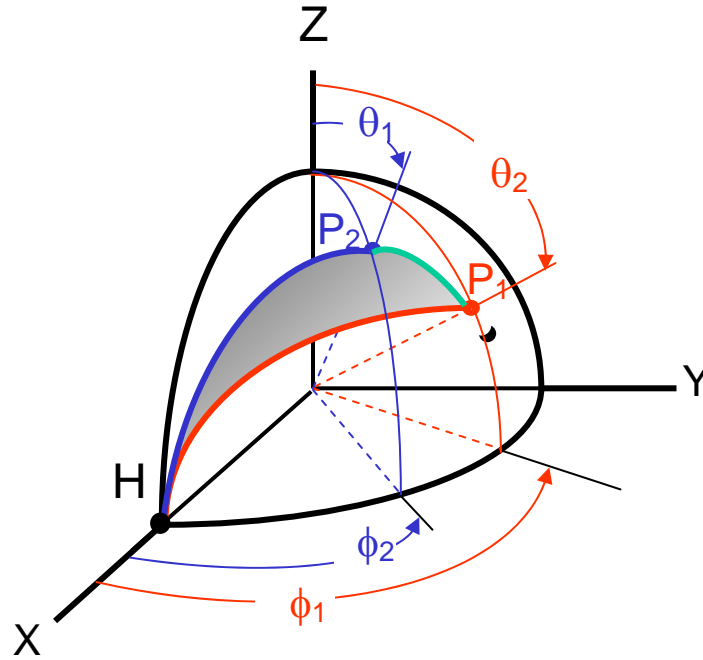


Fig. 48 – Location of two polarizations in terms of the axial ratio and the inclination of the major axis.

The spherical triangle H, P_1, P_2 then defines the arc P_1P_2 , a measure of the polarization difference between the points at P_1 and P_2 . Expressed as a function of the axial ratios ρ_1 and ρ_2 and their phase difference $(\tau_1 - \tau_2)$, the arc is

$$\cos \overline{P_1P_2} = \frac{-4\rho_1\rho_2 + (\rho_1^2 - 1)(\rho_2^2 - 1)\cos 2(\tau_1 - \tau_2)}{(\rho_1^2 + 1)(\rho_2^2 + 1)}. \quad (96)$$

In terms of a decibel difference between the two waves:

$$\Delta P_1P_2|_{dB} = 20 \cdot \log_{10} \left[\cos \frac{P_1P_2}{2} \right]. \quad (97)$$

Polarization filtering is, therefore, based on a signals characteristic relative to an inherently polarization-selective component, and its “selectivity” can be represented by the arc length on the Poincaré Sphere, as illustrated in Fig. 12. The most frequent utilization of polarization filtering is the rejection (or minimization) of rain clutter to enhance target detection. For most radar time-range-angle cells, target structural complexity assures reflection from any incident polarization. But since rain is near spherically shaped, an oppositely sensed circular polarized component dominates the backscatter, therefore facilitating target selectivity. Poelman [16] described a more selective approach. It is essentially a target decomposition approach. Visualized on a Poincaré Sphere, *all* of the received polarization parameters are reprocessed numerous times, each using a different scatter matrix transform that places its cross-polarized nulls close to the desired polarizations match; a ring about one polarization. In rain clutter, an improvement of about 6 dB over just a circular polarization technique is claimed.

ACKNOWLEDGMENTS

Much of the credit for my understanding of the general theory outlined in this report must go to three former and long retired NRL employees, M.L. Kales and J.I. Bohnert, and my first supervisor and mentor, at NRL, P.J. Allen, all of whom published their work in the early 1950s. At that time, the Radar Division work was motivated by the potential for improved target detection and classification requiring generation, reception, and control of EM waves with specific parameters. The recent renewed interest in the theory concerns its applicability to the generation and control of EM wave polarization of active phased arrays, important to the universality of future multifunction systems exemplified by the more recent work within the AMRFS program. Preparation of this report was done while under contract with the Naval Research Laboratory, Washington, D.C.

REFERENCES

1. V.H. Rumsey, G.A. Deschamps, M.L. Kales, and J.I. Bohnert, "Techniques for Handling Elliptically Polarized Waves with Special Reference to Antennas," *Proc. I.R.E.* **39**, 533-556, May 1951.
2. A.C. Ludwig, "The Definition of Cross Polarization," *IEEE Trans. Antennas and Propag.* **21**(1), 116-119, Jan. 1973.
3. J.E. Roy and L. Shafai, "Generalization of the Ludwig-3 Definition for Linear Copolarization and Crosspolarization," *IEEE Trans. Antennas and Propag.* **49**(6), 1006-1010, June 2001.
4. G.T.H. Knittel, "Comments on 'The Definition of Cross Polarization'," *IEEE Trans. Antennas and Propag.* **21**(6), 917-918, Nov. 1973.
5. G.F. Masters and S.F. Gregson, "Coordinate System Plotting for Antenna Measurements," www.nearfield.com/TechPapers, AMTA St. Louis, 2007.
6. W.R. Pickels, J.B.L. Rao, D.P. Patel, and R. Mital, "Coincident Phase Center Ultra Wideband Array of Dual Polarized Flared Notch Element," Antennas and Propagation Society International Symposium, 2007 IEEE, 4421-4424, June 9-15, 2007.
7. J.R. Huynen, "A Revisitation of the Phenomenological Approach with Applications to Radar Target Decompositions," Communications Laboratory, Electrical Engineering and Computer Science, University of Illinois at Chicago, May 18, 1982.
8. E.M. Kennaugh, "Polarization Properties of Radar Reflectors," Master of Science Thesis, Dept. of Electrical Engineering, The Ohio State University, Columbus, OH, 1952.
9. F.T. Ulaby and C. Elachi, *Radar Polarimetry for Geoscience Applications* (Artech House, Inc., 1990).
10. H. Mott, *Polarization in Antennas and Radar* (John Wiley & Sons, 1986), pp. 92-94.
11. C.D. Graves, "Radar Polarization Power-Scattering Matrix," University of Michigan Report 2144-45-T, August 30, 1955.

12. W.M. Boerner, M.B. El-Arni, C.Y. Chan, S. Saatchi, W.S. Ip, A.M. Mastoris, and B.Y. Foo, "Polarization Utilization in Radar Target Reconstruction," Communications Laboratory, Information Engineering Dept., University of Illinois at Chicago, January 15, 1981.
13. S.R. Cloude, "Polarimetric Techniques in Radar Signal Processing," *Microwave J.*, 120-127, July 1983.
14. E. Krogager, "Target Advances of Techniques for Utilizing Polarimetric Features of Radar Targets," RTO SET Symposium Oslo, Norway, October 11-13, 2004.
15. J.R. Huynen, "Comments on Target Decomposition Theorems," *Direct and Inverse Methods in Radar Polarimetry, Part I*. NAO ASI Series (Kluwer Academic Publishers, 1992).
16. J. Poelman, "The Effectiveness of Multi-Notch Logic-Product Polarization Filters in Radar for Countering Rain Clutter," *IEE Pro. F, Radars for Signal Processing* **138**(5), 427-437, October 1991.

Appendix A

CHARTS DEPICTING POLARIZATION LOSS

In the following tables, parameter combinations have been optimized for minimum circular polarization loss, as described in Section 5.5.

| δ (degrees) | | | | | $ E_R/E_L $ (dB) | | | | | E_L | | | | | | | | | | |
|--------------------|---------------|--------|---------------|--------|------------------|------|------------------|---------------|---------|---------------|---------|---------|------|------------------|---------------|-------|---------------|-------|-------|-------|
| | η_2 (dB) | -15 | η_1 (dB) | -25 | -50 | -100 | | η_2 (dB) | -15 | η_1 (dB) | -25 | -50 | -100 | | η_2 (dB) | -15 | η_1 (dB) | -25 | -50 | -100 |
| $k = 0$ dB | -15 | 114.79 | 108.09 | 105.08 | 104.90 | | $k = 0$ dB | -15 | -134.74 | -45.63 | -42.47 | -42.32 | | $k = 0$ dB | -15 | -0.71 | -0.35 | -0.24 | -0.23 | |
| $\xi = 85^\circ$ | -25 | 108.09 | 101.38 | 98.37 | 98.19 | | $\xi = 85^\circ$ | -25 | -45.63 | -191.97 | -52.70 | -52.20 | | $\xi = 85^\circ$ | -25 | -0.35 | -0.13 | -0.07 | -0.07 | |
| | -50 | 105.08 | 98.37 | 95.36 | 95.18 | | | -50 | -42.47 | -52.70 | -128.11 | -77.21 | | | -50 | -0.24 | -0.07 | -0.04 | -0.03 | |
| | -100 | 104.90 | 98.19 | 95.18 | 95.00 | | | -100 | -42.32 | -52.20 | -77.21 | -209.51 | | | -100 | -0.23 | -0.07 | -0.03 | -0.03 | |
| δ (degrees) | | | | | $ E_R/E_L $ (dB) | | | | | E_L | | | | | | | | | | |
| | η_2 (dB) | -15 | η_1 (dB) | -25 | -50 | -100 | | η_2 (dB) | -15 | η_1 (dB) | -25 | -50 | -100 | | η_2 (dB) | -15 | η_1 (dB) | -25 | -50 | -100 |
| $k = 0$ dB | -15 | 119.28 | 112.78 | 109.82 | 109.64 | | $k = 0$ dB | -15 | -145.08 | -39.55 | -36.39 | -36.23 | | $k = 0$ dB | -15 | -0.94 | -0.54 | -0.40 | -0.40 | -0.39 |
| $\xi = 80^\circ$ | -25 | 112.78 | 106.28 | 103.32 | 103.14 | | $\xi = 80^\circ$ | -25 | -39.55 | -159.41 | -46.61 | -46.11 | | $\xi = 85^\circ$ | -25 | -0.54 | -0.27 | -0.19 | -0.19 | -0.19 |
| | -50 | 109.82 | 103.32 | 100.36 | 100.18 | | | -50 | -36.39 | -46.61 | -131.71 | -71.12 | | | -50 | -0.40 | -0.19 | -0.14 | -0.14 | -0.14 |
| | -100 | 109.64 | 103.14 | 100.18 | 100.00 | | | -100 | -36.23 | -46.11 | -71.12 | -168.19 | | | -100 | -0.39 | -0.19 | -0.14 | -0.14 | -0.13 |
| δ (degrees) | | | | | $ E_R/E_L $ (dB) | | | | | E_L | | | | | | | | | | |
| | η_2 (dB) | -15 | η_1 (dB) | -25 | -50 | -100 | | η_2 (dB) | -15 | η_1 (dB) | -25 | -50 | -100 | | η_2 (dB) | -15 | η_1 (dB) | -25 | -50 | -100 |
| $k = 0$ dB | -15 | 136.10 | 130.76 | 128.21 | 128.05 | | $k = 0$ dB | -15 | -163.28 | -29.25 | -26.10 | -25.95 | | $k = 0$ dB | -15 | -2.49 | -1.94 | -1.73 | -1.73 | -1.72 |
| $\xi = 60^\circ$ | -25 | 136.10 | 125.42 | 122.87 | 122.71 | | $\xi = 60^\circ$ | -25 | -22.68 | -128.44 | -36.31 | -35.81 | | $\xi = 60^\circ$ | -25 | -2.31 | -1.54 | -1.39 | -1.39 | -1.38 |
| | -50 | 128.21 | 122.87 | 120.31 | 120.16 | | | -50 | -26.10 | -36.31 | -122.44 | -60.82 | | | -50 | -1.73 | -1.39 | -1.26 | -1.26 | -1.26 |
| | -100 | 128.05 | 122.71 | 120.16 | 120.00 | | | -100 | -25.95 | -35.81 | -60.82 | -131.59 | | | -100 | -1.72 | -1.38 | -1.26 | -1.26 | -1.25 |
| δ (degrees) | | | | | $ E_R/E_L $ (dB) | | | | | E_L | | | | | | | | | | |
| | η_2 (dB) | -15 | η_1 (dB) | -25 | -50 | -100 | | η_2 (dB) | -15 | η_1 (dB) | -25 | -50 | -100 | | η_2 (dB) | -15 | η_1 (dB) | -25 | -50 | -100 |
| $k = 0$ dB | -15 | 151.49 | 147.73 | 145.86 | 145.75 | | $k = 0$ dB | -15 | -118.02 | -22.98 | -19.85 | -19.69 | | $k = 0$ dB | -15 | -5.41 | -4.74 | -4.45 | -4.45 | -4.44 |
| $\xi = 40^\circ$ | -25 | 147.73 | 143.97 | 142.10 | 141.99 | | $\xi = 40^\circ$ | -25 | -22.98 | -123.50 | -30.02 | -29.52 | | $\xi = 60^\circ$ | -25 | -4.74 | -4.25 | -4.04 | -4.04 | -4.03 |
| | -50 | 145.86 | 142.10 | 140.23 | 140.12 | | | -50 | -19.85 | -30.02 | -147.32 | -54.52 | | | -50 | -4.45 | -4.04 | -3.86 | -3.86 | -3.85 |
| | -100 | 145.75 | 141.99 | 140.12 | 140.00 | | | -100 | -19.69 | -29.52 | -54.52 | -203.02 | | | -100 | -4.44 | -4.03 | -3.85 | -3.85 | -3.84 |

| δ (degrees) | | | | | $ E_R/E_L $ (dB) | | | | | E_L | | | | |
|--------------------|--------|--------|--------|--------|------------------|--------|--------|--------|--------|------------------|-------|-------|-------|-------|
| η_z (dB) | | | | | η_z (dB) | | | | | η_z (dB) | | | | |
| $k = -0.5$ dB | | | | | $k = -0.5$ dB | | | | | $k = -0.5$ dB | | | | |
| $\xi = 85^\circ$ | | | | | $\xi = 85^\circ$ | | | | | $\xi = 85^\circ$ | | | | |
| -15 | 114.79 | 108.09 | 105.08 | 104.90 | -15 | -29.98 | -29.00 | -28.56 | -28.54 | -15 | -0.96 | -0.60 | -0.48 | -0.48 |
| -25 | 108.09 | 101.38 | 98.37 | 98.19 | -25 | -32.03 | -30.65 | -30.06 | -30.03 | -25 | -0.60 | -0.38 | -0.32 | -0.31 |
| -50 | 105.08 | 98.37 | 95.36 | 95.18 | -50 | -33.04 | -31.45 | -30.78 | -30.74 | -50 | -0.49 | -0.32 | -0.28 | -0.28 |
| -100 | 104.90 | 98.19 | 95.18 | 95.00 | -100 | -33.10 | -31.50 | -30.83 | -30.79 | -100 | -0.48 | -0.31 | -0.28 | -0.28 |
| δ (degrees) | | | | | $ E_R/E_L $ (dB) | | | | | E_L | | | | |
| η_z (dB) | | | | | η_z (dB) | | | | | η_z (dB) | | | | |
| $k = -0.5$ dB | | | | | $k = -0.5$ dB | | | | | $k = -0.5$ dB | | | | |
| $\xi = 80^\circ$ | | | | | $\xi = 80^\circ$ | | | | | $\xi = 85^\circ$ | | | | |
| -15 | 119.28 | 112.78 | 109.82 | 109.64 | -15 | -29.63 | -27.59 | -26.80 | -26.75 | -15 | -1.18 | -0.78 | -0.64 | -0.64 |
| -25 | 112.78 | 106.28 | 103.32 | 103.14 | -25 | -33.69 | -30.46 | -29.31 | -29.25 | -25 | -0.79 | -0.52 | -0.44 | -0.43 |
| -50 | 109.82 | 103.32 | 100.36 | 100.18 | -50 | -36.23 | -32.08 | -30.68 | -30.60 | -50 | -0.65 | -0.44 | -0.38 | -0.38 |
| -100 | 109.64 | 103.14 | 100.18 | 100.00 | -100 | -36.41 | -32.18 | -30.77 | -30.69 | -100 | -0.64 | -0.44 | -0.38 | -0.38 |
| δ (degrees) | | | | | $ E_R/E_L $ (dB) | | | | | E_L | | | | |
| η_z (dB) | | | | | η_z (dB) | | | | | η_z (dB) | | | | |
| $k = -0.5$ dB | | | | | $k = -0.5$ dB | | | | | $k = -0.5$ dB | | | | |
| $\xi = 60^\circ$ | | | | | $\xi = 60^\circ$ | | | | | $\xi = 60^\circ$ | | | | |
| -15 | 136.10 | 130.76 | 128.21 | 128.05 | -15 | -27.64 | -22.81 | -21.31 | -21.23 | -15 | -2.73 | -2.18 | -1.96 | -1.95 |
| -25 | 130.76 | 125.42 | 122.87 | 122.71 | -25 | -49.09 | -29.04 | -26.11 | -25.96 | -25 | -2.20 | -1.79 | -1.63 | -1.62 |
| -50 | 128.21 | 122.87 | 120.31 | 120.16 | -50 | -37.75 | -34.44 | -29.54 | -29.32 | -50 | -1.99 | -1.64 | -1.51 | -1.50 |
| -100 | 128.05 | 122.71 | 120.16 | 120.00 | -100 | -37.12 | -34.89 | -29.80 | -29.57 | -100 | -1.98 | -1.63 | -1.50 | -1.49 |
| δ (degrees) | | | | | $ E_R/E_L $ (dB) | | | | | E_L | | | | |
| η_z (dB) | | | | | η_z (dB) | | | | | η_z (dB) | | | | |
| $k = -0.5$ dB | | | | | $k = -0.5$ dB | | | | | $k = -0.5$ dB | | | | |
| $\xi = 40^\circ$ | | | | | $\xi = 40^\circ$ | | | | | $\xi = 60^\circ$ | | | | |
| -15 | 151.49 | 147.73 | 145.86 | 145.74 | -15 | -24.41 | -18.12 | -16.37 | -16.27 | -15 | -5.64 | -4.95 | -4.65 | -4.63 |
| -25 | 147.73 | 143.97 | 142.10 | 141.99 | -25 | -35.27 | -26.22 | -22.13 | -21.94 | -25 | -5.01 | -4.49 | -4.27 | -4.25 |
| -50 | 145.86 | 142.10 | 140.23 | 140.12 | -50 | -25.87 | -36.31 | -26.94 | -26.61 | -50 | -4.74 | -4.29 | -4.10 | -4.09 |
| -100 | 145.75 | 141.99 | 140.12 | 140.00 | -100 | -25.53 | -37.53 | -27.34 | -26.99 | -100 | -4.72 | -4.28 | -4.09 | -4.08 |

| δ (degrees) | | | | | | $ E_R/E_L $ (dB) | | | | | | E_L | | | | | |
|--------------------|------|--------|--------|--------|--------|------------------|------|--------|--------|--------|---------------|------------------|------|-------|-------|-------|-------|
| η_z (dB) | | | | | | η_z (dB) | | | | | | η_z (dB) | | | | | |
| η_z (dB) | -15 | -25 | -50 | -100 | | η_z (dB) | -15 | -25 | -50 | -100 | η_z (dB) | -15 | -25 | -50 | -100 | | |
| $k = -1$ dB | -15 | 114.79 | 108.09 | 105.08 | 104.90 | $k = -1$ dB | -15 | -23.97 | -23.65 | -23.47 | -23.46 | $k = -1$ dB | -15 | -1.19 | -0.84 | -0.72 | -0.71 |
| $\xi = 85^\circ$ | -25 | 108.09 | 101.38 | 98.37 | 98.19 | $\xi = 85^\circ$ | -25 | -25.15 | -24.63 | -24.38 | -24.36 | $\xi = 85^\circ$ | -25 | -0.84 | -0.62 | -0.55 | -0.55 |
| | -50 | 105.08 | 98.37 | 95.36 | 95.18 | | -50 | -25.67 | -25.07 | -24.77 | -24.75 | | -50 | -0.73 | -0.56 | -0.52 | -0.52 |
| | -100 | 104.90 | 98.19 | 95.18 | 95.00 | | -100 | -25.70 | -25.09 | -24.79 | -24.77 | | -100 | -0.72 | -0.55 | -0.52 | -0.52 |
| δ (degrees) | | | | | | $ E_R/E_L $ (dB) | | | | | | E_L | | | | | |
| η_z (dB) | | | | | | η_z (dB) | | | | | | η_z (dB) | | | | | |
| η_z (dB) | -15 | -25 | -50 | -100 | | η_z (dB) | -15 | -25 | -50 | -100 | η_z (dB) | -15 | -25 | -50 | -100 | | |
| $k = -1$ dB | -15 | 119.28 | 112.78 | 109.82 | 109.64 | $k = -1$ dB | -15 | -23.62 | -22.75 | -22.36 | -22.34 | $k = -1$ dB | -15 | -1.42 | -1.01 | -0.88 | -0.87 |
| $\xi = 80^\circ$ | -25 | 112.78 | 106.28 | 103.32 | 103.14 | $\xi = 80^\circ$ | -25 | -25.71 | -24.45 | -23.91 | -23.88 | $\xi = 80^\circ$ | -25 | -1.03 | -0.76 | -0.67 | -0.67 |
| | -50 | 109.82 | 103.32 | 100.36 | 100.18 | | -50 | -26.75 | -25.28 | -24.66 | -24.63 | | -50 | -0.89 | -0.68 | -0.62 | -0.62 |
| | -100 | 109.64 | 103.14 | 100.18 | 100.00 | | -100 | -26.81 | -25.33 | -24.71 | -24.67 | | -100 | -0.89 | -0.68 | -0.62 | -0.62 |
| δ (degrees) | | | | | | $ E_R/E_L $ (dB) | | | | | | E_L | | | | | |
| η_z (dB) | | | | | | η_z (dB) | | | | | | η_z (dB) | | | | | |
| η_z (dB) | -15 | -25 | -50 | -100 | | η_z (dB) | -15 | -25 | -50 | -100 | η_z (dB) | -15 | -25 | -50 | -100 | | |
| $k = -1$ dB | -15 | 136.10 | 130.76 | 128.21 | 128.05 | $k = -1$ dB | -15 | -21.64 | -19.18 | -18.26 | -18.21 | $k = -1$ dB | -15 | -2.96 | -2.40 | -2.18 | -2.16 |
| $\xi = 60^\circ$ | -25 | 130.76 | 125.42 | 122.87 | 122.71 | $\xi = 60^\circ$ | -25 | -27.64 | -23.04 | -21.56 | -21.47 | $\xi = 60^\circ$ | -25 | -2.44 | -2.02 | -1.86 | -1.85 |
| | -50 | 128.21 | 122.87 | 120.31 | 120.16 | | -50 | -32.52 | -25.48 | -23.53 | -23.43 | | -50 | -2.24 | -1.88 | -1.74 | -1.74 |
| | -100 | 128.05 | 122.71 | 120.16 | 120.00 | | -100 | -32.91 | -25.65 | -23.67 | -23.56 | | -100 | -2.23 | -1.87 | -1.74 | -1.73 |
| δ (degrees) | | | | | | $ E_R/E_L $ (dB) | | | | | | E_L | | | | | |
| η_z (dB) | | | | | | η_z (dB) | | | | | | η_z (dB) | | | | | |
| η_z (dB) | -15 | -25 | -50 | -100 | | η_z (dB) | -15 | -25 | -50 | -100 | η_z (dB) | -15 | -25 | -50 | -100 | | |
| $k = -1$ dB | -15 | 151.49 | 147.73 | 145.86 | 145.75 | $k = -1$ dB | -15 | -18.43 | -15.07 | -13.93 | -13.87 | $k = -1$ dB | -15 | -5.84 | -5.13 | -4.82 | -4.80 |
| $\xi = 40^\circ$ | -25 | 147.73 | 143.97 | 142.10 | 141.99 | $\xi = 40^\circ$ | -25 | -28.72 | -20.22 | -18.10 | -17.99 | $\xi = 40^\circ$ | -25 | -5.26 | -4.71 | -4.48 | -4.46 |
| | -50 | 145.86 | 142.10 | 140.23 | 140.12 | | -50 | -69.71 | -24.15 | -20.95 | -20.79 | | -50 | -5.00 | -4.53 | -4.32 | -4.31 |
| | -100 | 145.75 | 141.98 | 140.12 | 140.00 | | -100 | -54.83 | -24.45 | -21.15 | -20.99 | | -100 | -4.98 | -4.52 | -4.32 | -4.30 |

Appendix B

SATELLITE COMMUNICATION

The polarization parameters within a given coordinate system in terms of any specific basis are well defined. But often the effect of separated coordinate systems must also be considered. The notable example is in satellite communication.³ At each communication site vertical polarization is readily defined by the local gravity vector and the horizontal polarization within an orthogonal plane, which then defines beam directions and polarization orientation in terms of the local coordinate system, usually spherical coordinates. The local coordinates of different sites, each with pointing beams at the same satellite will then differ, as will their vertical polarization reference. Optimum performance at each site requires the correct, albeit different, local directive angles and accounting for polarization alignment differences.

The relationship between an Earth communication site and a geostationary communication satellite is illustrated in Fig. B1. Along the line OC at the communication site, the local gravity vector \vec{r} defines the orthogonal horizontal “ground” plane. The line OS to the satellite also defines an orthogonal plane, that of the satellite directive antenna. For a geostationary orbiting communications satellite, the polarization angular orientation within that plane, defined by the E-field vector \vec{e} , is aligned with the Earth north-south polar axis. The location of the satellite, at a specific longitude and necessarily within the equatorial plane (0° latitude), and the communication site latitude and longitude are sufficiently descriptive for the intercommunication analysis following.

¹ D. Roddy, *Satellite Communications*, 2nd ed. (McGraw-Hill, New York, 1989).

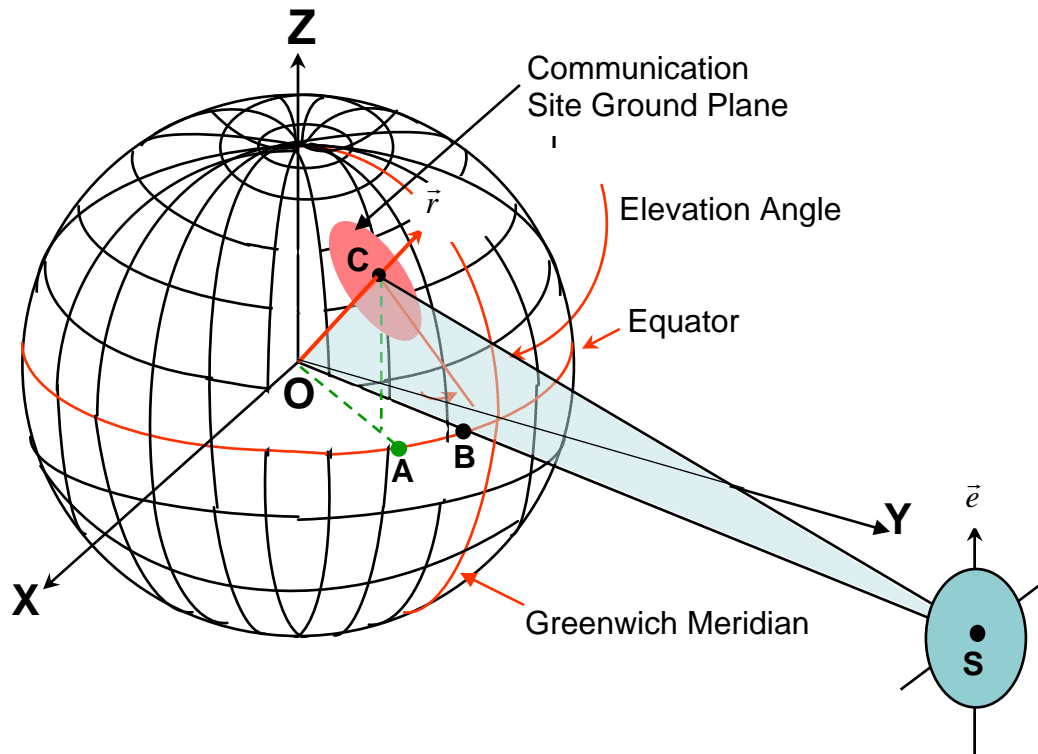


Fig. B1 –Satellite (S) and communication site (C) orientation. Communication and satellite azimuth along the Greenwich Meridian are at “A” and “B,” respectively. \vec{r} is the communication site local gravity vector and \vec{e} the satellite E-field vertical polarization vector.

SATELLITE DIRECTION ANGLES

The essential details are illustrated in Fig. B2: ζ_S and ζ_C are the respective longitudinal angles of the satellite and communication sites from the Greenwich Meridian, λ_C is the latitude of the communication site, and R_e and R_s are the distances from Earth center to surface (assuming a spherical Earth) and to the geostationary orbiting communications satellite.

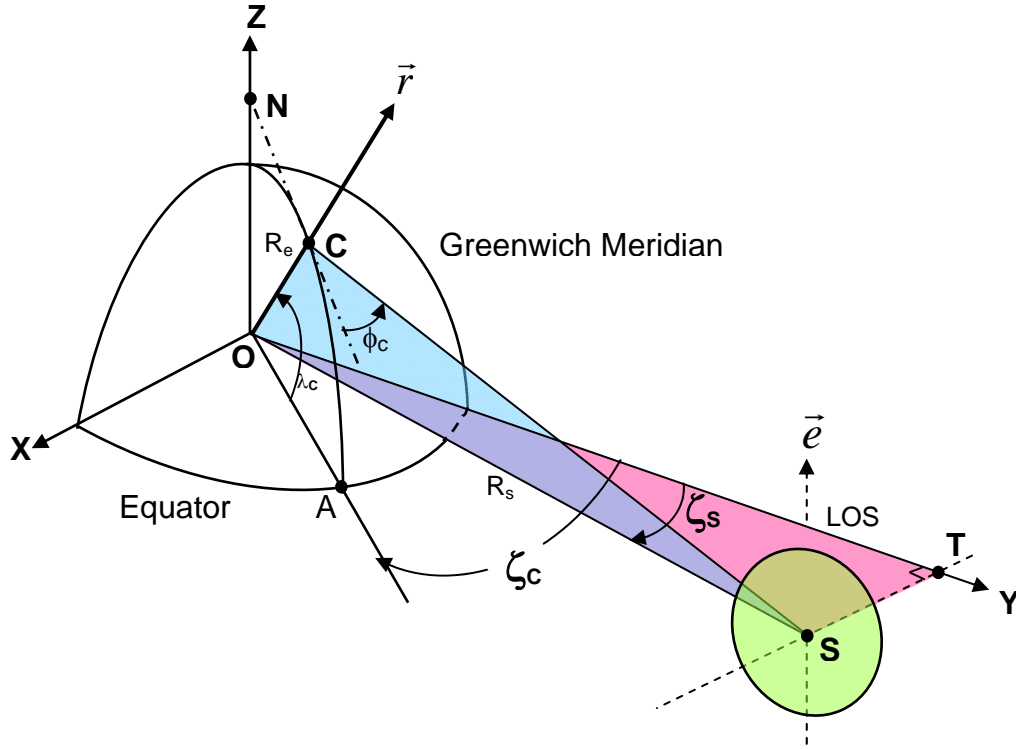


Fig. B2 – Angles associated with communications between the site at “C” and the satellite at “S”

Expressed as vectors, the line-of-sight (LOS) from communication site to satellite is $\overrightarrow{CS} = \overrightarrow{OS} - \overrightarrow{OC}$. In terms of Earth-centered spherical coordinates, these are

$$\overrightarrow{OS} = \vec{i} R_s \sin \zeta_s + \vec{j} R_s \cos \zeta_s + \vec{k} 0, \quad (\text{B1})$$

$$\overrightarrow{OC} = \vec{i} R_e \cos \lambda_c \sin \zeta_c + \vec{j} R_e \cos \lambda_c \cos \zeta_c + \vec{k} R_e \sin \lambda_c; \quad (\text{B2})$$

$\vec{i}, \vec{j}, \vec{k}$ are unit vectors in the x, y and z directions, respectively.

The LOS vector is then

$$\overrightarrow{CS} = \vec{i} (R_s \sin \zeta_s - R_e \cos \lambda_c \sin \zeta_c) + \vec{j} (R_s \cos \zeta_s - R_e \cos \lambda_c \cos \zeta_c) - \vec{k} R_e \sin \lambda_c. \quad (\text{B3})$$

The elevation angle of the satellite from the communication site is the complement of the angle between \overrightarrow{OC} and \overrightarrow{CS} :

$$\phi_c = \pi/2 - (\overrightarrow{OC} : \overrightarrow{CS}) . \quad (B4)$$

As a result,

$$\sin \phi_c = \frac{\overrightarrow{OC} \cdot \overrightarrow{CS}}{|\overrightarrow{OC}| |\overrightarrow{CS}|} = \frac{\cos \lambda_c \cos(\zeta_c - \zeta_s) - R_e/R_s}{\pm \sqrt{1 + (R_e/R_s)^2 - 2(R_e/R_s) \cos \lambda_c \cos(\zeta_c - \zeta_s)}} . \quad (B5)$$

In general, $\cos \lambda_c \cos(\zeta_c - \zeta_s) > R_e/R_s$, so the that the final result is

$$\sin \phi_c = \frac{\cos \lambda_c \cos(\zeta_c - \zeta_s) - R_e/R_s}{\sqrt{1 + (R_e/R_s)^2 - 2(R_e/R_s) \cos \lambda_c \cos(\zeta_c - \zeta_s)}} . \quad (B6)$$

Referenced to the north direction, the angle ξ , between the communication site north, characterized by a vector \overrightarrow{CN} in Fig. B2, and the satellite LOS, \overrightarrow{CS} is

$$\cos \xi = \frac{\overrightarrow{CN} \cdot \overrightarrow{CS}}{|\overrightarrow{CN}| |\overrightarrow{CS}|} . \quad (B7)$$

From Fig. B2, $\overrightarrow{CN} = \overrightarrow{ON} - \overrightarrow{OC}$, and $\overrightarrow{ON} = \vec{i}0 + \vec{j}0 + \vec{k} R_e/\sin \lambda_c$.

Applying these together with Eq. (B3), the result is

$$\cos \xi = \frac{\sin \lambda_c \cos(\zeta_c - \zeta_s)}{\pm \sqrt{1 + (R_e/R_s)^2 - 2(R_e/R_s) \cos \lambda_c \cos(\zeta_c - \zeta_s)}} . \quad (B8)$$

The relationship among the angles ξ , ϕ_c , and the satellite azimuth θ_c and the angles ξ and ϕ_e in the local communication site coordinates is illustrated in the right spherical triangle shown in Fig. B3, from which it is seen that

$$\cos \theta_c = \frac{\cos \xi}{\cos \phi_e} . \quad (B9)$$

Expanding this,

$$\cos \theta_c = \frac{\sin \lambda_c \cos(\zeta_c - \zeta_s)}{-\sqrt{1 - \cos^2 \lambda_c \cos^2(\zeta_c - \zeta_s)}} \quad (\text{B10})$$

(The radical is negative since $\theta_c = 180^\circ$ when $\zeta_c = \zeta_s$.)

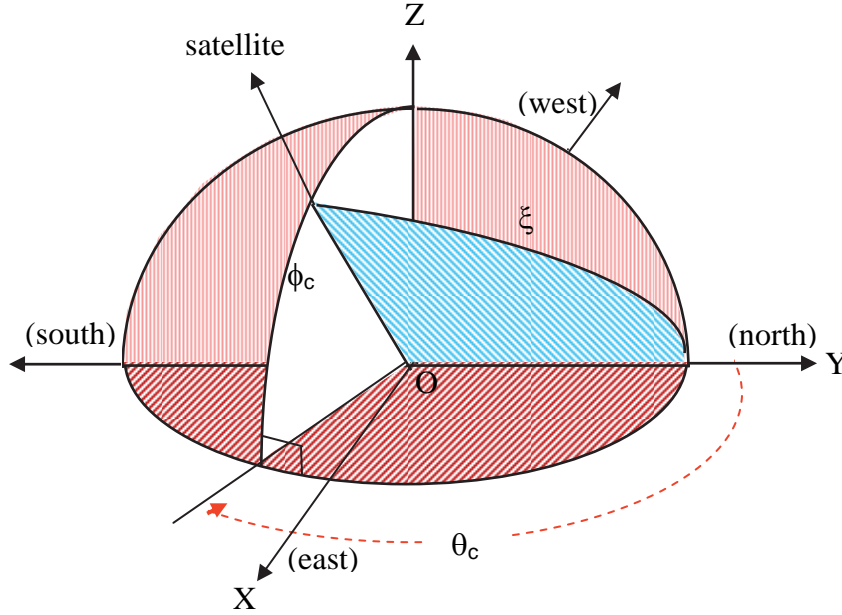


Fig. B3 – Satellite direction in terms of the communication site angles, θ_c , and ϕ_c .

Equation (B10) can then be rewritten as

$$\tan \theta_c = \frac{-\tan(\zeta_c - \zeta_s)}{\sin \lambda_c} \quad (\text{B11})$$

SATELLITE POLARIZATION

The approach is to calculate the difference between the satellite and communication site polarization vectors when they are referred to the common plane, OSC, as illustrated in Fig. B2. The communication site polarization plane is represented by the normal vector \vec{r} , defined by the Earth radius and the latitude and longitude angles λ_c and ζ_c . The satellite polarization plane, essentially defined by the station-keeping

direction along OS when the meridian angle ζ_s is specified, remains fixed while serving communication sites over a wide area.⁴

The outward-directed normal to the satellite and communication site planes, OTS and OCS, are given by vector cross-products of their respective vectors, $\overrightarrow{OS} \times \overrightarrow{OT}$ and $\overrightarrow{OS} \times \overrightarrow{OC}$, where

$$\overrightarrow{OS} = \vec{i} R_s \sin \zeta_s + \vec{j} R_s \cos \zeta_s + \vec{k} 0 \quad (\text{B12})$$

$$\overrightarrow{OT} = \vec{i} 0 + \vec{j} R_s \cos \zeta_s + \vec{k} 0. \quad (\text{B13})$$

From Eq. (B2): $\overrightarrow{OC} = \vec{i} R_e \cos \lambda_c \sin \zeta_c + \vec{j} R_e \cos \lambda_c \cos \zeta_c + \vec{k} R_e \sin \lambda_c$.

Then, combining these with Eq. (B2), the angle between the normals of these two planes is

$$\cos \psi = \frac{(\overrightarrow{OS} \times \overrightarrow{OT}) \cdot (\overrightarrow{OS} \times \overrightarrow{OC})}{|\overrightarrow{OS} \times \overrightarrow{OT}| |\overrightarrow{OS} \times \overrightarrow{OC}|} = \frac{\cos \lambda_c \sin(\zeta_s - \zeta_c)}{\pm \sqrt{1 - \cos^2 \lambda_c \cos^2(\zeta_s - \zeta_c)}}. \quad (\text{B14})$$

The angular directions and their relationships with reference directions can be somewhat confusing. Viewed from the satellite, ψ increases counterclockwise as $\zeta_c > \zeta_s$. The vertical polarization vector of the communication site is parallel with the OCS plane, i.e., 90° greater than the normal to that plane. However, the satellite vertical polarization vector is normal to the plane OST. Therefore, the angle from the vertical polarization of the satellite to the vertical polarization of the communication site is the complement, $90^\circ - \psi$, in a clockwise direction. To maximize the coupling between the communication site and the satellite, as well as minimizing any cross-polarization effects, these two directions must be matched. Looking at the satellite from behind the communication site, rotating the communication site component in a counter-clockwise direction achieves this result. Representing the required polarization rotation by ψ' , and using Eqs. (B2), (B12), (B13) and (B14), the required rotation is

$$\tan \psi' = \frac{\sin(\zeta_s - \zeta_c)}{\tan \lambda_c}, \quad (\text{B15})$$

in which a negative value signifies a counter-clockwise rotation.

An example of the directional and polarization orientation angles is a vertically polarized communication link between NRL's CBD ground site at 38.657° north latitude, and 76.528° west longitude with Telstar11, located at 37.500° west longitude.

Using Eqs. (B6), (B11), and (B15), with $\zeta_c = 76.528^\circ$, $\zeta_s = 37.500^\circ$, and $\lambda_c = 38.657^\circ$, $R_e = 6.37814 \times 10^6$ m and $R_s = 4.216414 \times 10^7$ m, the results are

$$\phi_c = 29.804^\circ, \theta_c = 127.618^\circ, \text{ and } \psi' = -38.210^\circ.$$

⁴ Small angular differences among the multiple satellite beams covering different geographic surfaces from the same satellite location are ignored.

Effects of Polarization Misalignment

Correct polarization alignment between the communication site and satellite is clearly required to optimize intercommunication power transfer. Small angular differences will have negligible impact on this transfer. For example, the one-way reduction in power transfer from a misalignment of 5° is only 0.03 dB. The greater impact of misalignment is the independent use of dual polarized channels, which then provide “a frequency reuse” characteristic. For this purpose, polarized component orthogonality is paramount. Requirements will depend on the waveform coding used, but a typical baseline is -25 dB. Cross-polarization characteristics at both the communication site and the satellite depend on the technology used to form orthogonal beams. A well-designed system may have an isolation of -30 dB or more and a poor one of -20 dB or less. Achieving good isolation depends on many factors; of course, these include antenna element or feed design, but other factors will also impact performance. At the communication site, for example, one factor is multipath caused by site topography and nearby structures, fixed or moving and, depending on operating frequency, magnetic effects (Faraday rotation) may also impact performance. Additional factors can even include atmospheric inhomogeneities. Figure B4 illustrates the impact of polarization alignment errors on a ground-satellite link with various cross-polarization levels. Assuming that a -25 dB cross-polarization level is required for effective frequency reuse and that the cross-polarization levels of the ground and satellite systems are -30 dB, the misalignment must be less than 1.5° .

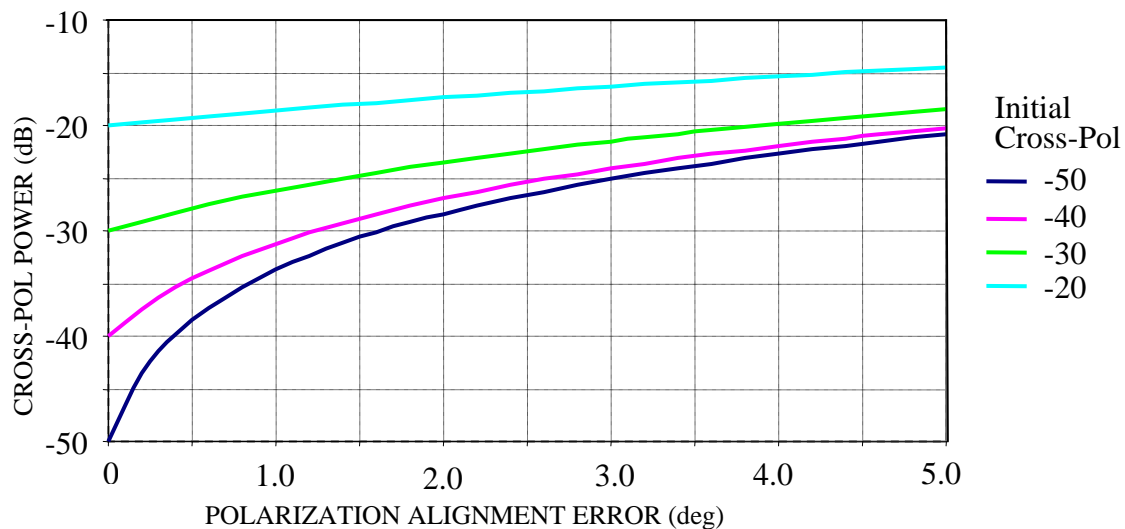


Fig. B4 – Effect of polarization misalignment on cross-polarization level